ERDC TR-06-6

US Army Corps
of Engineers®
Engineer Research and
Development Center

A GIS System for Inferring Subsurface Geology and Material Properties: Proof of Concept

Lawrence W. Gatto, Michael V. Campbell, Judy Ehlen,
Charles C. Ryerson, Lewis E. Hunter, and Brian T. Tracy

September 2006

Engineer Research
and Development Center

ERDC TR-06-6
September 2006

A GIS System for Inferring Subsurface Geology and Material Properties: Proof of Concept

Lawrence W. Gatto, Charles C. Ryerson, and Brian T. Tracy

Cold Regions Research and Engineering Laboratory
U.S. Army Engineer Research and Development Center
72 Lyme Road
Hanover, NH 03755-1290

Michael V. Campbell and Judy Ehlen

Topographic Engineering Laboratory
U.S. Army Engineer Research and Development Center
7701 Telegraph Road
Alexandria, VA 22315-3864

Lewis E. Hunter

Sacramento District
U.S. Army Corps of Engineers
1325 J Street
Sacramento, CA 95814-2922

Prepared for U.S. Army Corps of Engineers
Washington, DC

Abstract: This report describes the concept for a geographical information system (GIS) that can infer subsurface geology and material properties. The hypotheses were that a GIS can be programmed to 1) follow the fundamental logic sequence developed for traditional terrain- and image-analysis procedures to infer geologic materials; 2) augment that sequence with correlative geospatial data from a variety of sources; and 3) integrate the inferences and data to develop "best-guess" estimates. Structured logic trees were developed to guide a terrain analyst through an interactive, geologic analysis based on querying and mentoring logic primarily using imagery and map data as input. The logic trees allow a terrain analyst with limited geology background and experience to rapidly infer the most likely geologic material. A new surface projection method was also developed to estimate depth to bedrock, and an existing method to determine depth to the water table was significantly expanded. The concept was proven to be feasible during blind evaluations conducted at Camp Grayling, MI, a cool, temperate, vegetation-covered site, and at Yuma Proving Ground, AZ, and Fort Irwin, CA, both hot, arid, barren sites. The results show that an analyst can infer the correct geologic conditions 70–80% of the time using these inferential methods.

Contents

Figures and Tables

Figures

Tables

Preface

This report was prepared by Lawrence W. Gatto, Environmental Sciences Branch, Cold Regions Research and Engineering Laboratory (CRREL), U.S. Army Engineer Research and Development Center (ERDC), Hanover, NH; Michael V. Campbell, Geospatial Applications Branch, Topographic Engineering Center (TEC), ERDC; Judy Ehlen, Data and Signature Analysis Branch, TEC, ERDC; Charles C. Ryerson, Snow and Ice Branch, CRREL, ERDC; Lewis E. Hunter, Sacramento District, U.S. Army Corps of Engineers; and Brian T. Tracy, RS/GIS and Water Resources Branch, CRREL, ERDC.

The ERDC 6.1 basic research B52C program provided funding for this project, Geologic Structure Analysis (# 61110252C00). The authors thank Connie Gray (TEC), B52C Program Manager, for her interest, guidance, and support throughout the project; Tommy Hall (CRREL) for being the analyst for the July 2003 evaluation; SGT Chris Kennedy (TEC) for being the analyst for the October 2003 evaluation; Dr. Mark Moran (CRREL) for supporting this project throughout; Dr. Moran, Dr. Tom Anderson, and Dr. Steve Ketcham (all of CRREL) for discussions on seismic-wave modeling and requirements for geologic data and for supporting this project from its inception; Charles Shuey, a summer hire at TEC, for developing the slope projection algorithm in 2003; Connie Gray (TEC), Dr. Moran (CRREL), Dr. Keith Wilson (CRREL), Dr. Justin Berman (CRREL), and Randy Hill (CRREL) for participating in the final concept demonstration in July 2004; and Carla Elenz, Camp Grayling Environmental Office, and Rosa Affleck, CRREL, for the Camp Grayling imagery and GIS data layers. The participants at all three demonstrations provided useful and insightful comments for improving the logic trees and elements of the system concept and for developing the steps for follow-on research and development. The authors thank Dr. Moran, CRREL, and J. Ponder Henley, TEC, for technically reviewing this report.

This report was prepared under the general supervision of Dr. Terry Sobecki, Chief, Environmental Sciences Branch; Dr. Lance Hansen, Deputy Director; and Dr. Robert Davis, Director, CRREL.

The Commander and Executive Director of ERDC is COL Richard B. Jenkins. The Director is Dr. James R. Houston.

1 Introduction

A variety of Future Combat System components, including Hornet, Raptor, and Rattler, as well as unattended, advanced, intelligent seismic and acoustic ground sensor networks, will be used on the battlefield to collect and analyze seismic and acoustic surface waves for non-line-of-site detection and tracking of troop and vehicle locations and movements (Fig. 1). These surface waves follow curving ray paths and are highly sensitive to surface and near-surface geologic conditions. Ketcham et al. (2002) described ongoing research to develop high-fidelity, numerical analysis software to model the characteristics of seismic surface waves in denied areas (areas where ground access in not possible). They reported that knowledge of changes in subsurface boundary conditions and material properties within the upper 30 m of the earth's surface in denied sites was unavailable. And yet that knowledge is critically important to such modeling efforts because these changes generate refracted and reflected waves. The geologic conditions that most affect wave propagation are 1) contrasts between different soil and rock types, 2) depth to bedrock, 3) water table depth, 4) fracture locations, orientations, and spacings, and 5) material properties (e.g., bulk density, compressional velocity).

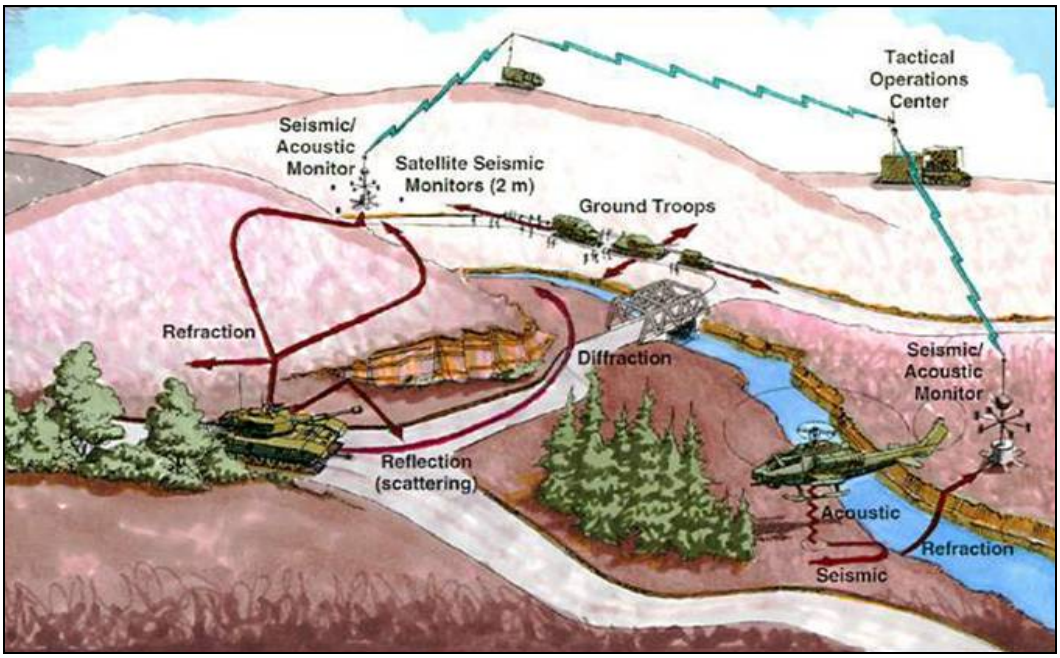

Figure 1. Ground sensor networks on a battlefield.

Even though available wave-modeling algorithms consider the complex influences of terrain and near-surface geological conditions on seismic-wave propagation, the current geologic models only approximate simplified, multi-layered, subsurface geology. Such models reflect neither the real geologic conditions nor the locations of important changes with contrasting compressional wave velocities within the upper 30 m. However, more-realistic geologic data that may exist for denied areas are not readily available, the specific subsurface features of importance are usually not known, and no method currently exists to collect the required information in denied areas. Clearly, the ability to more realistically infer the needed geologic complexities will dramatically improve the utility of seismic-sensor networks.

A rapid method is needed to infer geologic conditions and material properties in denied areas to maximize the information gained from sensor networks. These inferred geologic data can then be used to build an initial geologic model for the area where a seismic network will be established to provide initial parameters for wave-propagation models. These models will subsequently be modified as the network becomes active.

We propose that a method based on traditional terrain-analysis procedures that will infer the geologic parameters of importance to the depths of concern (20–30 m) can be devised in a GIS environment. This procedure will provide estimates of material properties that will be integrated into the numerical analysis software to model seismic waves.

Our overall objective is to create and evaluate a proof-of-concept GIS-based system that follows a systematic and logical protocol to infer geologic parameters to depths of about 30 m. We did not attempt to develop a functioning GIS system; such development is only appropriate in follow-on efforts. Our proof-of-concept currently unifies geologic associations, terrain-analysis techniques, and database procedures in a GIS environment, allowing a terrain analyst to predict subsurface seismic properties, a capability not currently available.

Our specific objectives are:

1. To devise a conceptual model for an interactive, GIS-based system that uses analytical and inferential procedures based on geoscience, image analysis, and terrain-analysis principles to infer geologic parameters;

2. To define, compile, and integrate the elements of the conceptual model to prove the feasibility of such a system (proof-of-concept); and
3. To evaluate the concept at sites where remotely sensed imagery and geologic data are available to assess the potential accuracy of the system and to identify necessary system modifications.

This report describes our initial concept for the method, the general geological-analytical processes followed, the logic behind the detailed inferential and estimation procedures, the results of the evaluations of that logic, the general operation of the system when it is developed, demonstrations of the proof-of-concept model to various groups, and the requirements for future development, demonstration, and validation.

2 SYSTEM CONCEPT

Capabilities and Assumptions

A GIS designed to manipulate geospatial data and interrogate databases is the target platform for our method. A GIS is ideal for unifying the different elements of our inferential system, including spatial data analysis techniques, image processing, and database manipulation procedures. GIS can be used to generate three-dimensional (3-D) geologic models. We expect that a GIS can be programmed to operate interactively with a terrain analyst who systematically analyzes geospatial imagery and map data by following logical steps that are the basis for traditional image and terrain analyses. Our GIS is specifically designed to infer the above-stated geologic parameters.

Our project team consisted of geologists and geomorphologists with extensive knowledge and experience in geologic processes, image processing, and image and terrain analysis; a climatic geographer with extensive experience in structured logic trees; and a forester with extensive experience in vegetation mapping, GIS applications, and automated image analysis and classification procedures.

Our concept was developed assuming that the latest versions of ESRI ArcGIS and ERDAS Imagine image-processing software will be used as the main processing and mapping platforms. These programs are commonly available and are widely used by Army terrain teams. We further assume that a military terrain analyst experienced with these software products is our target user and that additional training required for the analyst to use our system should be minimal and consist only of gaining familiarity with it. However, in developing the logic trees that form the backbone of our concept, we also assumed that the analyst would have minimal experience in classic photo interpretation and terrain analysis with respect to geology and landform identification. Thus, we designed the method to provide decision aids whenever the analyst might require ancillary information while being guided through the geological analysis sequence.

Furthermore, since the innovative component of our research was to develop the interactive logic sequence, we had to assume that some basic data layers such as those shown in Table 1 would be made available to the

Table 1. Data availability.

Primary data (globally available)	Secondary data (regionally available)	Tertiary data (site-by-site availability)
Climate data Glaciated vs. non-glaciated regions map Permafrost maps Digital elevation models (DEMs) Landsat digital imagery Soils maps Vegetation maps Land use maps Landform polygon maps Topographic maps with drainage patterns	Geologic maps: Surficial materials Tectonic history Bedrock types Large-scale structural geology maps with fractures Satellite/aircraft imagery with finer spatial and spectral resolution than Landsat	Well logs Water level data

analyst at the beginning of the process. We understand that the data available will vary with the specific location being analyzed and that not all data will be available for all sites. However, data layers with landform delineations without classifications and drainage patterns will always be generated and made available because they are critical to our analyses.

These assumptions of data availability allowed the team to focus on developing the logic process and identifying the needed supporting data and methods that will serve as decision aids. The team identified several steps that could be automated. However, automation was not a goal of this project and should be implemented during follow-on work. For this reason, our concept has been developed in a modular fashion so that as new algorithms or procedures are identified they can be inserted into the logic sequence.

We envision that an analyst will operate the GIS method, when fully developed, and will proceed through the inferential process by manipulating all available data to obtain the desired information. This process will be robust in that it must provide reliable inferences and estimates in all geologic terrains and climatic regions without site-specific data. It must also be sufficiently flexible to allow the analyst to proceed no matter what data are available to him and regardless of the scale or resolution of those data. We also envision that the system will be able to provide site-specific information when adequate data are available.

Although we believe that our concept is sufficiently generic to be globally applicable, due to time and resource constraints and the purpose of our project, we chose to develop it based on evaluations in two very different climatic environments. We focused our efforts on making our logic work at a cool, temperate site that has been glaciated (Camp Grayling, MI) and at two hot, arid sites (Yuma Proving Grounds, AZ, and Fort Irwin, CA).

We knew that none of the required geologic information is directly detectable on imagery, although the type of soil and bedrock present in landforms can be inferred using terrain analysis procedures. We were also aware that low-resolution, small-scale data (often digital) such as 1:500,000- or 1:1,000,000-scale soils and geology maps are likely to be available and can provide at least general information on the types of materials present. We assumed that adequate, high-resolution data were not available for most areas, and we designed our proof-of-concept evaluations to represent "worst-case-scenarios," e.g., 30-m-resolution imagery and 1:500,000- or 1:1,000,000-scale map data. Therefore, the desired information of surface material type, depth to bedrock, depth to the water table, and likely fracture patterns and characteristics must be inferred from whatever sources are available.

Basic material types and depth to the water table can be inferred from imagery analysis or surface topography, surface-water distribution (i.e., lakes), and drainage patterns. With regard to fracture patterns and characteristics, we knew that our potential user would not have the expertise required to make these determinations and that readily available software for so doing is lacking. To fill this gap, we designed a look-up table that uses proxy data to generate an estimate of fracture spacings based on rock type augmented by rudimentary lineation analyses to infer site-specific fracture orientations.* Similarly, seismic properties were compiled into a look-up table based on material types. The table used in the proof-of-concept model provides a "global" overview because of the availability of data and because our goal was to demonstrate the process, not to provide definitive answers. We assume that during a "true" application of the system, more specific site or proxy data, if available, would be used to populate the database.

* Lineations are features on the surface of the earth that reflect the presence of fractures at depth. They exhibit the properties of fractures (e.g., parallelism and length) and are typically delineated using patterns composed of straight stream segments, linear tonal patterns, lines of vegetation and topographic features such as aligned saddles.

Foundation in Terrain-Analysis Methods

We began with established geoscience and terrain-analysis principles that have previously demonstrated that surface features can be used to infer subsurface conditions as depicted in Figure 2. These principles show that shallow geologic structure can control the character of surface features and relief (Foster and Beaumont 1992). Dehn et al. (2001) explicitly stated that morphology directly reflects geologic history, including the processes that influenced morphologic and soils development. They also established that

a. Shallow geologic structure often controls the character of surface features and relief.

b. Morphology directly reflects geohistory and processes and affects soil development and water table depths (Dehn et al. 2001).

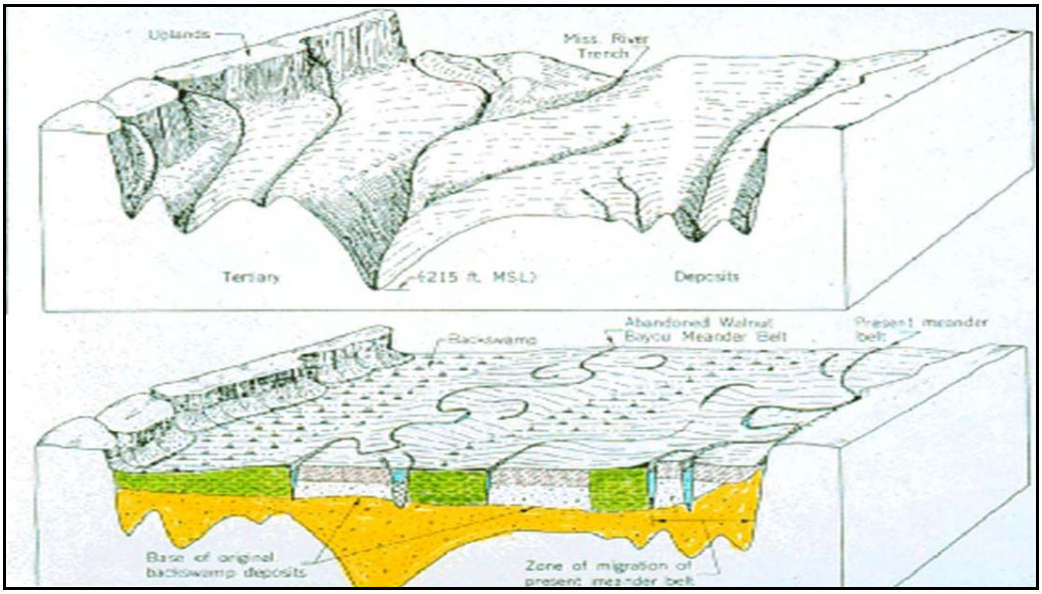

c. Landform identification and geomorphic context allow inference of physical characteristics of subsurface materials (Rinker and Corl 1984).

Figure 2. Geoscience principles to be used within the GIS environment to progress from analysis of surface features to estimation of subsurface conditions.

water-table depths are affected by surface morphology and subsurface conditions. Further, Frost (1950), Rinker and Corl (1984), and Leighty et. al. (2001), among others, have established that landform identification and geomorphic context allow inference of physical characteristics of subsurface materials. Consequently, traditional methods for obtaining geologic information from imagery have relied on analyses of surface terrain characteristics (e.g., Frost et al. 1953, Way 1973, Ehlen 1976, Blodget and Brown 1982, Rinker and Corl 1984, Graff 1992).

Typically, boundaries between different landforms and vegetation types are identified, and drainage patterns and lineations are delineated. These data are then combined to infer the type of the materials comprising each landform. Inferences are often based on the use of image identification keys (e.g., Liang et al. 1951a, b, c, d, e, f, Loelkes et al. 1983, Rinker and Corl 1984), the experience of the analyst, or a combination thereof.

Terrain analysis can be accomplished either manually through stereo viewing or digitally using high-resolution, digital elevation models (DEMs). Traditional analytical methods have relied on visual interpretation of stereo aerial photographs. However, readily available multi-scale digital images, automated methods to extract topographic and landform data from them, and enhanced computer capability to display those data in 3-D have been developed to replace traditional analytical methods. There is continuing debate as to the quality of the interpretations and products from these automated methods. Our experience with automated methods for delineating drainage networks, for example, clearly illustrates that the current capability is insufficient to produce the detail required to infer material types.

We know of no automated methods that are fully functional or that produce the detail adequate for our needs. Automation is a “black or white” process, whereas terrain analysis is an interpretive process. Furthermore, we are skeptical that knowledge-based systems, e.g., artificial intelligence, will be developed to the point that they will completely replace human-based interpretations in the terrain-analysis process. The Topographic Engineering Center has attempted to develop such knowledge-based systems over the past 20-30 years, but these systems do not produce results comparable to those produced by a human being.

The System

Traditional terrain analysis is based on identifying differences in landform characteristics and drainage patterns. Certain combinations of landform and drainage patterns are indicative of certain material types or conditions, e.g., a radial drainage pattern associated with a hill with a depression on the top indicates a volcano, and thus volcanic rock. Our overarching concept was to unify previously independent, unconnected geologic associations or rules of thumb, geomorphic principles, and terrain-analysis principles that allow inferences of subsurface features from surface conditions. Our conceptual model for the general analytical logic behind the entire inferential and estimation process consists of multiple, but linked, geologic analysis modules or approaches (Fig. 3). Each would be utilized to infer and estimate the required geologic parameters, and all would be integrated in a GIS to provide an operational framework with the required spatial analytical capabilities (Gatto et al. 2002). The basis for our concept is a flexible, interactive GIS system wherein input, analyses, and output modules could be swapped and modified as necessary. This initial concept guided us as we developed, evaluated, and modified the various modules.

The interactive analytical sequence begins with a query of all available data for a specified location from global, continental, and regional databases and the literature to provide input (Fig. 3). The primary types of data that are available globally include climate, DEMs, and Landsat digital imagery. Secondary types, which may be limited to continents or regions, include large-scale maps of structural geology showing fractures and faults, surficial geology with gross sediment and bedrock types, delineations of glaciated and non-glaciated regions, permafrost extent, soils, vegetation, and land use. Geologic literature may include descriptions of the regional tectonic history and geologic setting. Such geologic information will help constrain the possible material types likely to be present in a particular location, e.g., a non-permafrost area would not have extensive ground ice. In addition, satellite or aircraft imagery of much finer spatial and spectral resolution than Landsat, SPOT, or similar imagery is available for many regions, as are large-scale, topographic maps. Tertiary, site-specific data include well logs and water-level data. We doubt that well logs will be available for many sites, but if they are, they would provide valuable information on material types, depth to bedrock, and water-table depth.

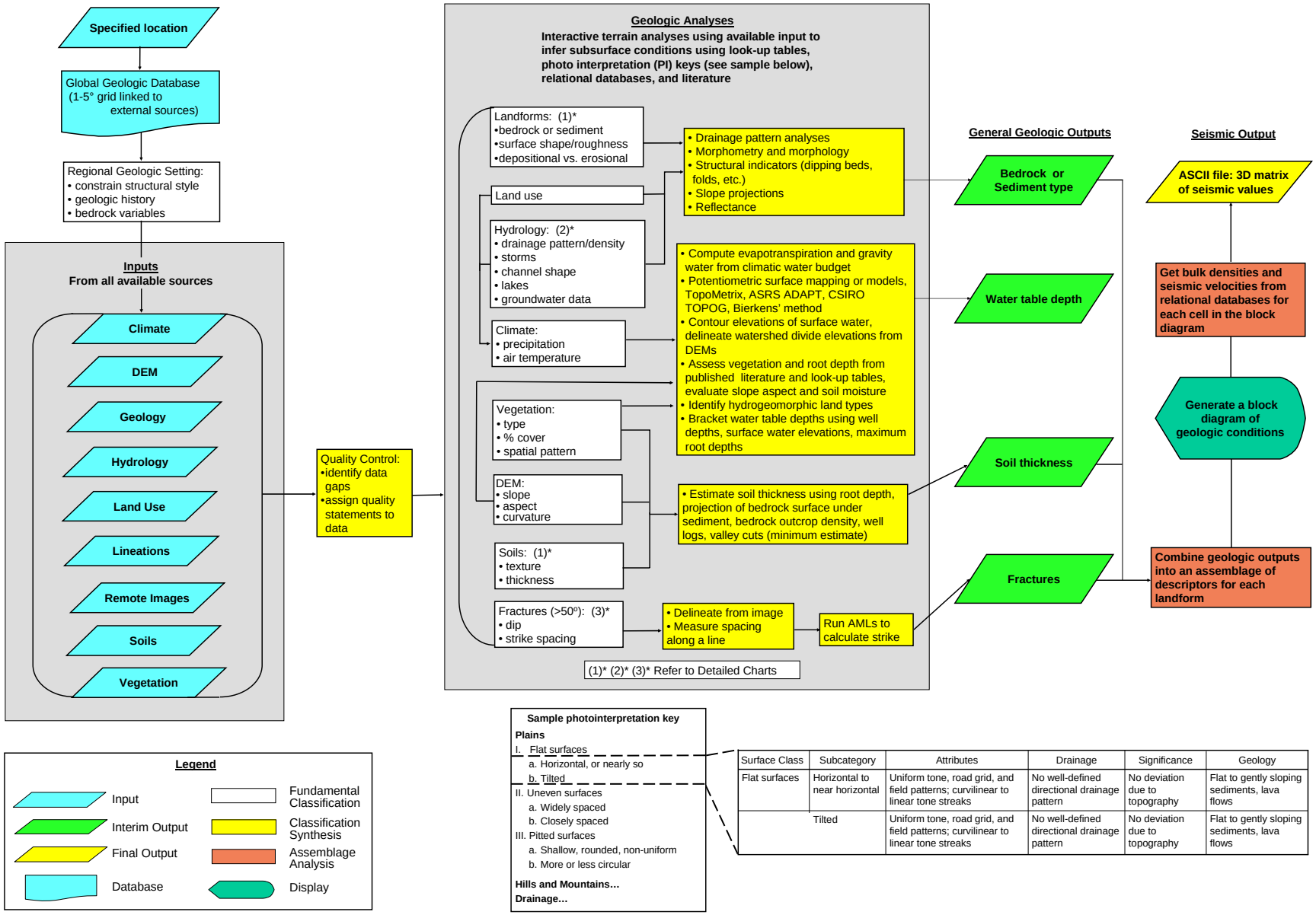

Surface Class	Subcategory	Attributes	Drainage	Significance	Geology
Flat surfaces	Horizontal to near horizontal	Uniform tone, road grid, and field patterns; curvilinear to linear tone streaks	No well-defined directional drainage pattern	No deviation due to topography	Flat to gently sloping sediments, lava flows
	Tilted	Uniform tone, road grid, and field patterns; curvilinear to linear tone streaks	No well-defined directional drainage pattern	No deviation due to topography	Flat to gently sloping sediments, lava flows

Figure 3. Analytical logic of the conceptual model.

We visualize that the data inputs will be hierarchical, going from global to continental scales, with regional terrains defined based on climate and tectonics, which would minimize the number of landforms and material types likely to be present. Glaciated and permafrost terrains would also be delineated to constrain landform and material-type options. Ultimately, we will include algorithms that will operate in the background to screen out options that are unlikely to occur. For example, permafrost landforms and frozen soil will not be an option for sites in a hot, arid area such as Yuma Proving Ground, AZ.

The concept for the geologic analyses (Fig. 3) incorporates separate modules for inferring material type, depth to bedrock, depth to the water table, and fracture characteristics. The details of the geologic analysis modules are shown in Figure 4. The first and last of these modules (Fig. 4a and c) utilize established image analysis techniques in a sequential process to make the geologic inferences. Figure 4a is used to infer gross constituent materials from landform analyses; Figure 4b, to estimate water-table depth; and Figure 4c, to infer fracture orientations and spacing. The GIS system will link these general geologic outputs to relational databases containing general and site-specific rock property data to extract the needed geophysical parameters. For this project, the data of interest were values that affect seismic wave propagation, particularly the compressional wave velocity of a material and the fracture characteristics that may impart seismic asymmetry. The GIS system will use these output parameters to generate a 3-D layered model.

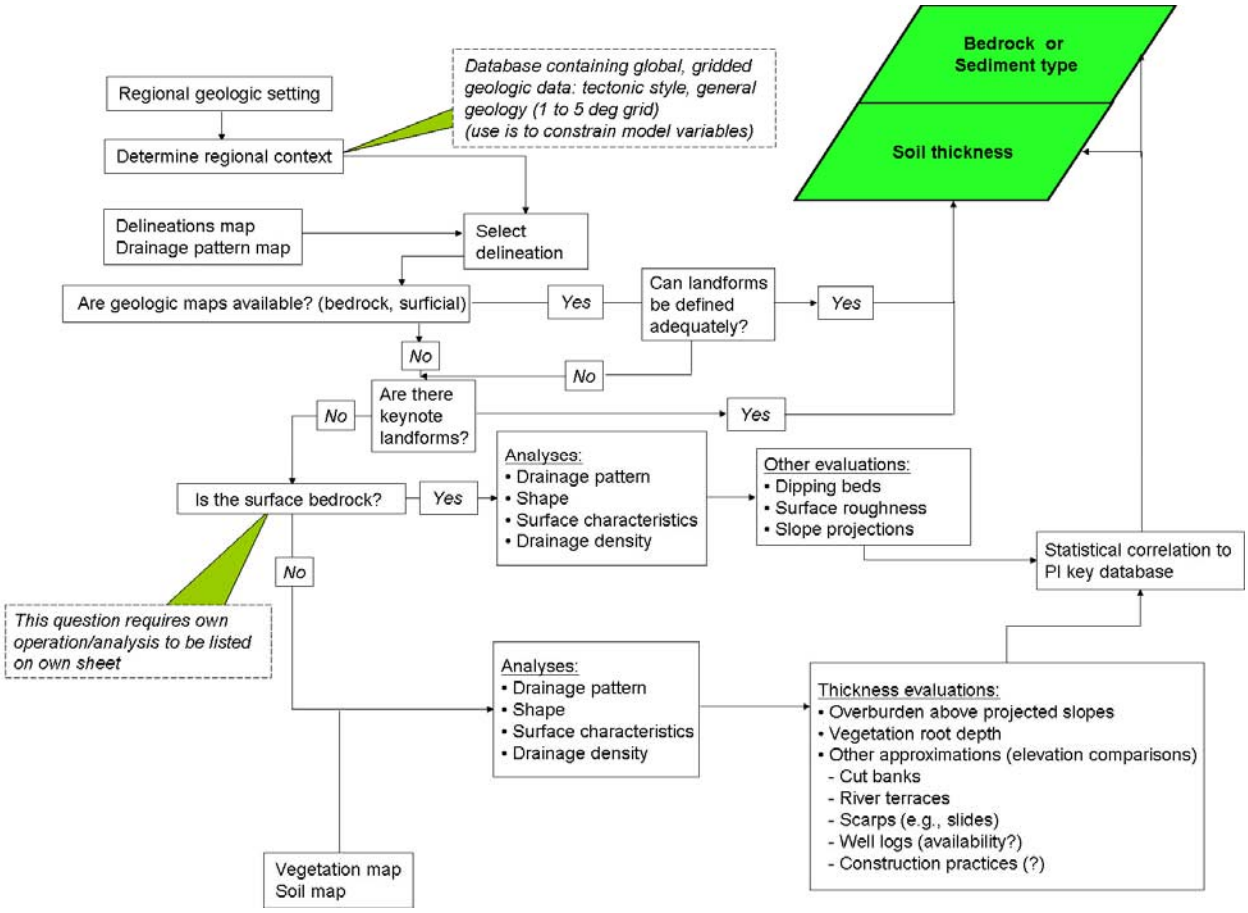

a. Landform analysis.

Figure 4. Conceptual models of geologic analyses.

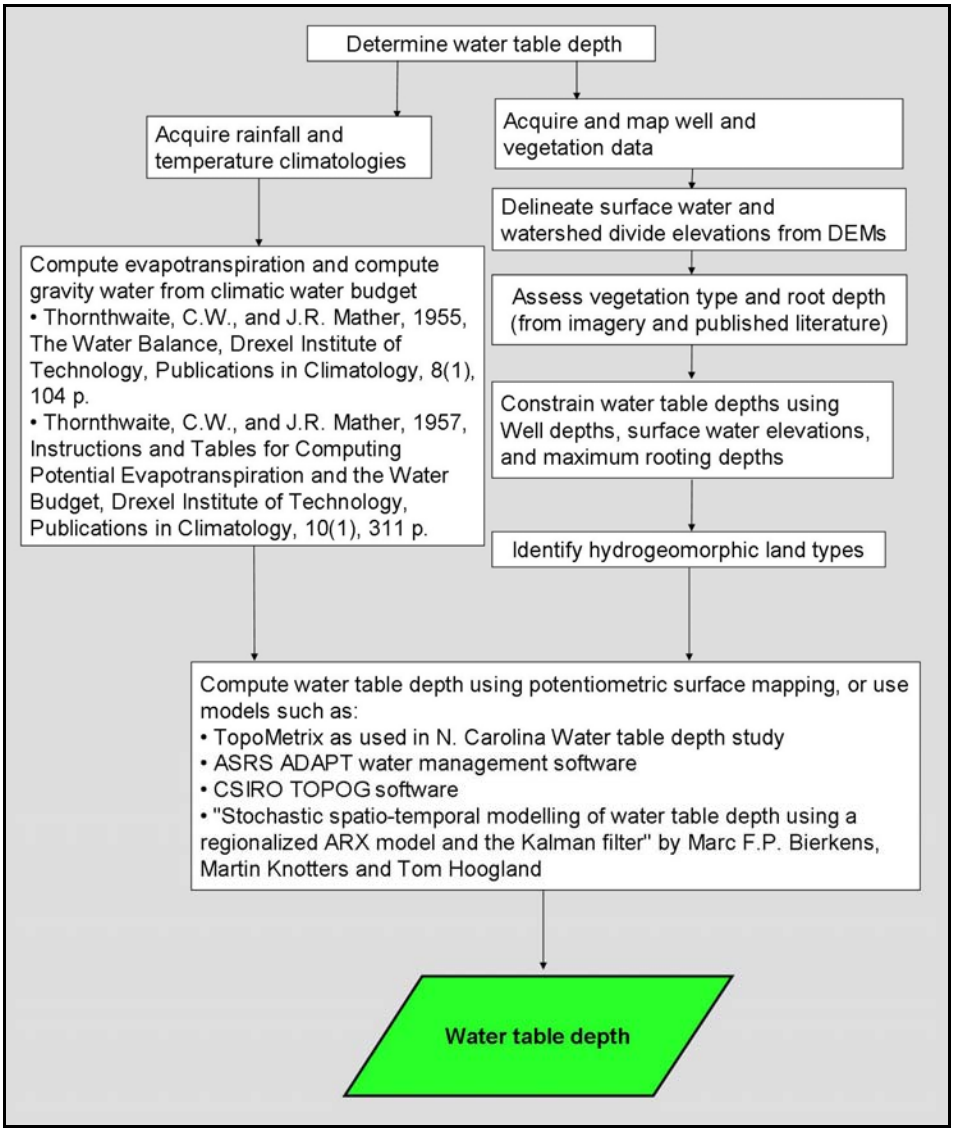

b. Hydrologic analysis.

Figure 4. (cont.).

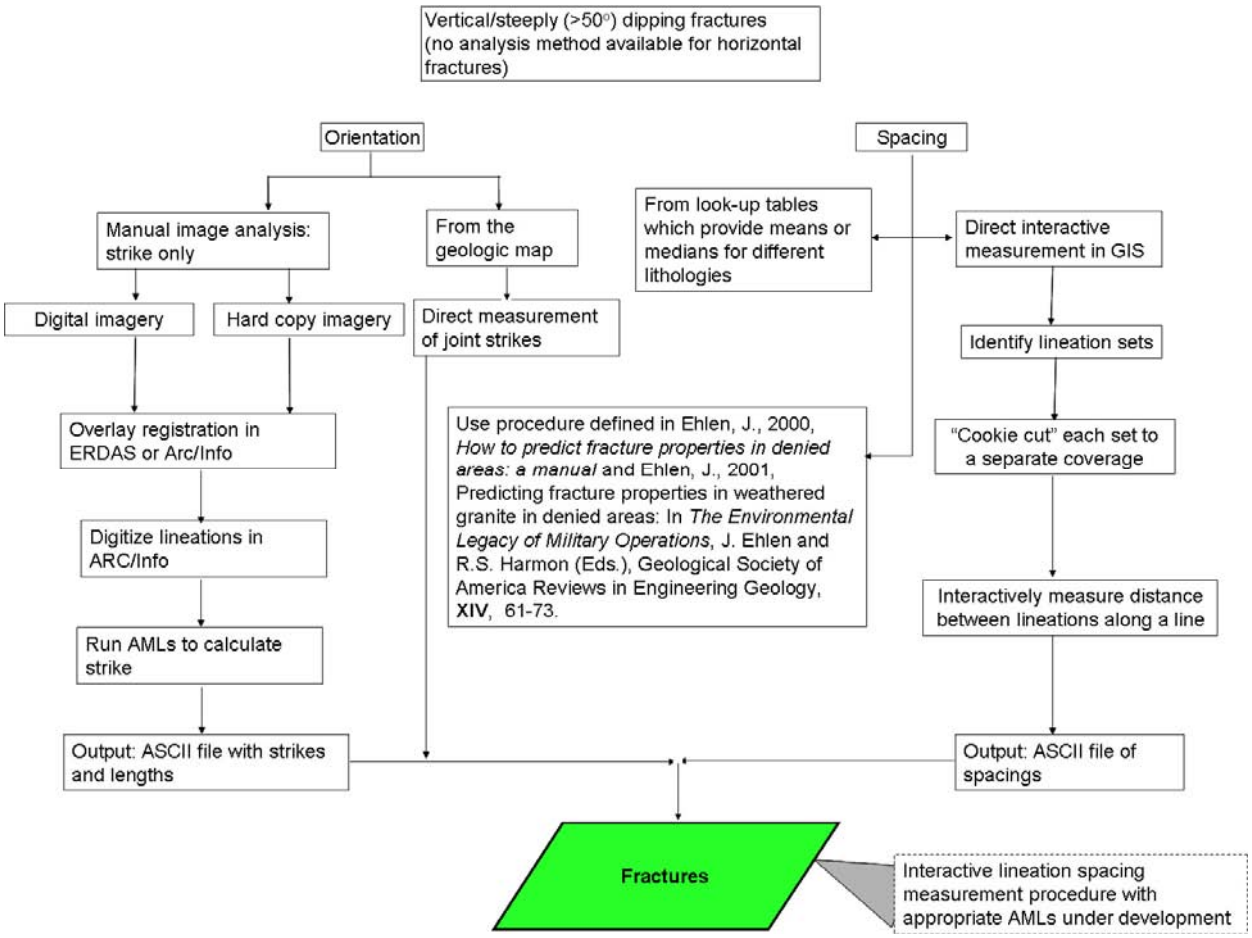

c. Fracture analysis.

Figure 4. (cont.).

3 LANDFORM CONSTITUENT MATERIALS

The core of our GIS-based system is a set of structured logic trees that 1) translates the classic terrain analysis process into an interactive querying and mentoring procedure, and 2) guides a terrain analyst from raw imagery and map data through a geologic analysis to infer surface and near-surface material types in different landforms. In building the system, we developed three such logic trees. Two trees are based on drainage pattern analyses, the third on landform analysis. These trees were evaluated in a series of tests, modified, and re-evaluated, eventually leading to the selection of the best overall performer.

We intentionally developed three separate logic trees so as to evaluate which inferential approach would most often provide the correct answer. All three trees will be in the final GIS system to provide the analyst with multiple routes, which will improve confidence in the inferred results if two or more trees generate complementary results. Thus, a multi-route approach would provide additional flexibility to the final GIS system.

All three trees use a logical flow of questions that require “yes” or “no” answers to systematically arrive at end-state material types for each landform unit. All three are founded on geologic associations and rules, geomorphic principles, and professional terrain-analysis experience. They are augmented by image-analysis procedures and techniques and are integrated with relational database procedures. For our proof-of-concept work, we evaluated each tree to determine which gave the most accurate and consistent results. Each was modified and expanded after each of four blind evaluations and the first two demonstrations (described below).

The first step in developing these logic trees was to compile a table (Table 2) based on published photo-interpretation keys from Liang et al. (1951a, b, c, d, e, and f), Way (1973), Rinker and Corl (1984), and Gerrard (1988). Table 3 is a portion of the Rinker and Corl (1984) table we used for the compilation. These reference tables describe each landform’s appearance and drainage pattern characteristics as seen on imagery and provide information on the materials that comprise the various landforms. We devised the logic trees to use the fundamental landform feature–constituent relationships defined in these tables.

Table 2. Portion of the table we devised from multiple sources that formed the basis for our logic trees.

Drainage pattern	Landform	Level I attributes	Level II attributes	Level III attributes	Tone	Land use	Material type
angular dendritic; medium texture	hills and ridges, irregular, connected	massive	bold, steep-sided hills	small pits and depressions	light gray tones with minor mottling; white-fringed gullies	cultivated, irregularly-shaped fields; wooded; cohesive materials	dolomitic/cherty limestone (humid)
dendritic	hills and ridges, irregular, connected	branching ridges	stepped slope changes and angular contours; sharply defined shadow tones	steep slopes, talus at bases of slopes; conical hills or plateaus			andesite (arid)
discontinuous	hills and ridges, irregular, connected	massive	smooth rounded forms; primarily as lowlands and valleys	depressions may be present			marble
parallel	plain, horizontal to near horizontal	level or gently sloping plain near sea level; broad, shallow, tidal stream channels	open tidal flats, swamps, and drainage ditches		light to mottled in clear areas; dark where forested	generally cultivated or heavy forest cover	sand, silt, clay - young coastal plain
radial; fine texture	hills, unconnected	shield-shaped hills that can be very large often with deep, steep-sided, rounded depression at the top			dark tone		basalt
rectangular; well-integrated; closely spaced, parallel gullies with few branches; fine to medium texture; structural control	hills and ridges, rolling	undulating terrain, low ridges alternating with shallow depressions; moderate to high relief; steep, convex slopes	smooth, rounded hills and ridges (ridges may be razor-sharp where glaciated)		uniform light grays; gullies dark-toned; possibly banded	rolling hilltops cultivated; steeper slopes forested; contour farming may be practiced; deep soils	schist
trellis with some parallelism if regional slope uniform; fine texture; often meandering	hills and ridges, irregular, connected	parallel ridges	asymmetrical straight ridges with sharp, saw-toothed crests; stair-step topography where gently dipping		definite parallel banding; limestone is brightest, followed by sandstone and shale	scattered grasses and scrub, occasionally concentrated along outcrops of water-bearing rock	tilted, interbedded sedimentary rocks (arid); shale can form conical hills; limestone is the ridge-former if present - if not, sandstone

Table 3. Portion of the landform tables from Rinker and Corl (1984) showing the details for some plains landforms.

Landform	Attributes	Drainage		Tone	Land use	Material type
		Plan	Cross section			
Plain, horizontal to nearly horizontal	level or gently sloping plains; jagged or lobate well-defined boundaries that can be very steep or stepped; mesas or plateaus, with some pear-shaped appendages; talus common at bases of slopes along boundaries; strongly vertically jointed; vertical escarpments; columnar jointing along major streams	parallel regionally; poorly developed, coarse texture	box-like, but with few gullies	dark tone with scattered light spots common or light; flow marks or blisters may also be visible	generally barren in arid or semiarid climates; intensively cultivated with rectangular and square field patterns in subhumid, humid, or tropical climates; highways follow straight lines and grid patterns	lava flows - darker tone indicates basalt; lighter tone, rhyolite or andesite
Plain, horizontal to nearly horizontal	flat with some surface irregularities caused by abandoned channels; natural levees slightly elevated; slackwater deposits in lower areas; terraces may occur along valley walls	meandering; major drainage channel that meanders through the valley bottom or is braided; many undrained swamps and ponds may produce deranged pattern; in arid/semiarid regions, patterns may not be apparent	varies; local changes in tone indicate surface irregularities; broad level areas will be uniform light to dark gray	varies, indicating well- to poorly-drained soils and fine to coarse textures	rich soils with high moisture content; intensively cultivated; where water table high, dense vegetation; in arid regions alkali deposits prevent dense growth	waterlaid materials (flood plains)
Plain, pilted	apparently flat, but with gradual slope away from the highlands; bounded by mountainous areas	braided; many dry, parallel, channels		uniform white or light gray; alkaline deposits have scrabbled pattern	scattered scrub growth in drainage channels; if irrigated, valley fills may be intensively cultivated with vegetables	waterlaid materials - alluvial valley fills
Plain, pitted	circular depressions; gently undulating; alignment noticeable; depressions bowl- or funnel-like with varying depths and symmetrical; transitional boundaries with other sedimentary rocks	discontinuous; circular, point, or short lineal drains; segments of branched drainage; few streams with short, steep gradients; radial around pits		overall light gray, but tone changes between dry and water-filled depressions	roads adjusted; vegetation scattered, isolated clumps; cultivated around pits	limestone
Plain, pitted	flat to gently undulating; non-uniform depressions; numerous pits shallow, rounded (barn sized), non-symmetrical, with some alignment; may be elongate; pits wandering; few valleys	internal; unconnected, poorly developed	valleys box shaped	generally light but speckled; pits are dark toned	grass covered in arid areas; forested or cultivated in humid areas	sand and gravel (glacial outwash); darker-toned areas probably finer-grained soil
Plain, dissected	originally flat plains now dissected; undissected areas appear as flat plains	dendritic; medium texture		uniform light tones with white-laced gullies or dull and uniform without white-laced gullies	cultivated, with square fields and gridded road systems; some tree cover, emphasizing the dendritic drainage pattern in humid climates; grass and scattered scrub cover in arid climates	thick, old glacial till

Detailed Drainage Logic Tree (Drainage 1)

This drainage-pattern tree (designated Drainage 1) was designed with a highly detailed, hierarchical sequence of questions on drainage patterns and drainage densities leading to an identification of material type (Fig. 5). It is based primarily on identification of the two-dimensional (2-D) drainage pattern (e.g., dendritic, pinnate, rectangular) within each mapped landform unit, followed by analysis of relative drainage densities (i.e., high, medium, or low) in each landform occasionally in conjunction with topographic characteristics. Three-dimensional data are sometimes required to make inferences using topographic characteristics. Instances when 3-D is necessary are at the decision points, shown in yellow, on Figure 5.

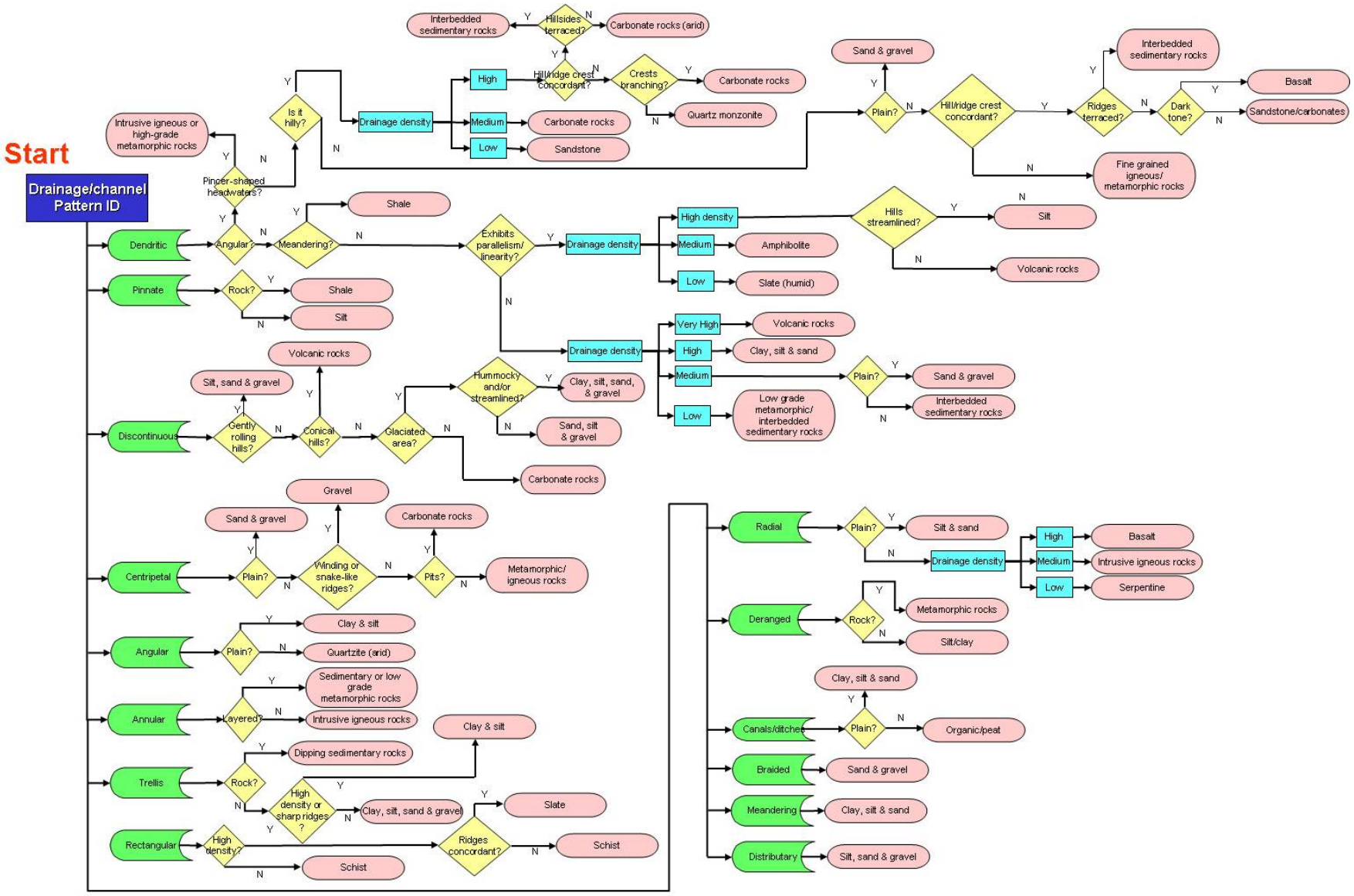

Figure 5. Drainage 1 logic tree.

General Drainage Logic Tree (Drainage 2)

The second drainage-based logic tree (designated Drainage 2) was derived from Drainage 1. The rationale behind this alternate approach was based on the results of initial evaluations of Drainage 1, which showed that several decision points assumed more geologic knowledge than the analyst had and were thus ambiguous. Consequently, the analyst was often misdirected down incorrect paths in the logic tree.

In addition, Drainage 1 focused on rock-type identification and was severely limited where bedrock was not exposed at the ground surface or where its presence could not easily be inferred. To alleviate this problem, we developed Drainage 2, a simplified, less detailed, more generic, drainage-based logic tree, which goes directly from drainage pattern to material type with few, if any, intervening questions (Fig. 6).

There are three key differences between the Drainage 1 and Drainage 2:

1. The number of potential surface material types is reduced in Drainage 2 to minimize potential erroneous inferences.
2. Drainage 2 relies exclusively on 2-D data sources.
3. Drainage 2 assumes that automated image analysis to determine whether or not surface material is bedrock is conducted prior to beginning the inference process.

For a rock surface to be defined, it must be exposed and not covered with vegetation. This is easily done using supervised classification or ratioing (Lillesand and Kiefer 1987, Jensen 1996). The identification of bare rock surfaces is common in land use/land cover classifications as well, such as the Anderson Level II Land Cover classification system (Anderson et al. 1976).

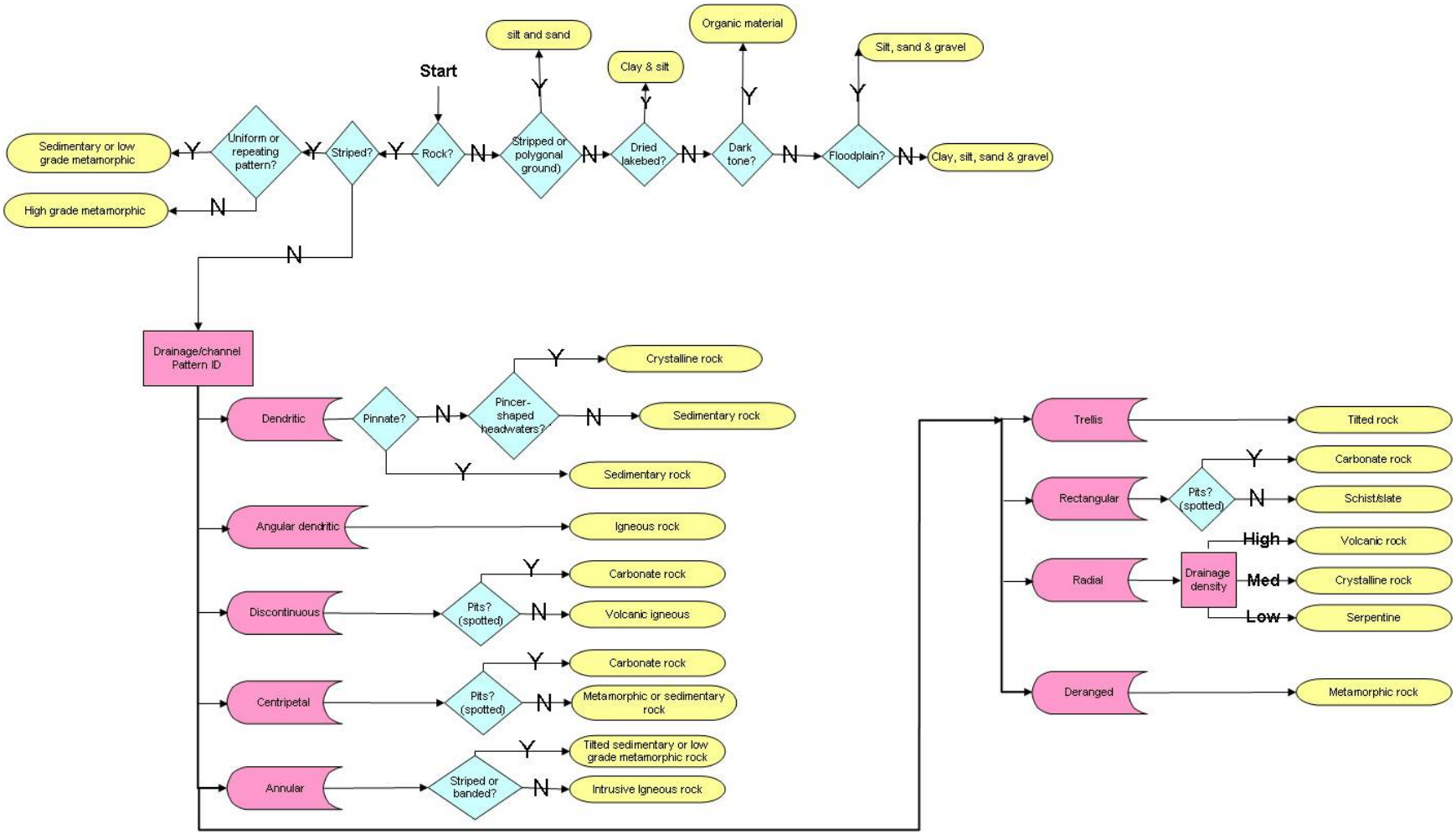

Figure 6. Drainage 2 logic tree.

Landform Logic Tree

The questions in the landform tree do not address drainage pattern but concentrate primarily on the surface features and topographic conditions of landforms and only rarely address drainage density (Fig. 7). This tree allows classification of geologic origin (such as erosional or depositional), slope shape and roughness, land surface characteristics, and material type. These classifications in turn allow predictions of attributes such as internal structure, composition, and surface profiles that can be used to project surfaces and create boundary conditions (see Section 4, below). This logic tree is intermediate in complexity between Drainage 1 and Drainage 2 in that the decision paths are generally shorter and the material types are fewer than in the Drainage 1, but the number of options is greater than in Drainage 2. However, this landform tree can be used less often than either of the drainage-pattern trees because 3-D imagery is required to answer most of the questions it poses, and such imagery is frequently not available. Decisions that require 3-D imagery are indicated by green boxes in Figure 7.

Figure 7. Landform logic tree.

Logic-Tree Evaluations

We conducted four blind evaluations of the logic trees at Yuma Proving Ground, AZ, and Camp Grayling, MI. These sites were selected because:

- Remotely sensed imagery and GIS data layers were available,
- Geologic data to assess the accuracy of our inferences were available, and
- The sites represent the distinctly different terrain and climatic conditions that are needed to evaluate the robustness of the logic trees.

The results of the evaluations iteratively served as guidance on how to refine and improve each logic tree.

Yuma Proving Ground is located at the northern edge of the Sonoran Desert adjacent to the Colorado River in southwestern Arizona (Fig. 8). Our study area is located in the southwest corner of the Proving Ground near the cantonment. It consists of a range of dark-toned hills composed of granite and gneiss that form distinctive landform units on the imagery, alluvial fans of different ages forming an apron along the front of these hills, and a low-lying basin filled with unconsolidated, light-toned, sandy sediments. The climate is arid and the vegetation is very sparse, consisting primarily of small shrubs (Fig. 8). Data available included landform and drainage maps (Fig. 9) (Ehlen 1976), 30-m-resolution Landsat imagery, and a 30-m DEM (Fig. 10).

The Camp Grayling study area is located in northern Michigan, along the Manistee River (Fig. 11). There is a floodplain on both sides of the river, beyond which rise low bluffs composed of glacial moraine. Several lakes are present in the area. The vegetation is Eastern Deciduous Forest, a northern hardwood/conifer mix (e.g., birch, beech, maple, oak, hickory, jack pine, and red pine). Soils are present and are of moderate depth. Data available included landform and drainage maps generated by us for this project (Fig. 12), U.S. Geological Survey (USGS) orthophotos and panchromatic SPOT imagery, and an 11-m DEM (Fig. 13).

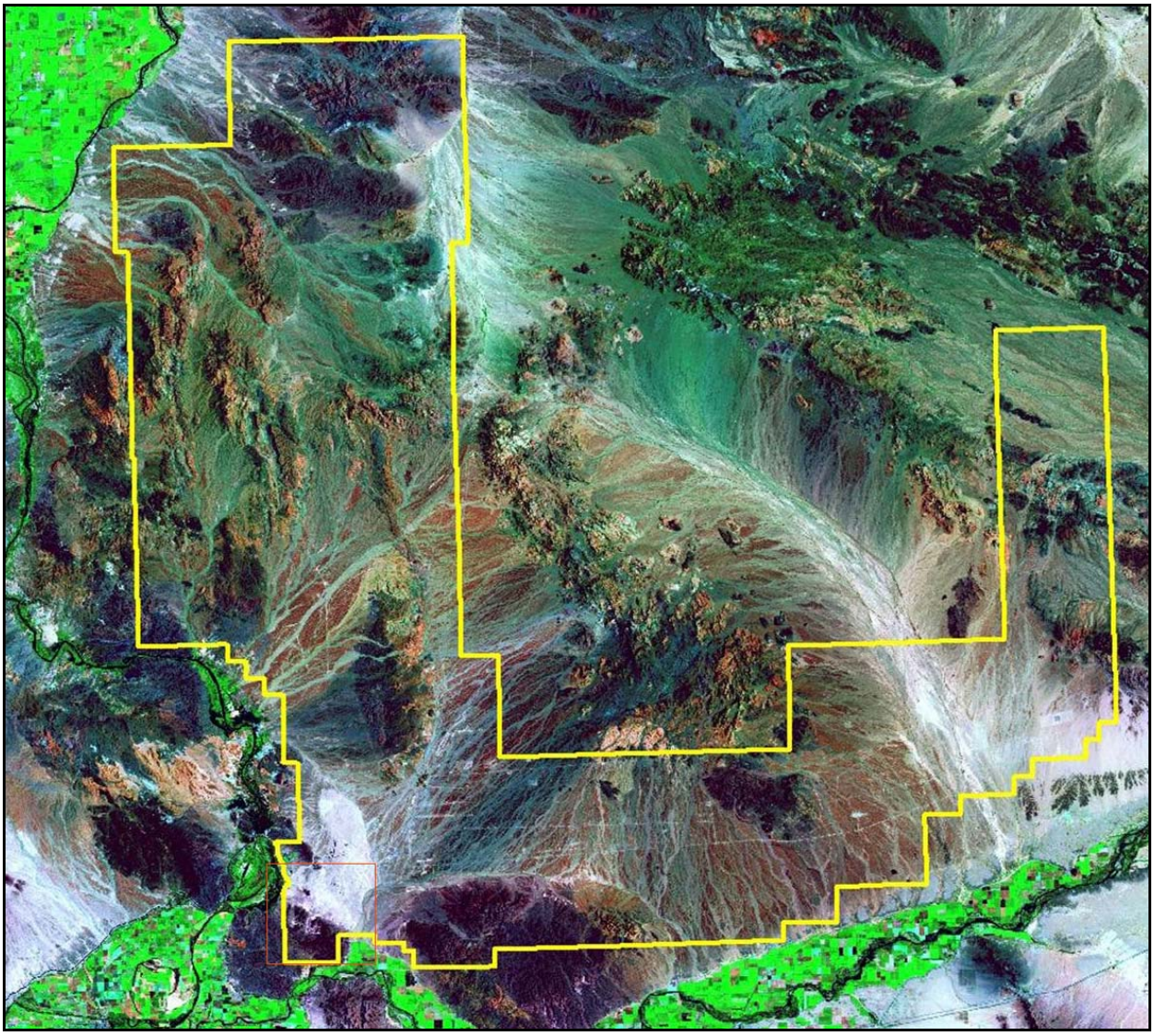

Figure 8. Landsat TM image (30-m resolution) showing the boundaries of Yuma Proving Ground, AZ, marked in yellow. The study area is located in the southwest corner, indicated by the red box.

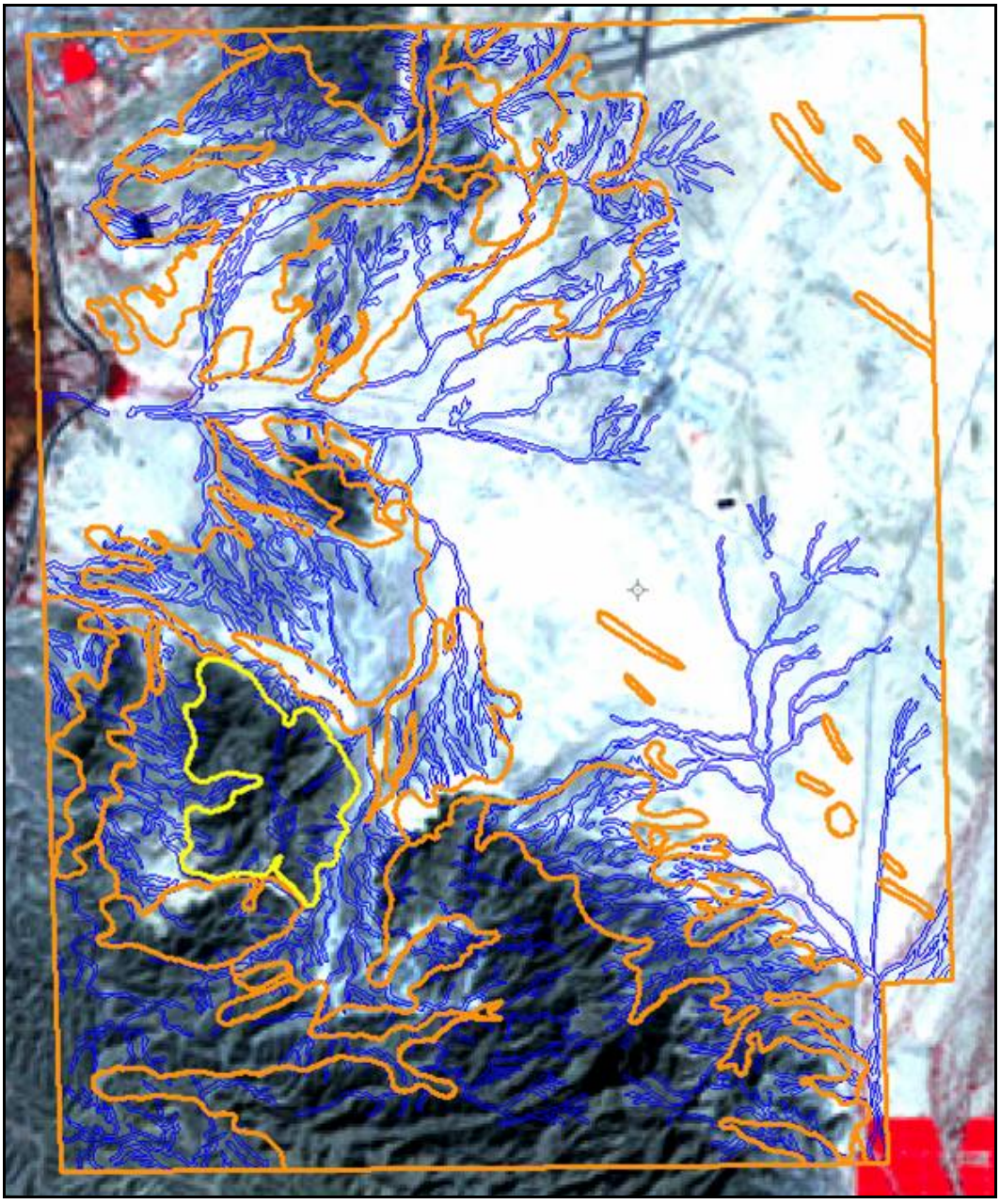

Figure 9. Subscene of the Yuma Proving Ground Landsat TM image with drainage network (blue) and delineated landform (orange) GIS layers; the area outlined in yellow is a landform elected for evaluation. The location of this area is shown on Figure 8 by the red box.

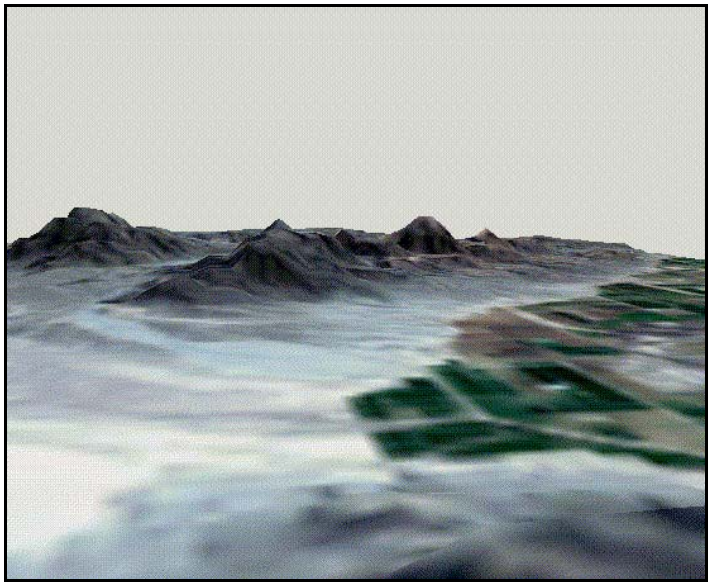

Figure 10. Merge of the Yuma Proving Ground Landsat TM subscene with a DEM to produce a 3-D perspective of the terrain surface. The viewing perspective is from west to southeast .

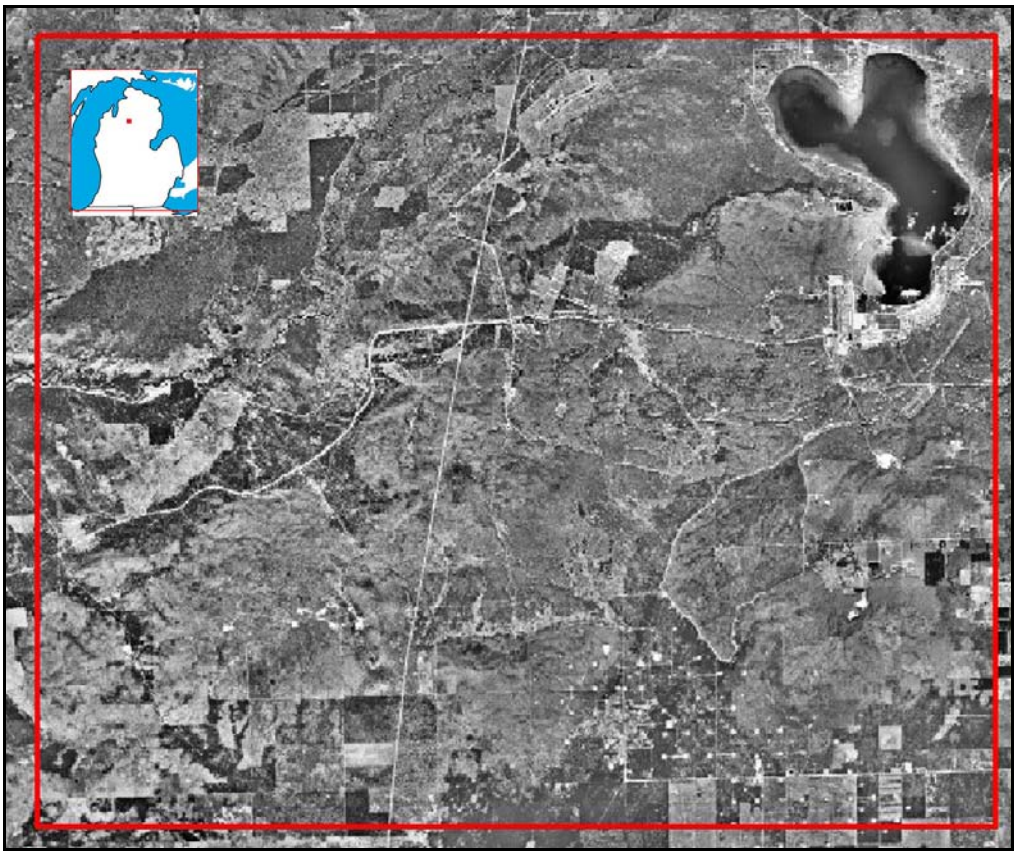

Figure 11. Camp Grayling MI study area and its location.

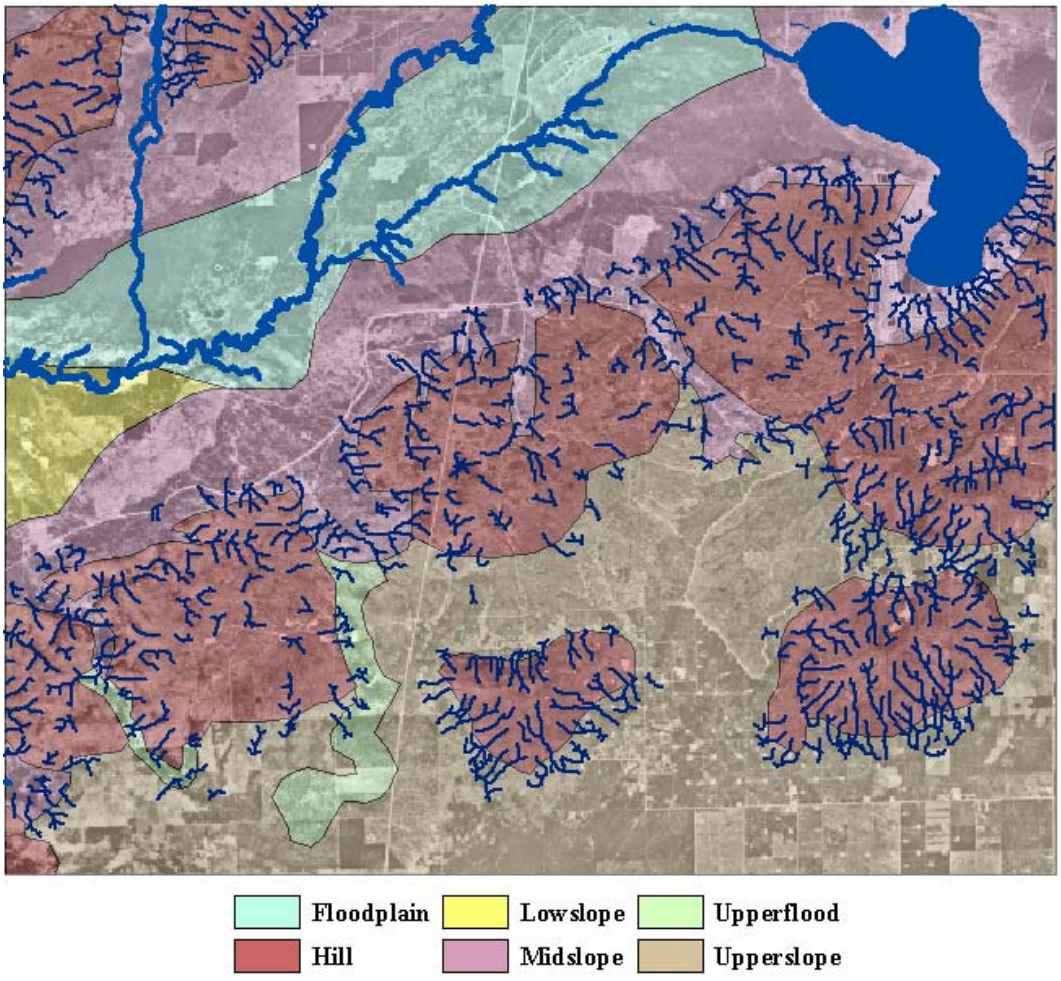

Figure 12. Landform and drainage patterns in the Camp Grayling study area.

During the evaluations, a moderator led the analyst through each logic tree while the analyst viewed selected landform units on imagery. The same landform units were used for all evaluations so that the results could be quantified and compared to determine how the logic tree modifications affected inference accuracy. The analyst could request manipulation of the imagery and the various data layers during the evaluations. We recorded such requests and compiled a list of capabilities our system would need to aid the analyst in making the best inferences possible. These decision aids are discussed in Section 7. Once the analyst proceeded through the logic trees and selected the material type, ground-truth data from the literature or results of field work by a team member were compared to the results to determine the accuracy of the analyst's decisions. These results were then tabulated so that the inferences from the different evaluations could be compared (Tracy et al. 2003).

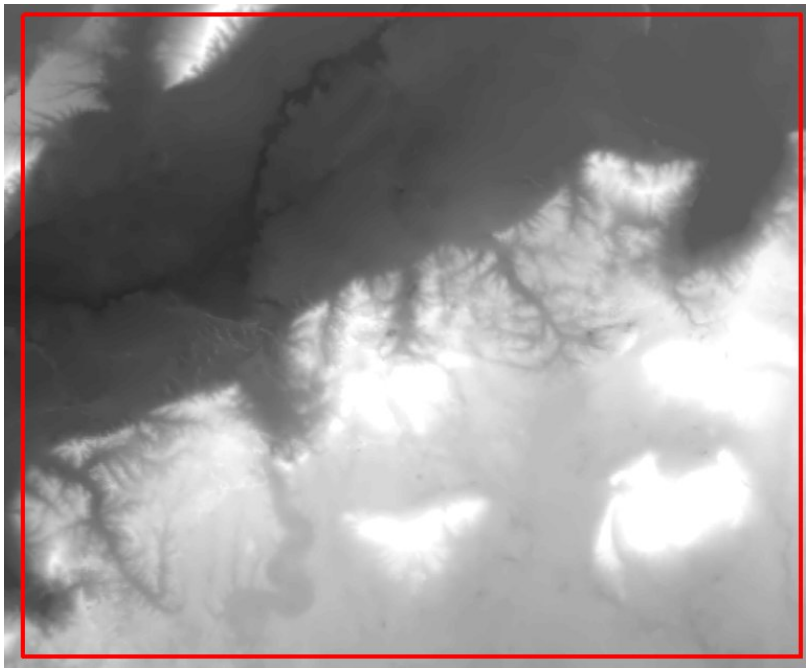

Figure 13. DEM covering the Camp Grayling study area. The original grid cell size has been resampled to 11 × 11 m.

Evaluation One

The first evaluation was done in April 2003, when the authors jointly analyzed a portion of Yuma Proving Ground. It became clear during this evaluation that even with very low-resolution, Landsat multispectral imagery, we could gain a perspective of the region and identify geologic features. We also easily integrated image-processing methods to extract specific physical characteristics of the landscape. The low resolution of the Landsat imagery, however, significantly restricted the level of inferences that could be made.

We compared the evaluation results to ground-truth data from the site (Ehlen 1976), which showed that the landform tree (Fig. 7) performed the best, with about 30% accuracy. Analysis of the evaluation results also showed us that some of our terminology could be confusing to the analyst and that ambiguity in some of the questions led to multiple wrong decisions. As a result, the three trees were modified to improve the decision-making process where incorrect decisions had been made.

Evaluation Two

Our second evaluation was conducted in July 2003 after improvements identified during the first evaluation were incorporated. The analysts included a trained geologist with skills in terrain analysis and image interpretation procedures, and a technician with a military background and extensive field experience but no formal geology background or experience in terrain analysis or image interpretation. The geologist analyzed the same portion of Yuma Proving Ground used in the first evaluation, and the technician analyzed this area as well as a portion of Camp Grayling.

During this evaluation, Drainage 2 achieved greater than 60% accuracy, and Drainage 1 and the landform tree achieved less than 20%. We again modified the three logic trees where problems were encountered or anticipated based on the "flow" of the evaluation. In many cases, errors and misleading questions could be foreseen as the evaluation progressed. Generally, these resulted from oversights we made during logic-tree development; minor alterations prevented future incorrect decisions. Although many of these changes could not be made mid-course during the evaluation, all steps were documented and evaluated post-evaluation, and corrections to the trees were recorded and implemented.

As a result of this evaluation, we determined that many of the decision steps brought the analysts to the correct inference: that line drawings of drainage patterns were useful in reducing selection errors, that the capability to drape a DEM and contours over an image aided in evaluating landform shapes, and that capabilities for viewing the image in 3-D, rotating it, and viewing it with the polygon of interest overlaid were very useful in answering many of the questions in the decision process. We also determined that we needed to include the capability to add and drop multiple data layers during the decision process, and that the data layers provided should include information on climate, soils, the global extent of glaciation, the direction of flow of rivers, lakes, and vegetation.

The successful use of the moderator in this evaluation indicated that a storyboard approach* to the inference process would make the analyst

* A storyboard approach involves a graphic, sequential visual script depiction of a multimedia project in which each page represents a screen to be designed and developed and that collectively demonstrate an approach or philosophy. Storyboards are useful for illustrating concepts to customers and checking that the steps of a process make sense once the details are sketched.

more confident while progressing through the decision process. We also found that we needed to:

- Highlight all like landform polygons in a region to make them visible relative to one another;
- Generate a rock-vs.-sediment data layer;
- Provide terrain-variables data layers, i.e., slope and aspect, drainage density, relief ratio, and slope convexity and concavity, to assist the analyst in evaluating landform surfaces;
- Provide a highly detailed, drainage-pattern overlay with the smallest channels shown;
- Provide ridge crest and hilltop data layers as a function of slope and maximum elevation; and
- Include a method to determine ridge-top spacing (e.g., to determine whether ridges are closely or widely spaced).

We also determined that it would be useful to include a variety of images at different scales that can be displayed in 3-D and in multiple vertical exaggerations to allow better definition of landforms and landform conditions to assist the analyst in making topography-based decisions.

Prior to this evaluation we postulated that a military terrain analyst would easily recognize certain landforms such as volcanoes and sand dunes. We called these keynote landforms. This led us to develop a path by which the analyst could bypass the logic trees when a keynote landform was recognized. The goal for having this shortcut was to provide flexibility in the system to allow more rapid inferences of a landform's constituent materials. Also, by using the GIS system the analyst would become more familiar with keynote landforms and gain proficiency in using all elements of the system. We determined during this evaluation, however, that our choices of keynote landforms had to be expanded and that photographs of all keynote landforms should be included.

Evaluation Three

Unfortunately, we were unable to incorporate all of the modifications to the logic trees and develop all the decision aids determined useful during Evaluation Two before Evaluation Three took place in October 2003. We did expand the list of keynote landforms (Table 4). The analyst for this evaluation was a trained military terrain analyst who had the skills and knowledge we expect from users of our fully developed system. This ana-

lyst was chosen as a proxy for the target user to evaluate the validity of our concept. This evaluation yielded 80% accuracy for Drainage 2, whereas accuracies for Drainage 1 and the landform logic tree remained below 20%. Both Yuma Proving Ground and Camp Grayling were used in the evaluation.

Table 4. Keynote landforms.

Arid		Cool temperate	
Landform	Material	Landform	Material
basin and range	basin gravel, sand, silt, clay; range of rock types	esker/esker complex	sand and gravel
lava flow	basalt	pitted outwash	sand and gravel
caldera	lava flows, tuff	kettle/kame topography	sand and gravel
volcano	lava flows, tuff	fluted ground moraine	clay, sand, gravel
sand dunes	sand	drumlin	clay, sand, gravel
deflation basin	fine sediment	end moraine	clay, sand, gravel
alluvial fans	sand and gravel	sink hole	limestone/dolomite
playa	silt, fine sand	disappearing streams	limestone/dolomite

We noted that many of the terminology problems encountered earlier had been eliminated, and because the user had considerable familiarity with the operating platforms and capabilities, prompts with respect to data manipulation that could aid in a decision could be eliminated. This analyst was able to easily identify the landforms, progress quickly through the decision process in all the logic trees, rapidly select material types, add and drop multiple data layers during that process, use the data layers provided much more effectively than the previous analysts, use drainage pattern and density drawings effectively, and take advantage of a ridge-line overlay. Consequently, this analyst's inferences were significantly improved over those made during previous evaluations. Unfortunately, because of his high skill level, we cannot determine how much of this improvement was due to improvements to the logic trees we made between Evaluations Two and Three.

One of the critical lessons learned from this evaluation was that material types rather than generic rock or landform names should be used in the logic trees, e.g., the end product should be sand rather than sand dunes; silt, sand, and gravel rather than alluvium; volcanic rock rather than basalt or andesite, and so on. We also determined that the terminology throughout the logic trees had to be illustrated (e.g., we need to include pictures of a pitted plain, a lakebed, etc.) and simplified and that technical terms

should be abandoned except where no alternative is available, e.g., the question should be “Are the hills the same height?” rather than “Are the hilltops concordant?”

This evaluation also emphasized that an automated method to distinguish “rock” from “not rock” needs to be included as a decision aid; that a shaded relief map and terrain profiles would be useful; that the drainage pattern must be delineated to show fine detail in the smallest tributaries; and, finally, that allowing the analyst to view the drainage in just the polygon(s) of interest, in addition to viewing the drainage pattern over the entire area, would assist him in his choices.

Evaluation Four

This final evaluation, in February 2004, was a self-evaluation; the team members were the analysts. Camp Grayling and Yuma Proving Ground were the study areas, and the same procedure was followed as for the previous evaluations. The purpose of this evaluation was primarily to remove any remaining inconsistencies from the logic trees and to make sure that the modifications we made to simplify the terminology for material type were successful and consistent. Again, Drainage 2 performed best, at approximately 80% accuracy; the results for the other two logic trees improved, with Drainage 1 achieving approximately 30% accuracy and the landform tree approximately 60%.

From this evaluation we learned that pictorial examples of different images tones (e.g., light, dark, uniform, mottled) should be included among the decision aids; that we need some form of automated method to distinguish a plain, which we have defined as a surface with a slope of 3° or less; and that minor inconsistencies still exist in the logic trees and terminology. Overall, the three logic trees worked well with the imagery and data layers currently available over the two areas used for evaluation.

Summary

The four evaluations helped us determine how to 1) iteratively modify and refine the three logic trees, 2) make the inferential process more functional and user friendly, and 3) enumerate the types of decision aids that must be available to the analyst when using the fully developed GIS system. The analysts suggested numerous modifications that were incorporated into the logic trees, as well as indicating the need for specific decision aids.

Table 5 lists the decision aids that should be provided to the analyst using the system. The decision aids will enhance the likelihood of the analyst answering the questions in the logic trees as rationally as possible and achieving the correct answers.

Results from Evaluations Two, Three, and Four are shown in Figure 14 with respect to the percentage of correct answers for each analyst and logic tree. It is apparent that the military terrain analyst achieved the highest level of accuracy and that Drainage 2 consistently produced the best results. We believe these results reflect differences in the capabilities of the analysts, with the terrain analyst being the most skilled, as well as the continuing improvements in the logic trees and the development of additional data layers as the need for them was identified.

For example, although the technician and the geologist both took part in Evaluation Two, the technician had drawings of all the drainage patterns from which to choose, whereas the geologist did not. The technician thus produced more correct answers than the geologist using both drainage logic trees. In some cases, there was no way the analyst could have gotten the correct answer, either because it was not included in the logic tree or, even if the correct answer was possible, analysis of the patterns would not have led him to it.

After Evaluation Two, the language in the flowcharts was streamlined, and all answers were changed to material compositions, e.g., sand, silt, and gravel, rather than waterlaid or glacial sediments. (The origin of the sediments is not important for our purposes.) This change increased the number of routes through the logic trees that could lead to correct answers. This evaluation also showed that image resolution could affect the likelihood of obtaining correct answers. For example, although the terrain analyst was following the right path in Drainage 1 to identify granite as the composition of one of the Yuma Proving Ground landforms, he was unable to get the correct answer because he could not discern “pincer-shaped headwaters” in the drainage pattern data layer. A resolution significantly greater than 30 m is required to identify this pattern. This suggests that the different levels of detail in our three logic trees may in fact be appropriate. Low image resolution may explain the poor performance of Drainage 1 in most of the evaluations. This logic tree requires the analyst to choose between many highly detailed patterns, the details of which were not apparent on the imagery used in the evaluations.

Table 5. Decision aids available to the analyst.

1. Ability to interactively move around an image to get a "feel" for the region of interest
2. All data, maps, and views for area available to analyst at all decision points upon request
3. Images and drawings needed at all feature identification points to define a term, illustrate the feature configuration, especially for uniform slopes, parallel ridges, irregularly connected hills/ridges, concordant crests, texture, pitted surfaces, rolling hills, ridge interfluves, angularity, and striped rock patterns (both plan and profile views)
4. Ability to toggle between the polygon of interest and neighboring polygons so the analyst can understand the context of the polygon of interest
5. Ability to add and drop data layers on demand
6. Ability to adjust data layer colors to suit the analyst's preferences
7. The global extent of glaciation
8. A topographic line map layer
9. 3-D visualizations including alternating views using different vertical exaggerations
10. Drainage pattern (DP) and density (DD):
    a. View all DP and DD patterns at once to include line drawings/images of each displayed side by side; when a particular type of pattern can have multiple versions, show all versions
    b. DP in polygon only and/or in neighboring polygons simultaneously or separately
    c. Stream order (automated routine); 1st-order streams if possible or the lowest order detectable
    d. DD using multiple spatial windows (e.g., 3, 7, 12 km^2) as well as map and classification
    e. Direction of flow
    f. Channel pattern, i.e., meandering
11. A shaded relief view, i.e., contour layer view
12. Ability to manipulate imagery:
    a. Multiple spatial scales and spectral resolutions
    b. Access and alternately show high- and low-resolution imagery upon demand
    c. Be able to show alternating views of larger and smaller areas surrounding the polygon of interest
    d. In color and grayscale
13. Ability to develop terrain models:
    a. Ridge-line and hill-top diagrams in plan view; quantifying ridge- and hill-top spacing
    b. Ridge profile view
        - LandSurf or ArcMap
        - Histograms indicating concordancy or lack thereof
    c. Landform slope characteristics:
        - Slope aspect, direction, and angle
        - Slope profile to define uniformity and smoothness
    d. Determine maximum and minimum relief ratios in each neighborhood
14. Illustrate keynote landforms with pictures and drawings prior to polygon analysis
15. Access relational databases and drop-down tables with various formats:
    a. Thickness of weathered material
    b. Total overburden thickness
16. Ability to estimate depth to bedrock:
    a. Slope projection using Matlab
    b. Soil type description including a minimum estimate of depth to bedrock
    c. Vegetation root depth estimation
    d. Location of area relative to glacial maxima
17. Perform unsupervised classification and spectral analyses/band ratioing to differentiate rocks vs. sediment

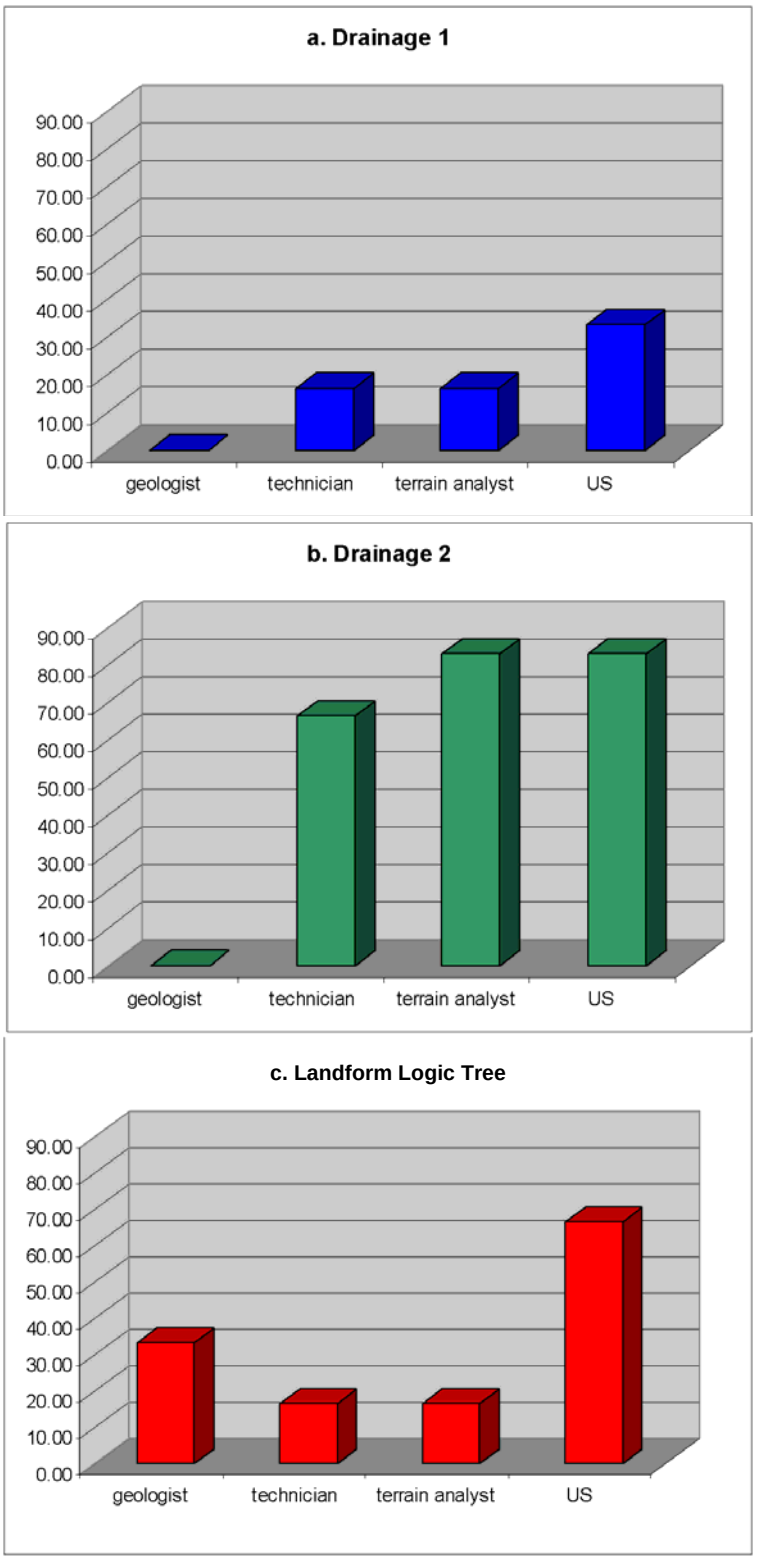

Figure 14. Analyst performance on the three logic trees. The geologist and the technician took part in Evaluation 2, the terrain analyst in Evaluation 3, and team members (US) in Evaluations 1 and 4.

Overall, the evaluations revealed the following. First, it is very important that the user of our GIS system, when fully developed, be a military terrain analyst with some level of geologic knowledge and image interpretation skills. Second, terminology used in the decision process must be consistent and familiar to the analyst. A glossary of terms should be provided. Third, the resolution of the imagery used and the data layers available have a major effect on the quality of the inferences. For example, if stereo imagery is available, the landform logic tree would most likely produce the best inferences. If high-resolution imagery were used, e.g., centimeter or meter resolution, Drainage 1 would be most appropriate. But if only low-resolution imagery, such as that from Landsat's 30-m Thematic Mapper, is available, reasonable inferences can be made using Drainage 2. Fourth, 3-D viewing is required for optimum evaluation of landforms in all of the logic trees. Fifth, automatically extracted drainage patterns usually do not provide adequate detail of the small tributaries, the patterns of which may be crucial for correct material type identification. The capability for the analyst to interactively draw drainage patterns onto imagery or a DEM may be required, rather than depending on drainage patterns as depicted on topographic maps currently available or generated with automatic methods. Such capability currently exists in ArcGIS.

Geologic complexity varies from area to area as well, and the different levels of detail in the three logic trees also accommodate these different degrees of complexity. For example, and assuming comparable imagery and resolution, Drainage 2 would be most effective in simple terrain and Drainage 1 would be applicable in highly complex terrain.

4 GEOLOGIC DISCONTINUITIES AND MATERIAL PROPERTIES

The landform constituent materials inferred by the three logic trees discussed above are required for estimating the seismic properties of the materials and the depths to the boundary between unconsolidated material (overburden) and bedrock and for inferring fracture characteristics, two of the three primary factors needed by seismic modelers.

Depth to bedrock

The true depth to bedrock can only be determined with borehole data or geophysical methods, which require on-site surveys and access. In the absence of such access, a variety of approaches are available to make inferences. Since the depth to bedrock cannot be determined directly from the analysis of imagery, we identified six approaches that could be used to infer or estimate depth depending on regional terrain. These approaches are:

1. Observation of bedrock in incised topographic features,
2. Extrapolation of vegetation root depth,
3. Inference from soil types,
4. Geologic “rules of thumb,”
5. Compilation of data from the literature, and
6. Projection of a bedrock surface into and under adjacent unconsolidated material.

All six approaches have strengths and weaknesses, but each can provide estimates and should be built into a fully functioning GIS system. However, the extrapolations of depth to bedrock from soil types (Approach 3) would require building a database so that estimates based on rock types (Approach 5), slope position (Approach 4), and climate (Approach 4) can be compared and matched to generate the best possible estimate of depth to bedrock.

Approaches 1–5

The ability to observe exposed bedrock in incised slopes such as deep stream channels or gullies (Approach 1) is unlikely at the resolutions and

scales likely to be available. If stereo imagery with appropriate resolution or scale is available, however, determination of the depth of unconsolidated material can easily be calculated using the "three-point" method (e.g., Billings 1954).

Depth-to-bedrock extrapolations using either vegetation root depth estimates (Approach 2) or soil types (Approach 3) may be useful to help constrain an estimate. The use of vegetation root depth is based on the fact that the maximum root depths of certain plants in certain environments are known, e.g., mesquite roots in an arid environment have been shown to reach 30 m. The development of this approach would require an extensive literature search and compilation of look-up tables.

Soil descriptions (Approach 3) may provide ranges of depth to bedrock, which in effect are typically generalized estimates of the depth of soil or unconsolidated sediments. In most cases, the total thickness of the unconsolidated material varies not only with soil type but, more importantly, with landform type and position within a specific landform. A precise landform classification and delineation will include knowledge of the local parent material and weathering processes that influenced the formation of a specific landform unit. Knowing the possible range in soil depth, however, does not necessarily provide a good answer about the depth of overburden, because the soil may be underlain by unknown thicknesses of weathered material. Such materials are not typically addressed in soil depth determinations or definitions (Ehlen, in prep.). Furthermore, maps giving soil depths rarely indicate the type of rock material the soils overlie, information required by our model. Neither Approach 2 nor Approach 3 is thus sufficiently accurate, and both would provide at best only a minimum estimate. If estimation of depth to bedrock from soil type is desired, the only current map that can provide relatively uniform global information is the United Nations Food and Agricultural Organization (FAO) 1:5,000,000 Soil Map of the World (United Nations FAO 1998).

The FAO Soil Map of the World, a compilation of information from about 11,000 maps at a variety of scales from many nations, is available digitally, with a 5-minute × 5-minute cell size, equating to 9 km × 9 km at the equator. Among the information available on the map are World Reference Base soil type, landform classification, slope class, and soil depth profile. Soil depth information is derived from the dominant soil type in a 1° × 1° cell that often does not extend to bedrock. Soil depth is one of several soil

attributes derived for global climate modelers, and as a result, attempts to extract soil texture, profile, and depth information from any one square is unreliable without referencing cautions in the original FAO map (http://daac.gsfc.nasa.gov/interdisc/readmes/soils.shtml). Webb et al. (1991) developed a set of decision rules to provide soil depth per cell, with 360 cm set as the maximum depth to allow more realistic hydraulic modeling. When more than one soil depth was found per cell, they were averaged, and when soil types were missing, information was pulled for the same soil type from another location. When a soil type had no depth information for any location, depth was estimated from a soil type with similar characteristics.

Other global soil maps have been produced, but they are of smaller scale. However, the National Geospatial-Intelligence Agency is reprocessing a 1:1,100,000 U.S. Department of Agriculture (USDA) global soils map that was produced in the 1960s and 1970s, but unpublished, to a global, digital 1:250,000 map using FAO and other ancillary information (McMahon 2003). As of this writing the map has not been released.

Three geologic rules of thumb (Approach 4) based on general observations that have been shown true when applied in a variety of geologic settings may also provide information on depth to bedrock. First, if the area of interest is located in terrain composed of fault-block mountains interspersed with basins, one can assume that the depth to bedrock in the basins is greater than 20–30 m. Because such topography is most common in arid and semi-arid environments, where soil depths are generally shallow in the mountains, one can also assume that the mountains are primarily bare rock with small pockets of shallow soil (0–2 m deep). Bedrock would be deeper in the transitional areas between the mountains and the basins, i.e., on alluvial fans. Second, in terrains where bedrock slopes are far from unconsolidated deposits, such as in wide floodplains along major rivers and in moist tropical environments where deep weathering has occurred, the depth to bedrock is also likely to be in excess of 30 m.

Depth to bedrock is most difficult to estimate in temperate climates and in areas along the margins of past continental glaciers where sediment thicknesses vary considerably. In addition, in areas near and beyond the limits of former glaciation, sediments may also be underlain by significant amounts of weathered bedrock, as noted above. However, a third rule that applies in such areas is that if bedrock exposures are visible, one can

assume that the bedrock is shallow but variable. If no bedrock is exposed, which is often the case, the overlying sediment is usually shallow on the mid-slope positions and convex slopes but deeper on hill or ridge crests, in foot slope positions, and on concave slopes. This third rule is a very broad generalization and does not apply in many situations, such as where landslides are common, but it can provide rough estimates of the relative depth to bedrock.

The published literature (Approach 5) provides abundant site-specific data on overburden thickness, which is defined as the combined thickness of soil and weathered material, i.e., depth to bedrock. Table 6 summarizes such information for granite and gneiss that was gleaned from an incomplete literature search. This table is not complete and was prepared only as a proof of concept. More complete tables could be compiled for all material types in the three logic trees, but that effort would be extremely time consuming and labor intensive. Although this type of information might be useful if nothing else were available, we do not believe it would be sufficiently accurate for use in our model.

Table 6. Example of the type of data on overburden thickness in granite and gneiss that can be found in the literature.

Climate	Position	Mean soil depth (m)	Range (m)	Mean weathering depth (m)	Range (m)
Tropical	hillcrest	3.66	0.5–10.5	65.6	2.4–200
	hillside	3.6	0.5–15	12.7	3.5–55
Temperate	hillcrest	1.5	0.5–2.5	7.5	2.0–13
	hillside	1.8	0.5–3.2	3.6	0.7–9.5
	valley	–	–	45	30–60

Approach 6

Within a region with a mix of landform units such as bedrock hills or mountains and adjacent, sediment-filled floodplains or basins, the depth and orientation of a bedrock surface as it passes beneath adjacent sediment can be predicted or estimated by modeling and projecting the gradient of the bedrock surface into the subsurface. This modeling was our primary effort for estimating bedrock depth because it is the most operationally feasible and is broadly applicable in mountainous areas where sloping bedrock surfaces are exposed (Fig. 15).

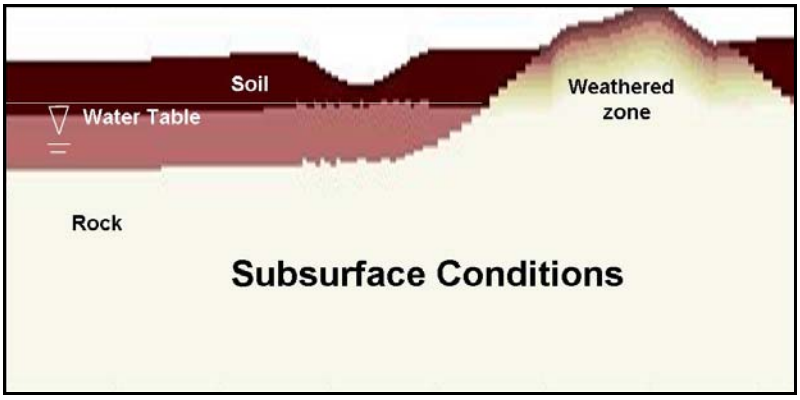

Figure 15. Schematic of a bedrock slope extending beneath unconsolidated sediments.

Our approach is based on the assumption that the slope and shape, including convexity, concavity, and roughness of an exposed bedrock surface, that we observe remain the same in the subsurface. We are aware that this is not always the case, e.g., granite landforms often intersect the surface of unconsolidated materials that surround them at close to vertical, but a short distance below this surface, at a nick point, the bedrock becomes flat; the above-ground slope does not extend to any great depth in the subsurface. However, because such morphological relationships cannot be determined from image analysis, we focused our efforts on devising a method to project the bedrock surface into the subsurface using the above-ground slope, which can be determined.

We used the Southern Boundary Area at Fort Irwin, CA (Fig. 16) to develop this approach. Fort Irwin is located in the Mojave Desert. Our study area consists of hills composed of very-dark-toned basalt as well as some lighter-toned sedimentary rocks. The bedrock hills are surrounded by very-light-toned, unconsolidated, basin-fill sediments. The vegetation consists of very sparse, small shrubs and grasses. As at Yuma, the soil is also sparse and, where present, is very shallow, typically less than 0.5 m thick. A typical hill landform may or may not have bedrock at the surface. In the case of the Fort Irwin study site, a land cover map derived from satellite imagery confirmed that bedrock surfaces existed within specific landforms. This area is thus ideal for our purposes because of the distinct contrast between the very-dark-toned bedrock hills and the very-light-toned basin fill, which allows the boundary between landform units to be very precisely located on the imagery. Furthermore, slopes, particularly in the basalts, are quite steep and contrast well with the very gently sloping basin surface.

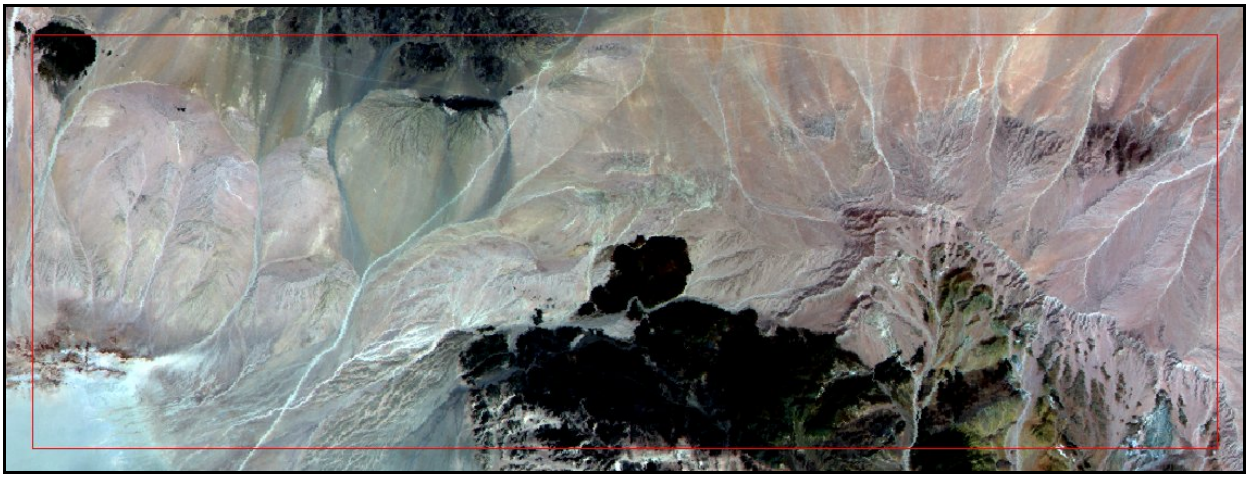

Figure 16. Five-meter-resolution SPOT image showing the Fort Irwin Southern Boundary Area. The study site, outlined in red, is 7 × 20 km in size.

The data layers required for this analysis include a landform map and a DEM derived from IFSAR (interferometric synthetic aperture radar) imagery. An available, good-quality surficial geology map of the Southern Boundary Area with 12 geologic units was used as a surrogate landform map (U.S. Army TEC 1996). We determined that several of these units were very similar with respect to their classification, so we combined them. The aggregated landform map included eight landforms units (Fig. 17). Of these, both the basalt and the interbedded sedimentary rock landform units have exposed rocky surfaces (Fig. 18).

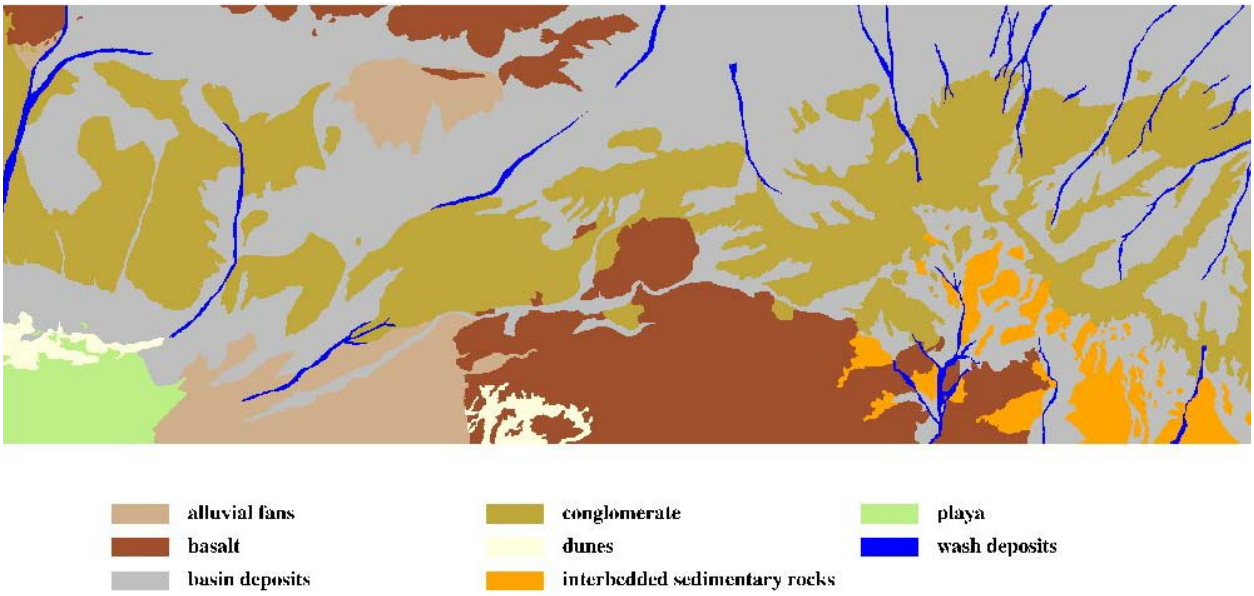

Figure 17. Modified landform map of the Southern Boundary Area derived from an available surface geology map. (After U.S. Army TEC 1996.)

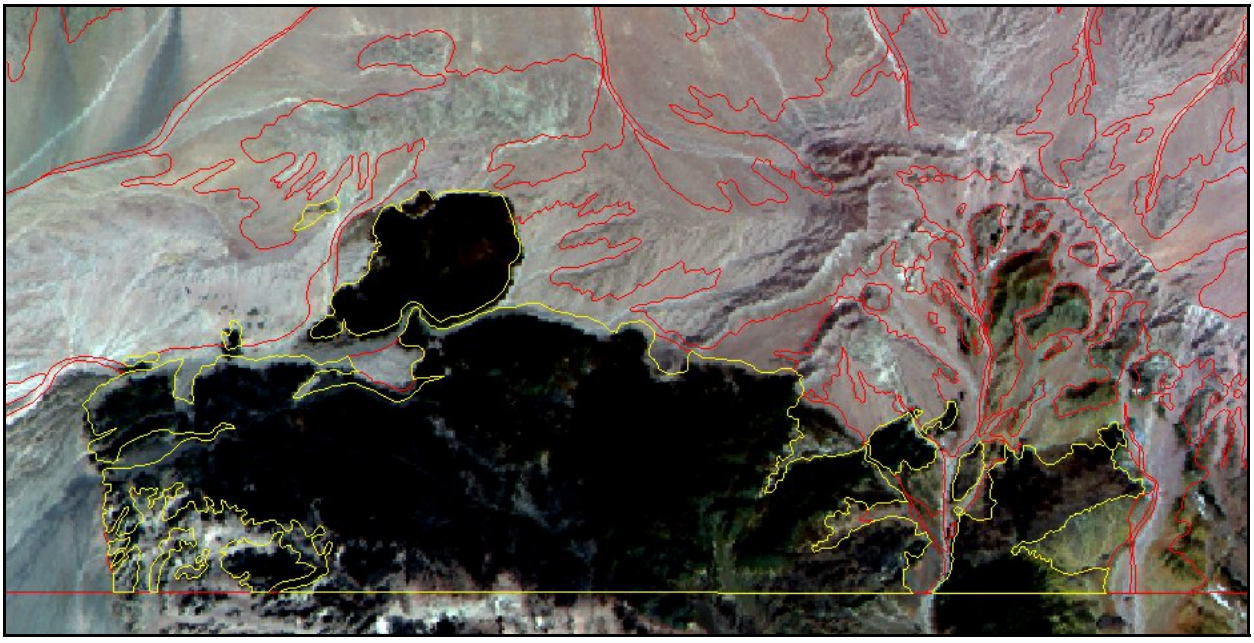

a. Basalt landforms (outlined in yellow), illustrating the dark tones of the exposed rock surfaces.

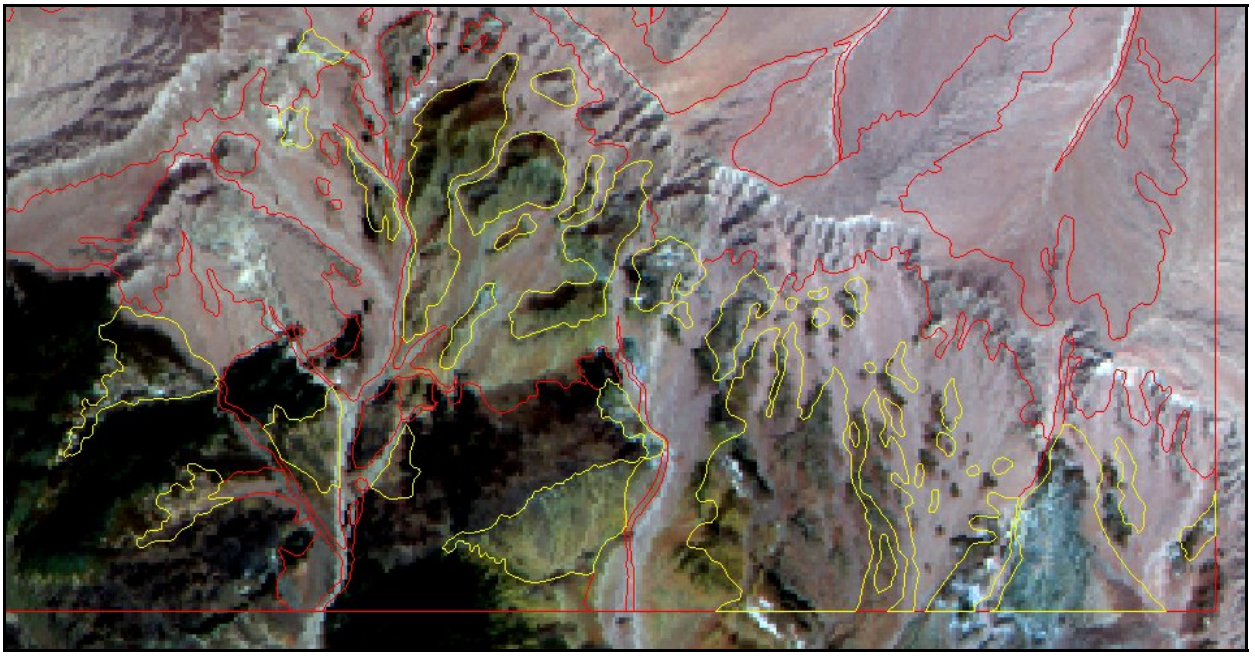

b. Interbedded sedimentary rock landforms (outlined in yellow), showing the uneven tones of the mixed rock types and thin soils.

Figure 18. Maps of sample landform units in part of the Southern Boundary Area.

The basalt and sedimentary rock polygons were used to subset, or clip, the elevation data. Clipping should occur precisely at the point where the hill landform slips beneath the unconsolidated material of the basin.

The output DEM had a spatial resolution of 2.5 m. Such fine-spatial-resolution digital terrain models are typically not available for most study sites. Therefore, the DEM was re-sampled to a 5-m spatial resolution (Fig. 19). We believed this degradation would not adversely impact the precision of the slope projection algorithm and would significantly decrease the processing time, as well as better represent data typically available for other areas. Figure 20 is a shaded relief map of the study area generated from the DEM.

Figure 19. Grayscale image of the IFSARE-derived DEM of the Southern Boundary Area. (IFSARE is IFSAR for elevation.)

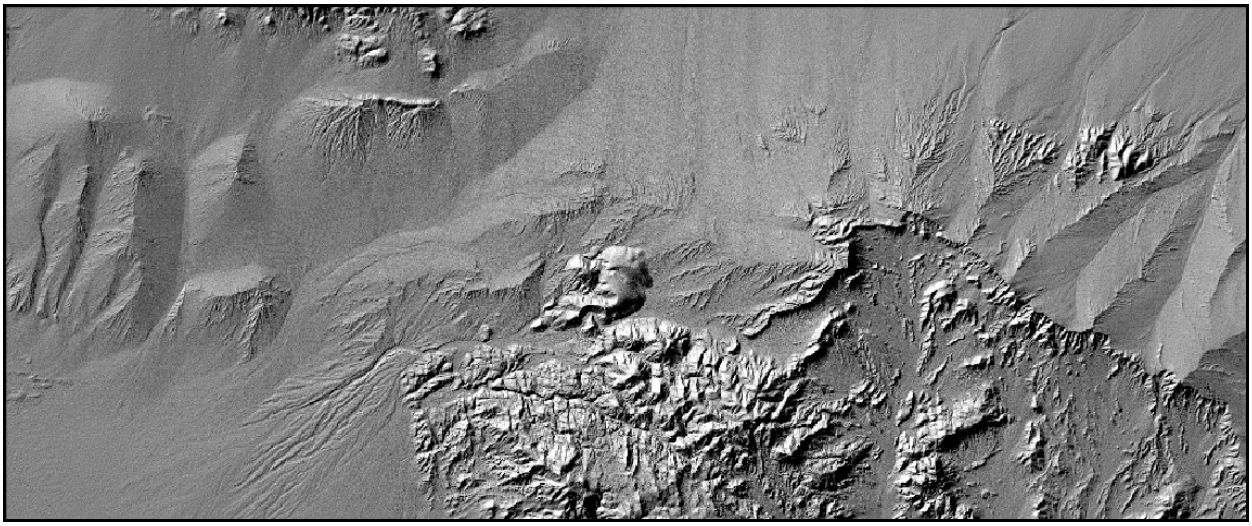

Figure 20. Shaded relief image of the IFSARE-derived DEM of the Southern Boundary Area.

The slope projection algorithm was written using MATLAB data analysis software. The basalt and sedimentary rock landform vector polygons were used to create a raster mask. The mask was then applied to the original 5-m DEM to select only those pixels that fell within the basalt and sedimentary rock polygons (Fig. 21). The masked grid cells (i.e., pixels without elevation data) are now identified as background.

Figure 21. Raster mask created by clipping the original 5-m DEM with the basalt and sedimentary rock landform polygons.

The algorithm proceeds by identifying all background pixels that are immediately adjacent to pixels with elevation data. This is accomplished by searching the four adjacent cardinal grid cells (i.e., up, down, left, and right) for a value greater than 0. For each pixel that is marked as "adjacent," the uphill slope gradients are calculated in eight possible directions (Fig. 22). The gradients are then averaged, and a new elevation value is calculated. Negative gradients are ignored. The routine also ensures that a minimum number of uphill elevation pixels are available for modeling the existing slope. This value can be user defined based on the spatial resolution of the DEM. Finally, whereas the gradient is modeled over the entire length of the existing slope, only the maximum gradient in any given direction is used in the averaging calculation.

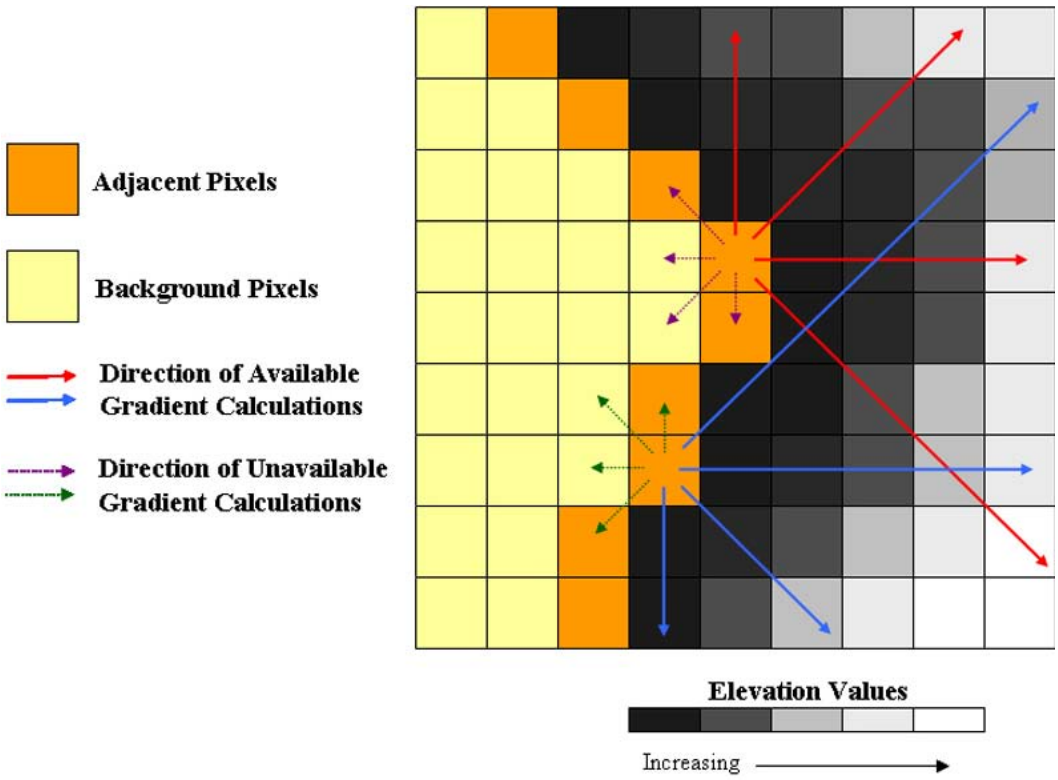

Figure 22. Simplified view of the eight possible directions that are searched for available slope gradient estimations.

The routine progresses through each of the marked pixels, checking for valid elevation values in eight directions, calculating the slope gradient, averaging the maximum gradients, and estimating the new elevation value. After processing the first ring of adjacent pixels, the program identifies the next ring of background grid cells that are adjacent to the newest cells with elevation values. In the current version, the user must set the number of iterative loops required to reach a predetermined projected slope depth. In this effort, the maximum depth is approximately 30 m.

Figure 23a shows the input to the slope projection algorithm. The final product of the algorithm is a DEM with the estimated elevation pixels expanding around the original, clipped DEM (Fig. 23b). Figure 23c compares the original overlay to the projected surfaces.

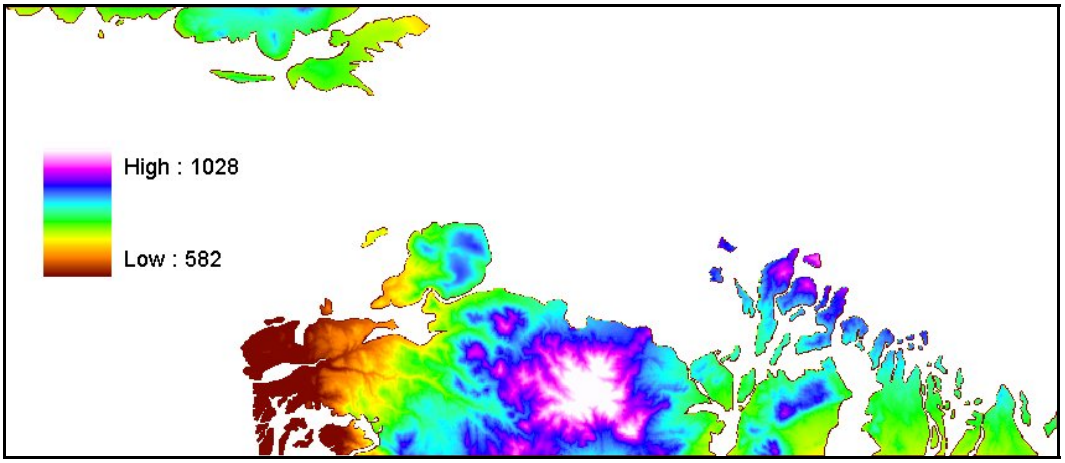

a. Color-coded elevation pixels used as input to the slope projection algorithm.

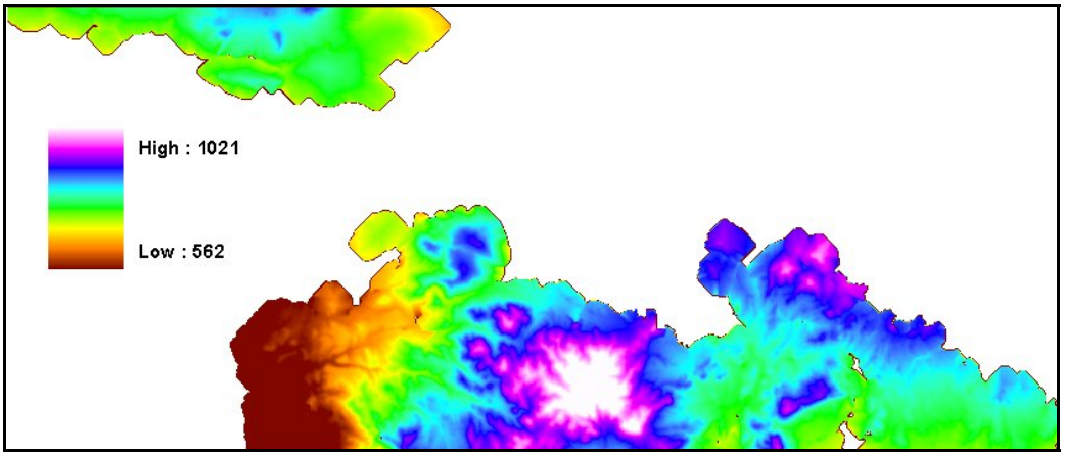

b. Color-coded slope projection algorithm output for basalt and sedimentary rock landform polygons.

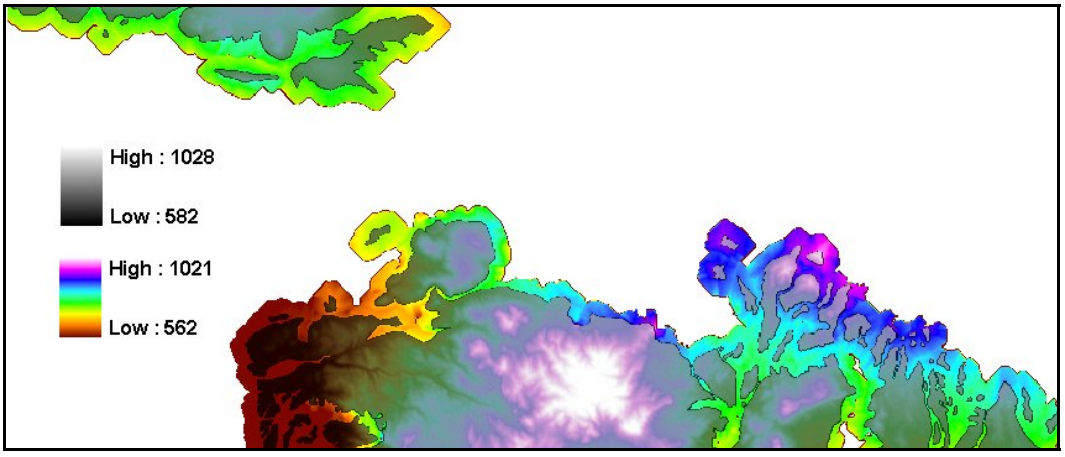

c. Comparison of a and b; the original clipped DEM draped over slope projection algorithm output.

Figure 23. Input to the slope projection algorithm and resulting DEM for basalt and sedimentary rock landforms.

The creation of the actual depth-to-bedrock layer required additional raster processing steps. The projected slope layer depicts a significant portion of the study area with an assumed depth to bedrock greater than 30 m. Therefore, the value of –30 was assigned to all grid cells in the original DEM that coincided with background pixels in the projected slope map. The projected slope layer was then subtracted from this DEM to calculate depths to bedrock estimated to be less than 30 m. These two layers were combined to create a contiguous depth map for the entire study site (Fig. 24a). Figure 24b depicts the detail of the depth estimates along the projected subsurface slopes.

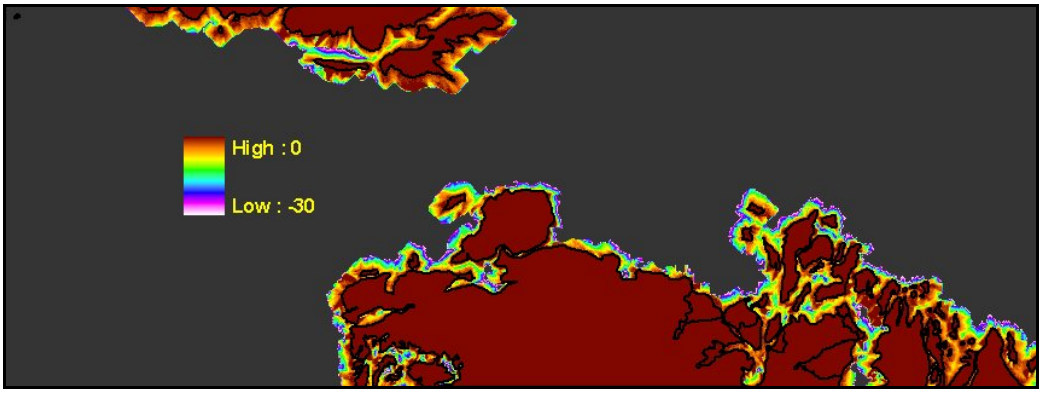

a. Completed depth-to-bedrock layer. The outlines of the original basalt and sedimentary rock landforms are displayed as black polygons. All pixels within these polygons logically have depth values of zero.

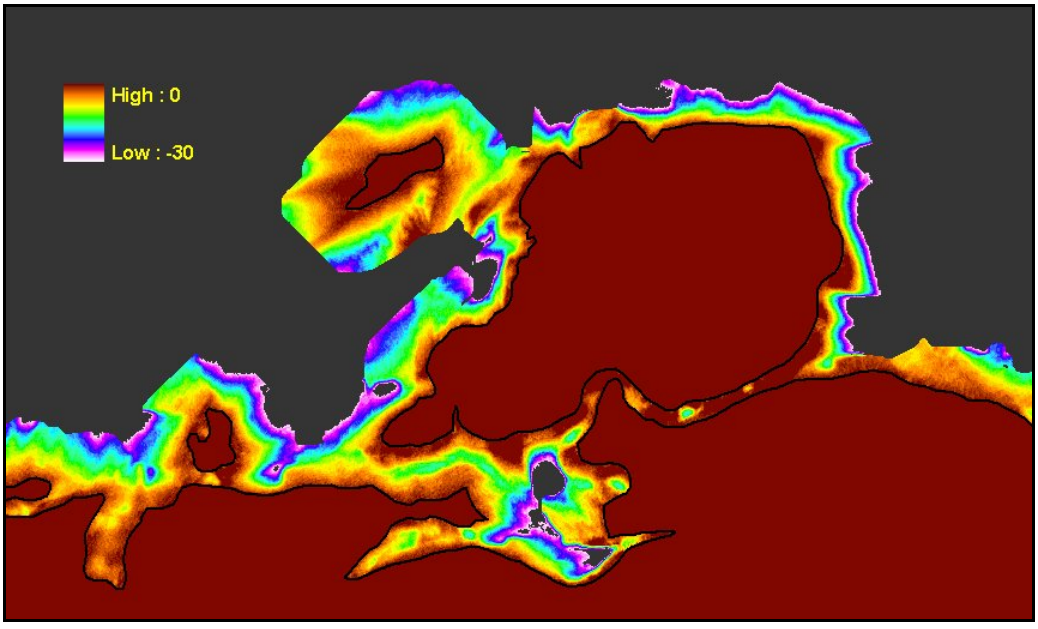

b. Detail of the depth-to-bedrock estimates along projected basalt slopes.

Figure 24. Depth-to-bedrock map of the entire study site.

Finally, the depth estimate for each pixel was subtracted from the original DEM to create a new digital terrain model representing the predicted elevation of the bedrock down to a maximum depth of 30 m. Viewed from above, the semi-transparent landform polygons are draped over the relief map using the heights of pixels in the original surface DEM (Fig. 25a). Figure 25b shows the same area but viewed from the below the ground surface (i.e., looking up into the landform polygons). The angle and orientation of the subsurface slope pixels can clearly be seen.

Overall, the conceptualization and implementation of the slope projection algorithm appear to provide a reasonable estimate of the depth to bedrock in this area. However, there are several shortcomings with the MATLAB code that degraded the accuracy of the final product. As described above, the precise location of the boundary between the bedrock and the basin-fill landforms will significantly influence the accuracy of the predicted depth to bedrock. Therefore, the availability of a highly detailed and accurate landform map will significantly enhance the accuracy of the projected slopes.

Another problem is associated with gaps in the ring of pixels that should be marked as “adjacent.” This initial process is critical since it determines which new pixels will be estimated. As shown in Figure 22, only those adjacent pixels with data in one of the four principal directions (i.e., up, down, left, right) are marked for processing. Background pixels that have only a diagonal connection (adjacent corners) to existing elevation grid cells are not marked for expansion. However, these diagonally adjacent pixels are cardinally connected to at least one cell that has been marked for prediction during the current execution loop and should, therefore, have been selected as cardinally adjacent at the start of the next loop. This was not always observed on a loop-by-loop basis as the code was tested. For example, if the algorithm was allowed to complete 25–30 loops, some pixels that were immediately adjacent to the original real elevation values were never expanded, leaving large gaps in the final product. An investigation into this phenomenon did not yield a definitive reason as to why some pixels were consistently ignored over many loops. The immediate solution was to stop the algorithm after every three to five loops and manually apply a smoothing filter to the projected DEM. This neighborhood operation was applied selectively only to the blank background pixels adjacent to existing valid elevation grid cells. The median of the elevation values within the 3 × 3 window was calculated and assigned to these adjacent

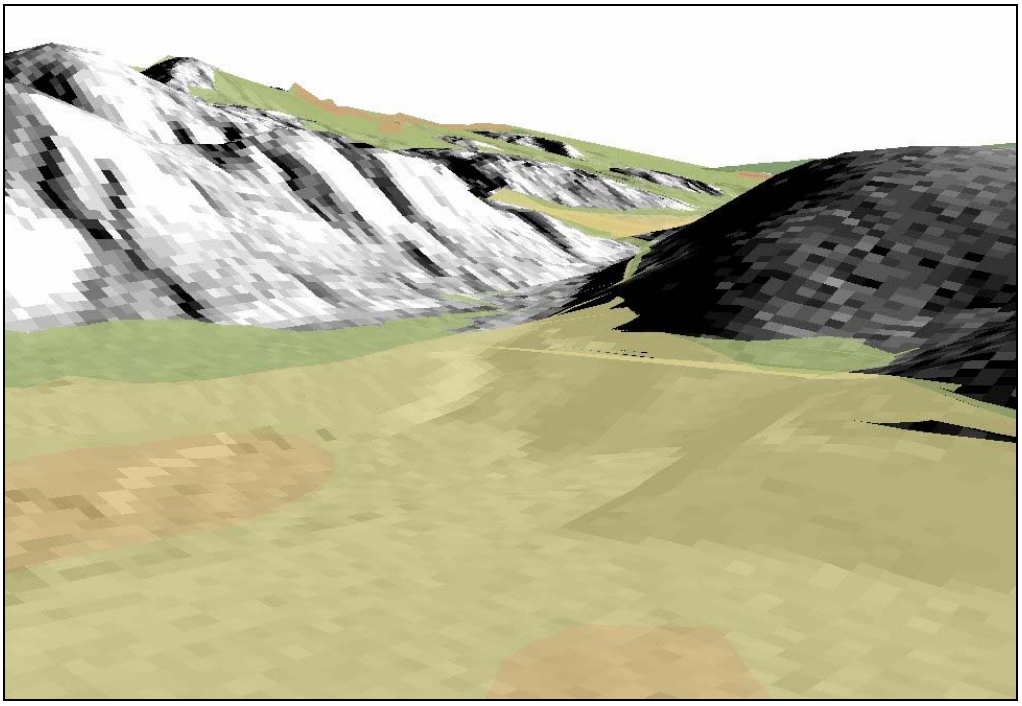

a. Small window of the bedrock elevation model as a shaded relief map. The semi-transparent landform polygons, set at the elevation of the original DEM, are draped over a shaded relief map of the estimated bedrock surface.

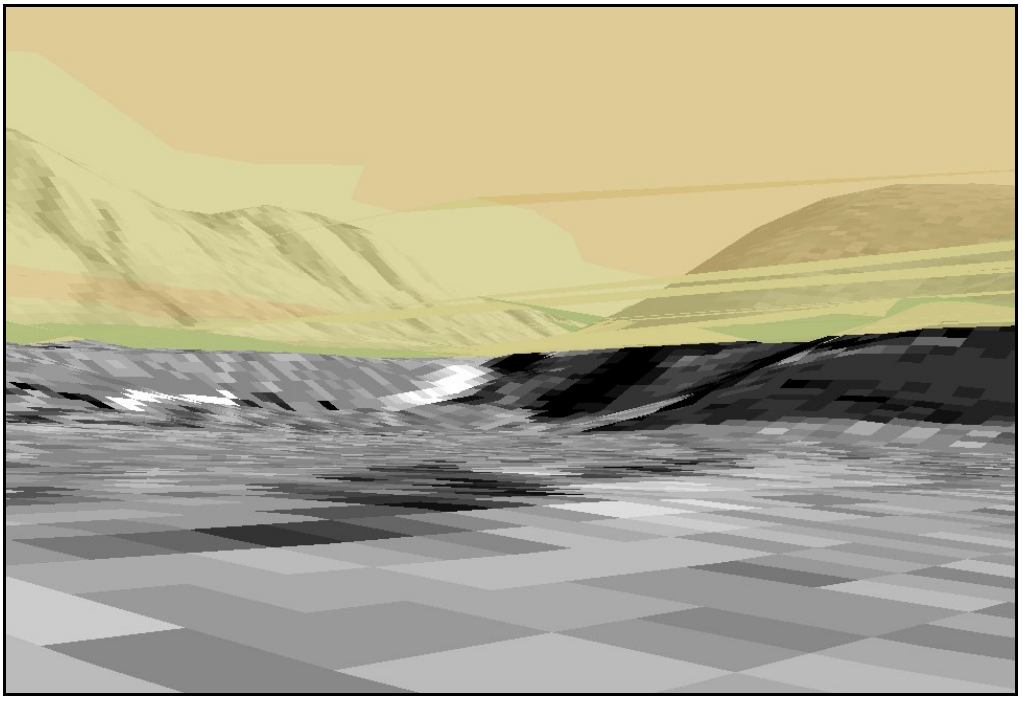

b. View from beneath the semi-transparent landform polygons. The angle and orientation of the projected slope pixels are visualized.

Figure 25. Digital terrain model representing the predicted elevation of the bedrock down to a depth of 30 m.

blank pixels. The manually modified DEM was then run through another three to five loops, and the median smoothing filter was applied again. This iterative process was continued until 30 loops were completed. This somewhat imprecise method was successful in smoothing out the gaps in the modeled pixels, but a more objective and quantitative routine is necessary.

Another computational shortcoming of the algorithm is its inability to compute and track the total depth of the projected slope. This effort focuses on material properties in the upper 30 m of the earth's crust, so the algorithm needed only to estimate the position of the bedrock layer in this relatively shallow depth. The routine does not include steps to determine when the slopes attained a depth of at least 30 m. A simple measure would be to determine the difference between the minimum elevation of the original DEM and the minimum elevation of the projected pixels. When the change in minimum value surpassed a target depth (e.g., 30 m), the algorithm would stop looping, but this only provides the maximum depth of the entire set of newly modeled grid cells. Logically, the steepest slopes would reach the target depth with fewer loops than shallower slopes would need to reach the user-defined minimum depth. The difference between the minimum value of the original DEM and the minimum value for the projected slope map was only 20 m. However, inspection of the elevation values in areas with steep hillsides showed total projected depths well in excess of 30 m. The areas with gentle slopes consistently had projected slopes with depths of less than 15 m. Additional code should be developed to measure and track the depth of the projected slopes.

Furthermore, the modeling of the slope gradient is performed without regard to the profile curvature at the base of the hill. This entire exercise in modeling the orientation and depth of the subsurface slope assumes that the buried gradient is linear. In actuality, the orientation of the bedrock surface will change with increasing depth, generally becoming less steep. This transition may be either abrupt or gentle, depending on the type of material, the climate, and the geologic structure of the area. Therefore, the slope projection algorithm should be enhanced to account for the nonlinear (e.g., concave) tilt of the bedrock surface as it disappears beneath the sediment. Furthermore, it is suggested that the profile curvature of the local terrain at the interface of the bedrock and sediment-filled landforms will influence the shape of the projected slope. These parameters are easily computed using existing raster-based GIS software routines. The inclusion

of this topographic variable into the slope projection model would likely significantly increase the complexity of the trigonometry employed in the current algorithm.

Lastly, in landscapes where soils and vegetation overlie bedrock, the thickness of the unconsolidated layer would have be subtracted from the surface elevation values before projecting the slope beneath the adjacent depositional landform, complicating algorithm development. The precise location of the boundary between two landforms in vegetated terrain would be more difficult to determine, thus making the point where the projection of the slope is to begin less reliable.

Depth to the Water Table

We required a method for mapping the water table that was computationally efficient; required little detailed weather, climate, and local soil information; and provided either annual or seasonal estimates of water-table depth per geomorphic unit. An ideal method would allow us to utilize GIS topographic analysis capabilities to provide better estimates of water-table depth. A search was conducted to locate and assess methods of estimating water-table depth principally using hydrologic models, although we considered using vegetation type, soil type, and other indicators such as surface water levels of lakes and streams as well. Most of the models located were rainfall-runoff models that use weather or climatic information to drive precipitation moisture supply and evapotranspiration losses, and soil information to assess runoff, infiltration, and subsurface flow losses. Some models use detailed deterministic approaches, and others are empirically based statistical approaches with little grounding in physics.

Matson and Fels (1996) reviewed the primary methods of computing water-table depth in areas where measurements are not available. They classified techniques as statistically based, landscape classification based, and deterministically based. Deterministic modeling approaches are most common and the most complex, but they provide reliable results if high-quality information is available to drive the model. Of these techniques, we demonstrate a statistically based approach for approximating water-table depth and apply it to the Camp Grayling area. We also describe a GIS-based deterministic approach that has been applied successfully to watersheds ranging from a few hectares to subcontinental in scale.

Statistical Approach

In general, the most accurate method for determining the vertical distance to the water table is to collect borehole data across the landscape and interpolate the depths between the boreholes. However, unless continuously monitored, borehole measurements provide information from only a moment in time, and they may not be representative of conditions during expected use of the area.

When borehole measurements are not available, other terrain parameters must be used to model the depth to the water table. Generally, such parameters include DEMs, landcover classifications, surface water (streams, rivers, lakes) delineations, and soil series or type maps. Matson and Fels (1996) proposed several methods for mapping the water table using available GIS techniques when well data are unavailable.

Foley et al. (1994) employed a terrain relaxation filter to generate a predicted, unconfined, near-surface water table with an averaging neighborhood filter to relax, or flatten, the surface topography while holding the elevations of surface waters fixed. Their method starts with a 500-m grid cell DEM and a surface waters map. The neighborhood operation, or digital filter, consists of a square matrix of pixels that is passed over the DEM. Using only odd-number-pixeled squares, the average of the elevation values within the filter was assigned to the center pixel. The filter is passed iteratively over the DEM, “flattening” the topography. The grid cells associated with surface waters were held constant during the relaxation filtering.

This method relies on two important assumptions. First, the surface of the water table must mimic the ground surface in that area, and the point at which water appears or flows onto the ground surface must reflect the vertical position of the water table at that location. Using these assumptions, the estimated water table surface can be depicted in 2-D by connecting the points between which water emerges onto the ground surface (D. Perscious, UTD, personal communication, 2002). Multiple 2-D profiles can then be combined, and an estimated 3-D water-table surface can be modeled. This filtering routine was explored within the Camp Grayling study area, with generally poor results. The primary shortcoming was the inability of the neighborhood operation to adequately flatten the topography to a below-surface depth that approximated the location of the actual water table.

Landscape Classification Method

Matson and Fels (1996) suggested a landscape classification approach to estimate water-table depth. This thematic-based scheme defines discrete depth-to-water-table classes or ranges throughout the landscape. These estimates can be based on any available landscape information, such as landform or geomorphic classes, that best characterizes the depth and behavior of the water table. Thus, a complete groundwater-elevation map is generated by simply adding the depth-to-water-table estimate to the GIS database for each landform feature. The availability of published groundwater-depth estimates, in relation to landscape position, is critical to the success of the method.

Matson and Fels (1996) described the application of this method to six physiographic regions of North Carolina. Landscape type and landscape position, such as slope, were used to develop a taxonomic classification scheme based on the relationship between the landscape features and the water-table-depth measurements. Although successful, their results showed that the degree of success depends on the quality of relationships made between topographic features and known water-table depths. And, because the method is empirical, accuracy can easily suffer when the relationships established in one area are applied to another, even slightly different, area.

We developed a variation of this filtering technique by developing an algorithm that employs a soil series polygon map. The average estimated depth to the water table within each soil class was determined for Camp Grayling. By subtracting the published average depths from an existing DEM, a map showing the vertical position of the water table was produced. A neighborhood mean filter was applied to the preliminary depth map to approximate a smooth groundwater gradient between adjacent soil types.

The soils map was provided as a vector-formatted shapefile within a suite of GIS layers for Camp Grayling (Fig. 26). Note that there are missing data in the northeastern and southern sections of the area. Soil descriptions covering these sections are outside of the boundary of Camp Grayling and were therefore not available. Table 7 lists the hydrologic group and the estimated depth to the uppermost-unconfined water table for each of the unique soils series. The hydrologic group codes, A through D, categorize soil infiltration and transmission rates. Group A soils are chiefly deep, well-drained sands or gravels with high water infiltration and transmission

rates. Groups B and C have increasingly higher silt and clay contents with progressively lower permeability and high surface runoff volumes. Group D soils are chiefly clays with high swelling potential and a perched water table. These discrete classes were developed by soil scientists for the Michigan Department of Environmental Quality (Mikula and Croskey 2003). Three combined soil series are also listed with their scaled depth-to-water-table estimates. Other combined series exist but are not listed because the two or more soil types have the same hydrologic group classification and therefore the same depth values. Depth-to-water-table values were extracted from several sources, including Brockway and Nguyen (1986), Kazmierski et al. (2002), and Mikula and Croskey (2003).

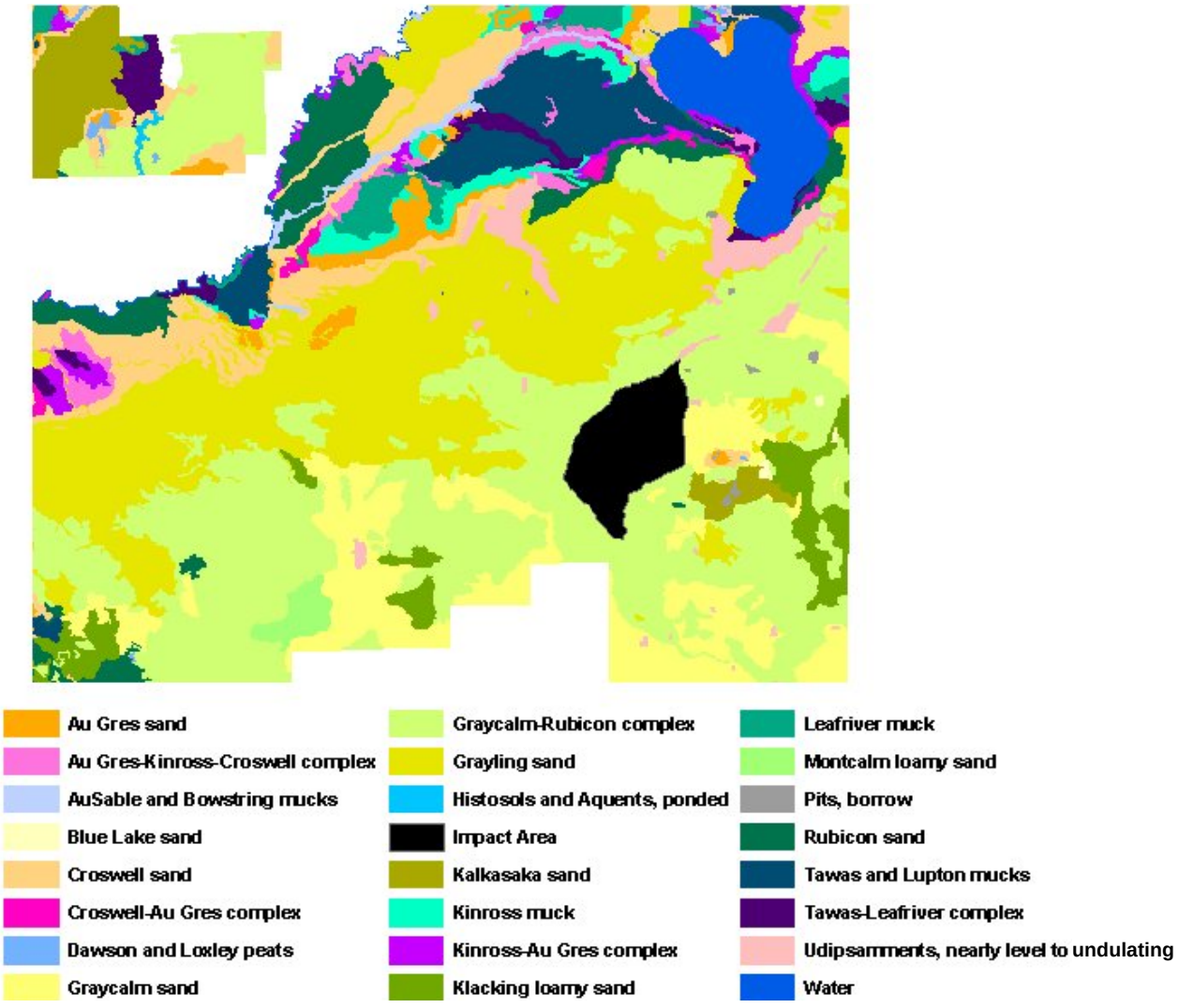

Figure 26. Soil series within the Camp Grayling study area.

Table 7. Soil series, hydrologic groups, and estimated depths to the water table in the Camp Grayling study area.

Soil Series	Hydrologic Group	Hydrologic Description	Depth to Water Table (m)
Croswell sand, Blue Lake sand, Graycalm sand, Grayling sand, Kalkaska, Klacking, Montcalm, Rubicon, generic Udipsamments	A	deep, well-drained sands and gravels	25
Au Gress sand	B	moderately to well-drained sandy loams, loams, silty loams, and silts	15
Au Sable, Bowstring, Dawson, Kinross, Levfriver, Loxley, Lupton, generic ponded soils, Tawas	D	very poorly drained clays with permanent high water table	1
Au Gres-Kinross-Croswell	B-D-A	–	10
Crosswell-Au Gres	A-B	–	20
Kinross-Au Gres	D-B	–	8

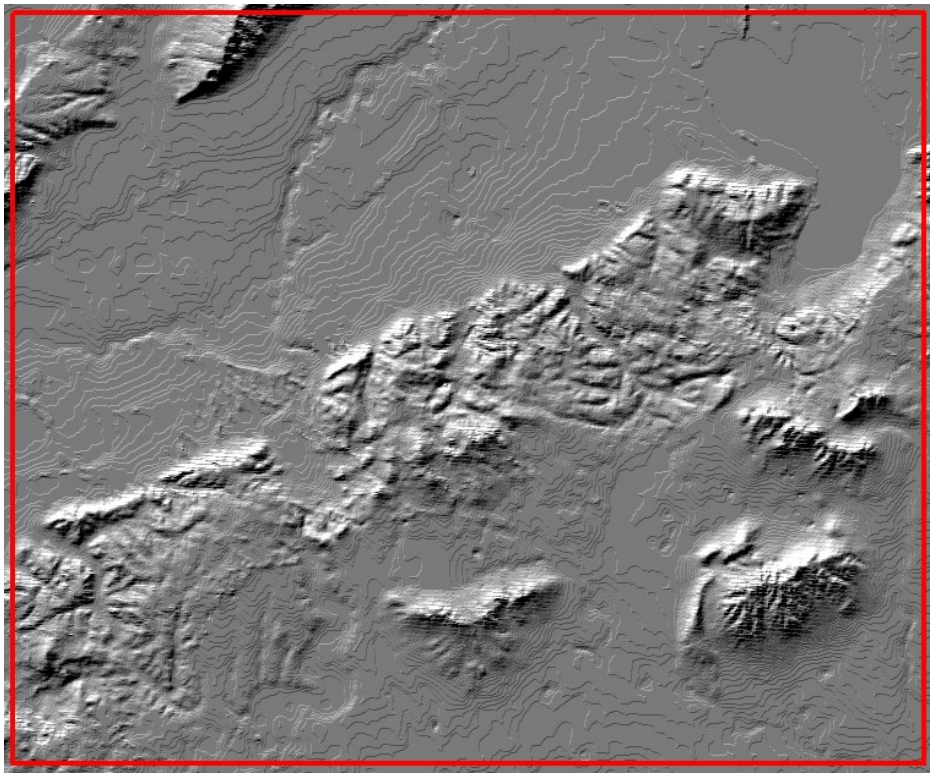

Figure 27. Shaded relief map of the Camp Grayling study area.

The original spatial resolution of the Camp Grayling DEM was 22 m. The data were interpolated to twice the grid cell density, creating a DEM with 11-m pixels (Fig. 13). Figure 27 is a shaded-relief map of the study area at this resolution.

The depth-to-water-table numbers were added as a new field for each polygon in the ArcGIS shapefile. The vector data were then converted to raster format using the same 11-m grid-cell dimensions as the DEM, with the depth-to-water-table integer value assigned to each pixel. At this point, a raster-map layer showing the estimated depth to the water table was available (Fig. 28).

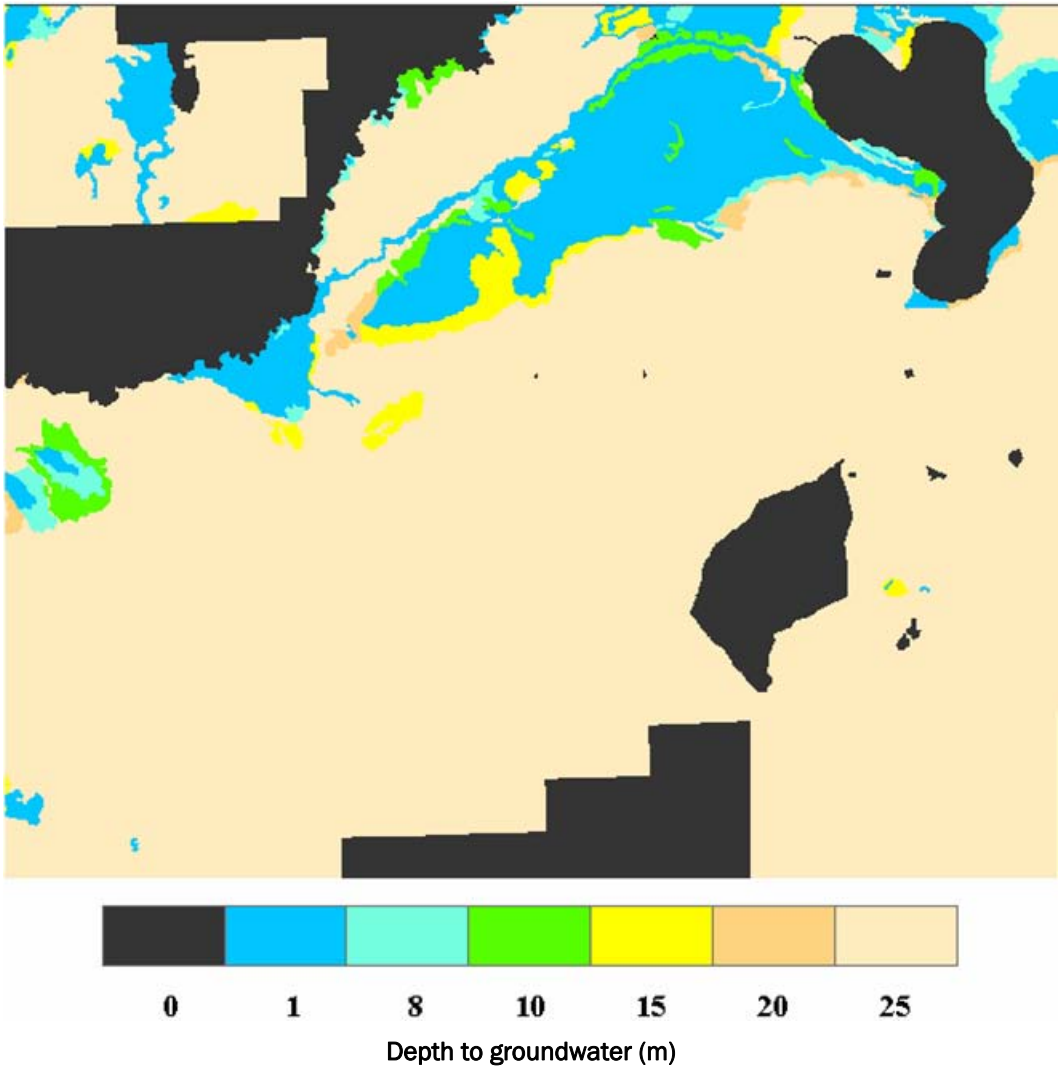

Figure 28. Color-coded depth-to-groundwater estimates determined from the soil series. Estimates are in meters. The black areas indicate where no soil series has been assigned. The irregularly shaped polygon in the center right is an impact area, and the black area in the upper right is Margrethe Lake.

A block diagram (Fig. 29) of a small subset of the study area clearly shows large steps in estimated groundwater depths in adjacent soil types. These abrupt changes in the vertical position of the water table are not realistic;

logically the gradient of the saturated layer between neighboring hydrologic units should be relatively smooth. Therefore, the next step was to smooth the depth-to-water-table raster map using a series of averaging neighborhood operations. Similar to the smoothing filter applied to the depth-to-bedrock projected surfaces, the square pixel matrix was passed over the water-table-depth raster map to create a more realistic groundwater-depth gradient between adjacent soil classes (Fig. 30). Figure 31 shows a block diagram of the smoothed water-table depths.

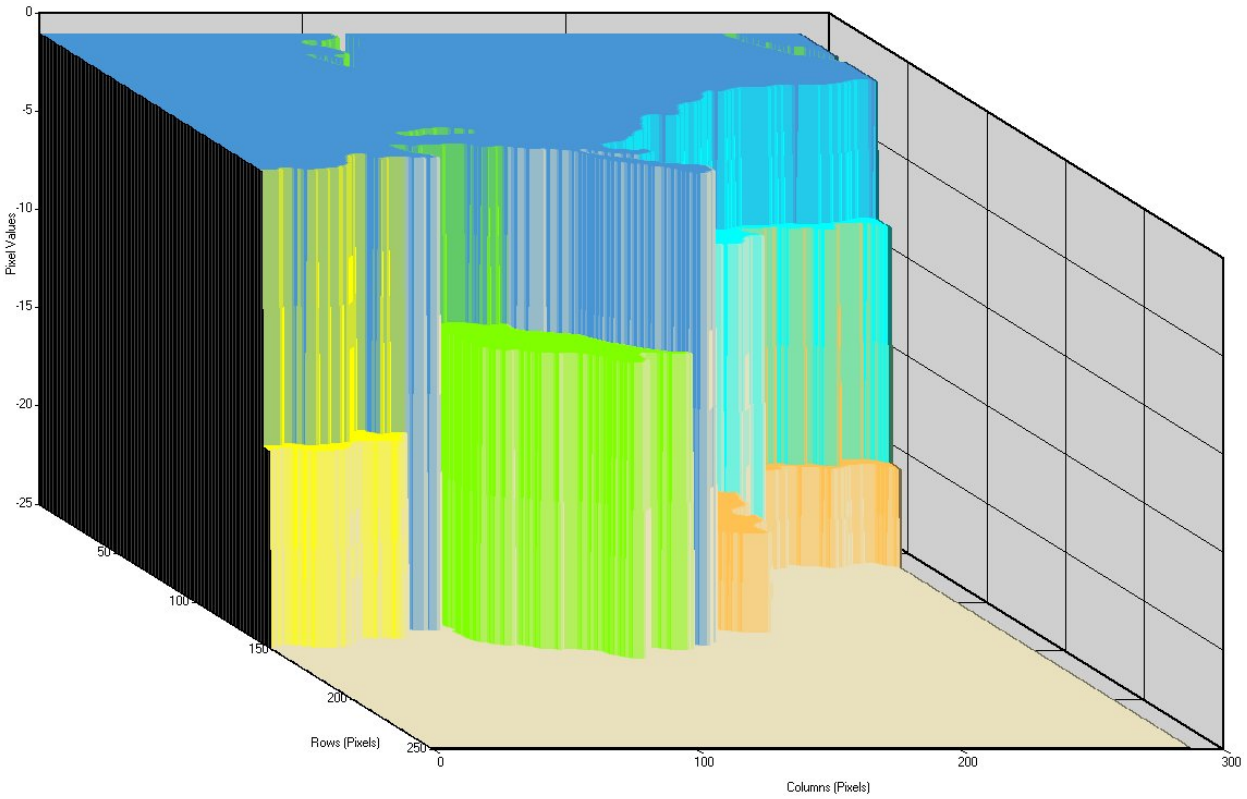

Figure 29. Surface profile of discrete depth-to-groundwater classes. Note the large steps between adjacent depth classes. The depths are in meters.

This enhanced depth-to-water-table map is missing the zero depths coincident with the surface waters throughout the study site. The surface waters were reintroduced using the original rivers and lakes vector ArcGIS shapefiles. The rivers vector data were initially created as discrete-line features. Because line features in vector format are one dimensional (i.e., they do not have area), a line buffering operation was applied to the rivers vectors to produce approximate river polygons. The buffer distance was set to 30 m on both sides of the line defining the location of the river channel.

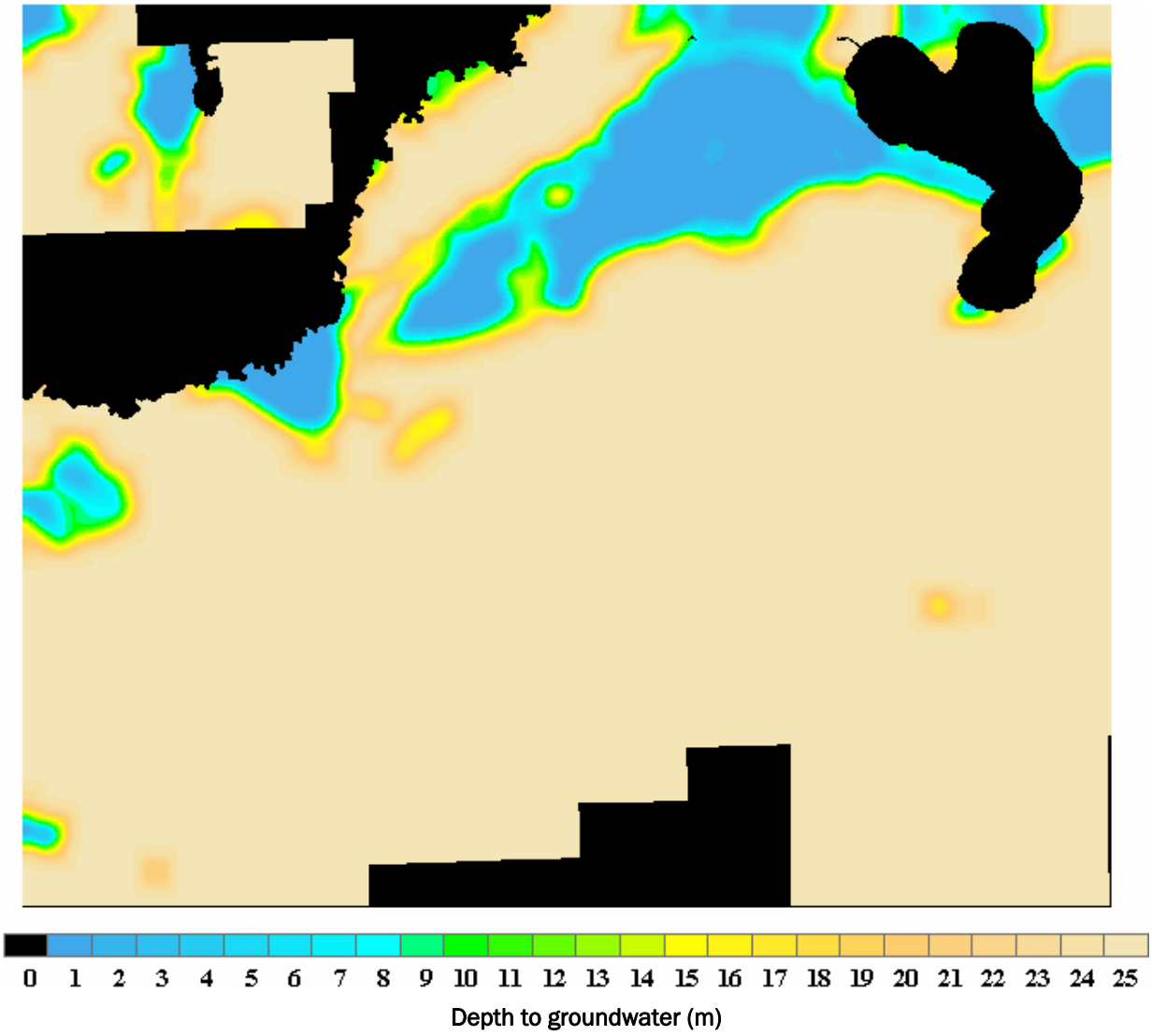

Figure 30. Map view of depth-to-groundwater estimates after application of the smoothing filter.

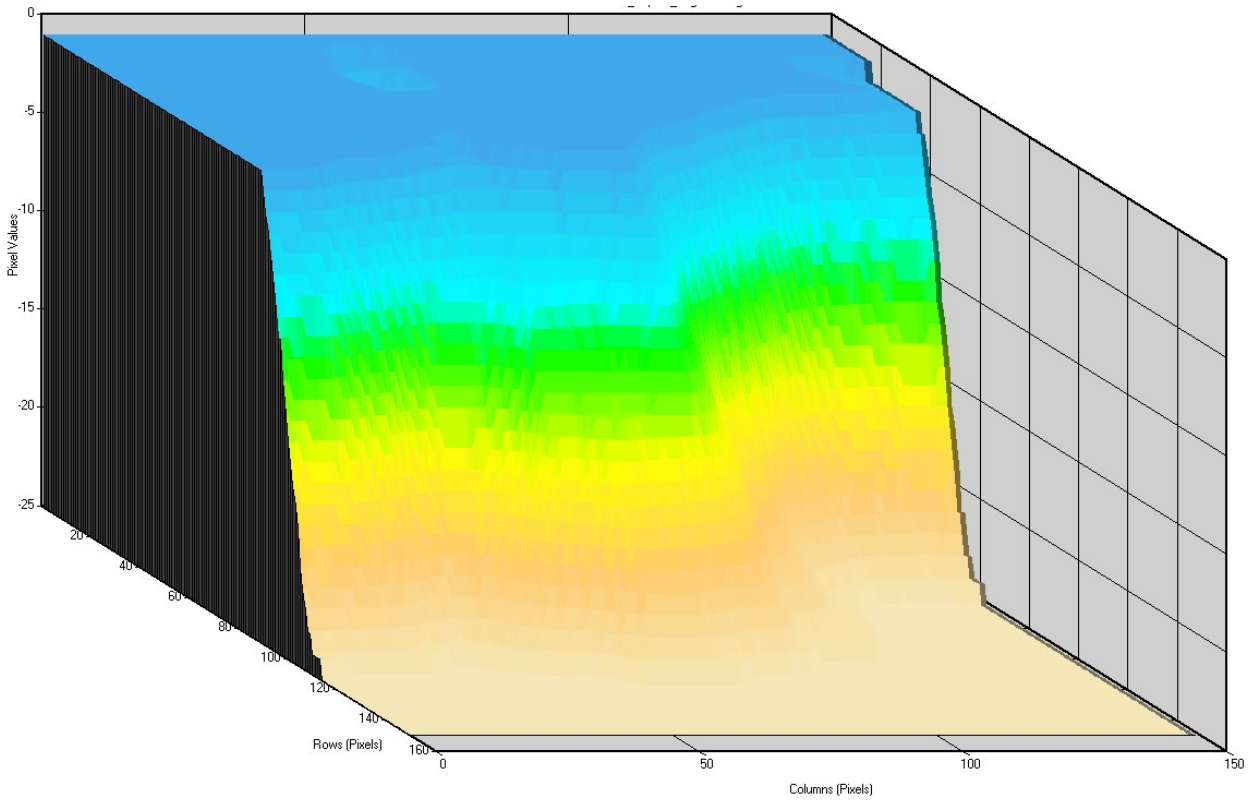

Figure 31. Surface profile of smoothed depth-to-groundwater classes after application of the smoothing filter. Note the gradual, more realistic gradient between adjacent depth classes. The depths are in meters.

The river polygons, now with 2-D area attributes, were converted to raster data with a grid cell size of 11 × 11 m. The 30-m line buffer ensures a minimum two-pixel buffer on either side of the original river channel. The pixels that correspond to the river polygons were renumbered to a value of 0, while the non-river pixels were designated as background with a value of 1. This output file effectively acts as a mask. By multiplying this rivers mask and the depth-to-water-table map, depth pixels that intersect (i.e., overlie) the rasterized river channel are reset to a depth of zero. All non-surface water pixels are multiplied by the value of 1 and therefore remain unchanged. A series of smoothing filters was again applied to remove any large changes in groundwater depths at the interface with the river pixels. Figure 32 shows the results.

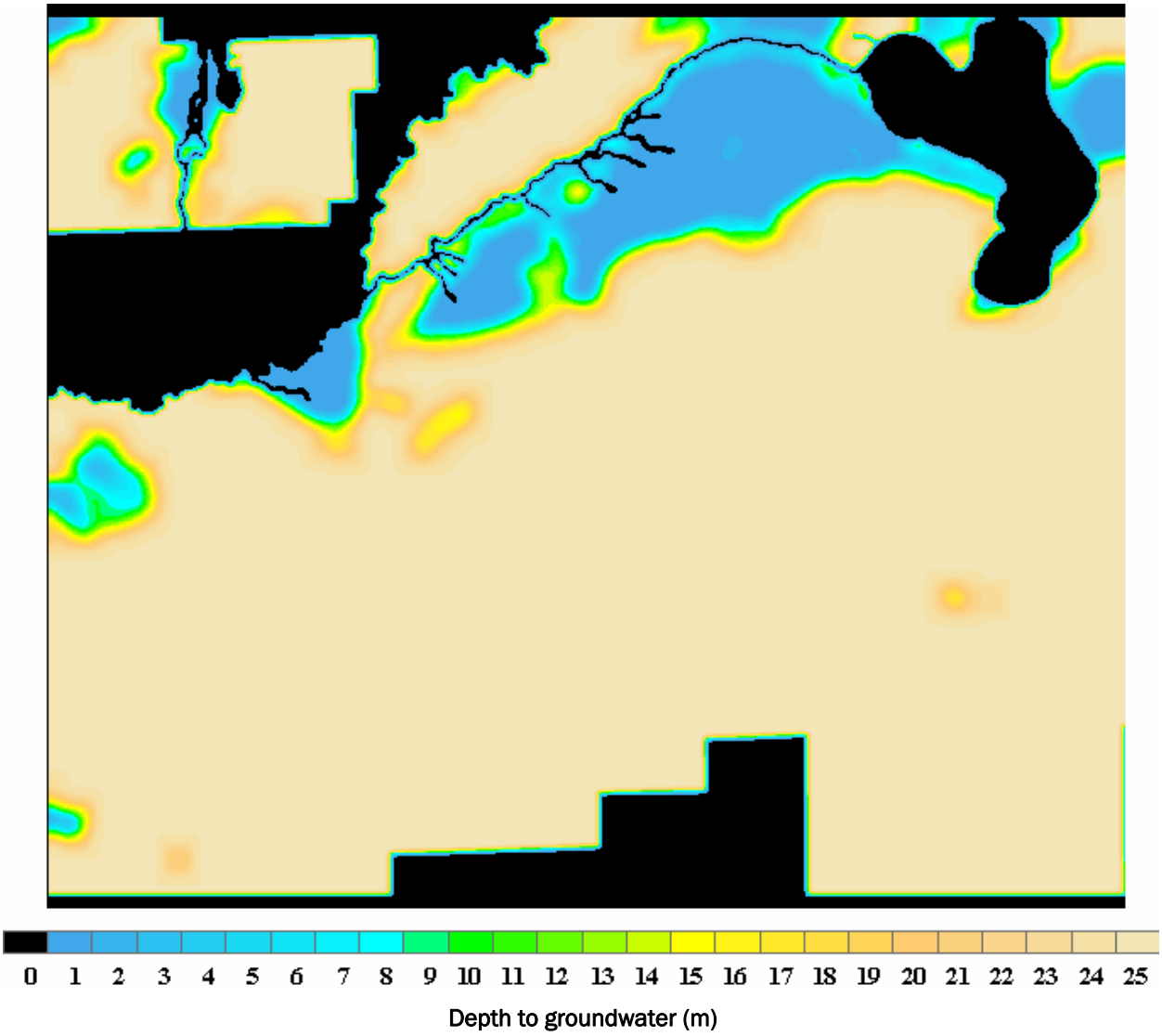

Figure 32. Depth-to-groundwater estimates after overlaying surface-water pixels and applying a smoothing filter.

Lake Margrethe is located in the northeastern corner of the study site (Fig. 11). The pixels associated with this lake had already been assigned depth values of 0 from the soil series map layer. However, a procedure identical to the rivers mask could have been applied to set lake pixels to a groundwater depth of zero.

The next step was to subtract the estimated groundwater depths from the original DEM to create an actual elevation model of the location of the water table. This below-ground DEM (Fig. 33) is similar to the original surface DEM (Fig. 13). However, on closer inspection, this groundwater DEM shows much different subterranean topography, particularly over the

poorly drained soils within the river floodplain. Much of the more complex upland areas, in the central and southern parts of the study area, mimic the surface topography because these soils are uniformly well drained with predicted water-table depths of 25 m.

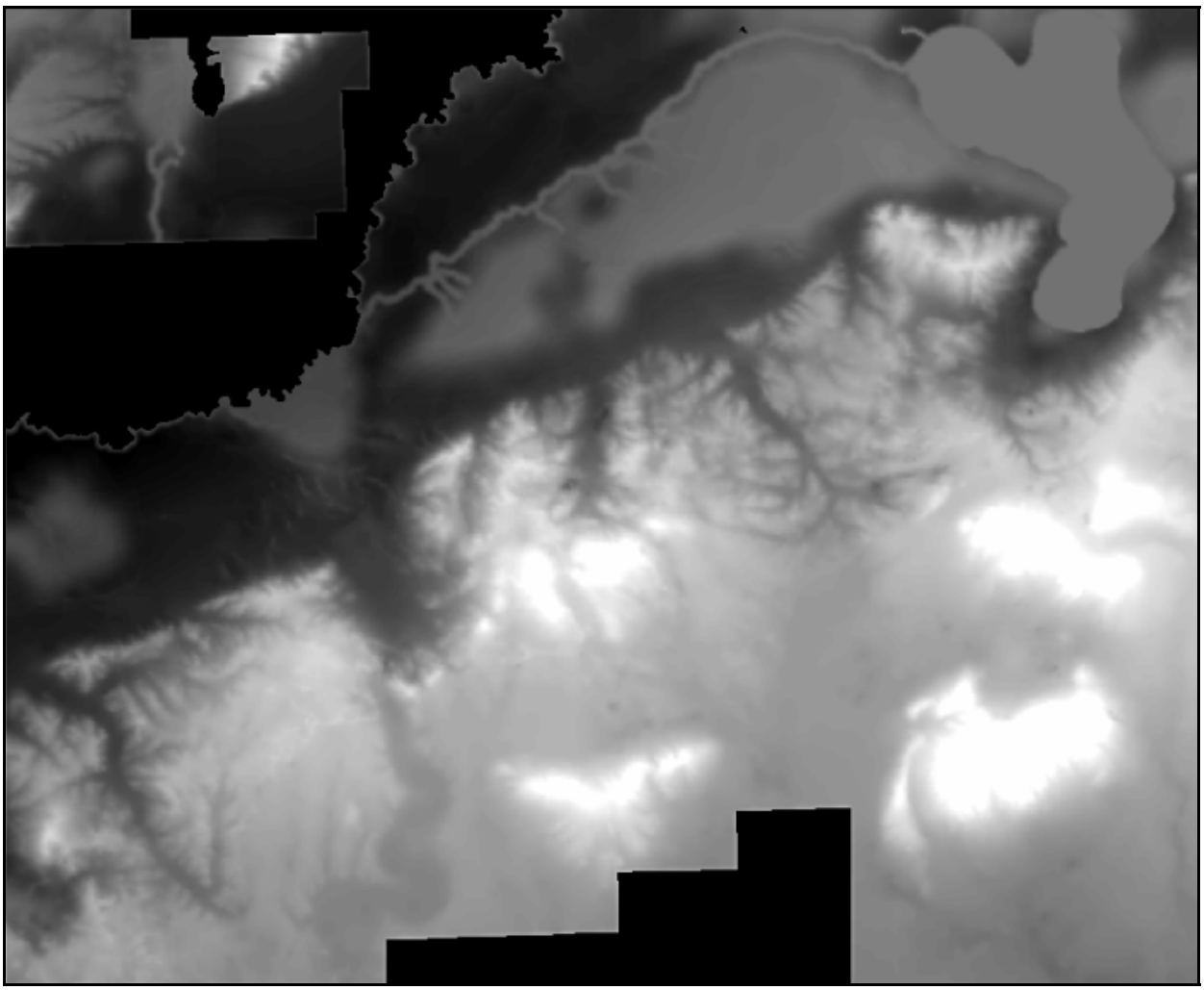

Figure 33. Depth-to-groundwater DEM.

Figure 34 provides a perspective view of the depth to the water table across the river floodplain. Note that the soil classes south of the river channel (the deep blue areas near the bottom of the image) generally have shallow water-table depths; therefore, the water-table depths in this zone exhibit a smooth gradient to the base of the hills south and east of the main river channel. The soil series on the north bank of the river (the left side of the image) are classified as various sands, and here the modeled groundwater depths drop off very quickly from the main river channel.

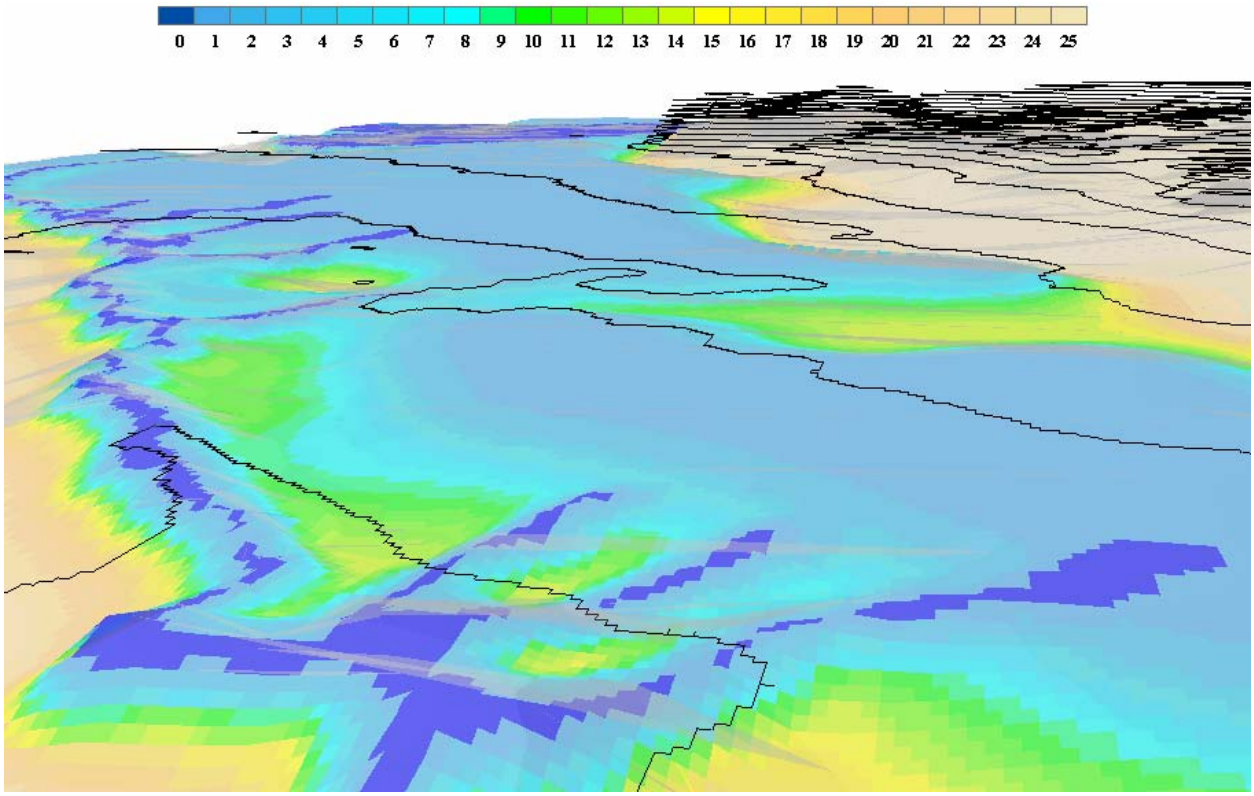

Figure 34. Perspective view of groundwater topography looking northeast across the floodplain. Surface elevations are shown by black, 5-m contour lines. The vertical exaggeration is a factor of 5. Depths are in meters.

Figure 35 shows another perspective view of water-table depths, with a vertical exaggeration of 10, looking southwest from Margrethe Lake along the transition from floodplain to hills. As the water table passes through the poorly drained soils of the riparian zone to the more porous sands of the uplands, there is a minor dip at the base of the hill before it rises to mimic the surface topography. The accurate portrayal of the vertical position of the water table over this transition area can only be tested with borehole data.

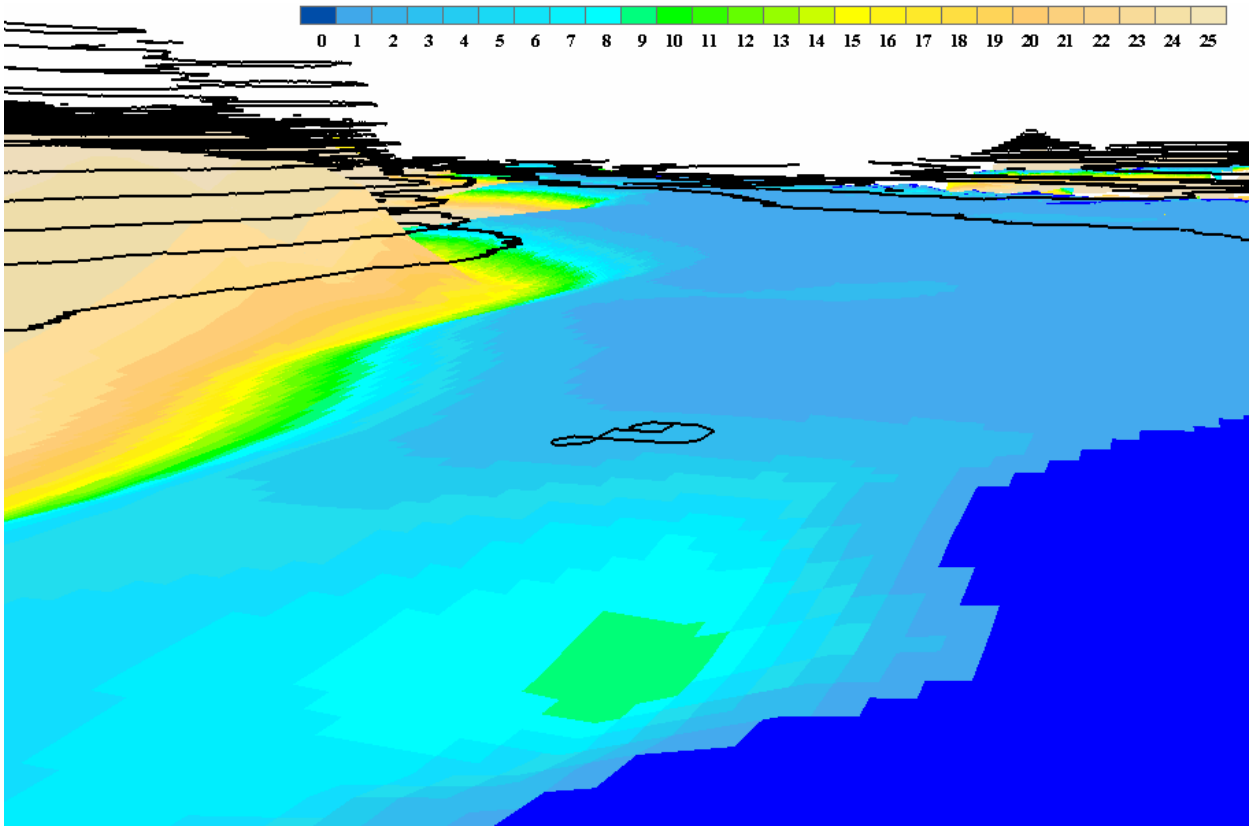

Figure 35. Perspective view of groundwater topography looking southwest from Margrethe Lake. Surface elevations are shown by black, 5-m contour lines. The vertical exaggeration is a factor of 10. Depths are in meters.

Figure 36a shows the topography of the water table, with the surface topography shown as a semi-transparent overlay. The view is from above the land surface. Figure 36b shows the same area but from below the surface. The area between the water table and the soil surface represents the thickness of the unsaturated unconsolidated material.

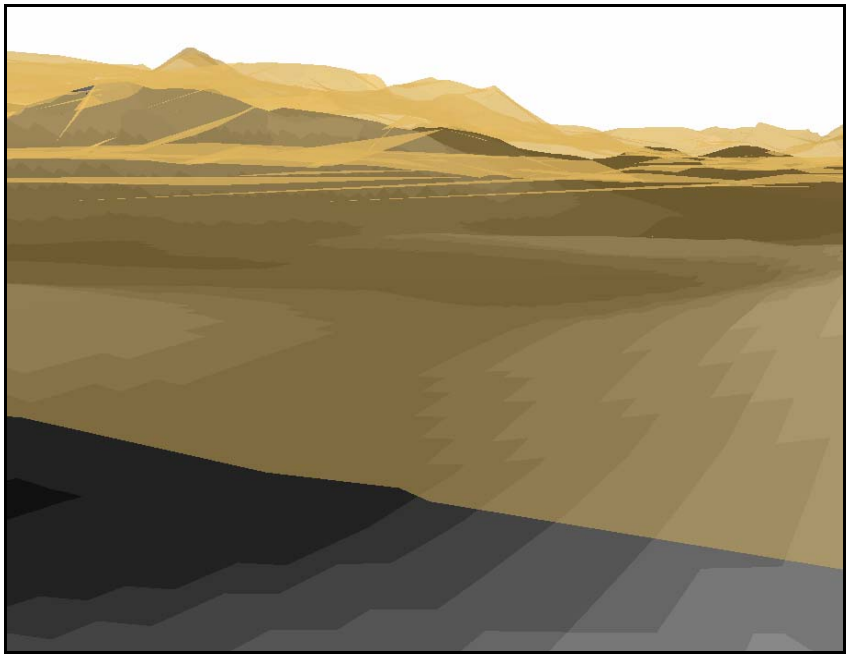

a. View from above ground level looking down.

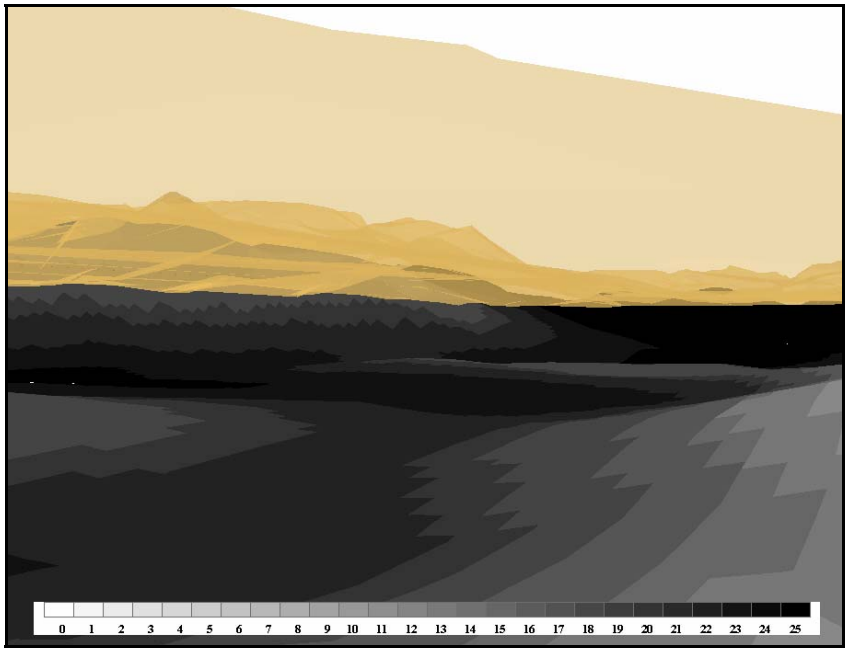

b. View from below the ground looking up. The area between the gold surface and the gray-tone water table approximates the total volume of sediment available to carry seismic waves.

Figure 36. Perspective views of groundwater topography. The ground surface is shown as a semi-transparent gold overlay, and the water-table surface is shown in gray tones. The vertical exaggeration is a factor of 5. Depths are in meters.

Deterministic Approach

Overall, the most physically "true" approach to estimating water-table depth is with deterministic models. Though not necessarily providing the most accurate answers because of the quality of input parameters and the algorithms themselves, these models attempt to simulate all of the physical processes occurring within a watershed.

The USGS *MODFLOW* (Modular three-dimensional finite-difference groundwater model) model is one of the most comprehensive and widely used deterministic models (USGS 1997). Its comprehensive design allows it to be used for stream flow, subsurface flow, infiltration, pollution tracking, water-table-depth estimation, and many other applications. In addition, it can be readily coupled to a GIS for inclusion of topographic information (USGS 1997). Though applicable to estimating water-table depth, its complexity and demand for data would make it difficult to apply to data-poor areas.

A model similar to *MODFLOW* is *TOPOG*, a terrain-analysis-based hydrologic modeling package from the Australian Commonwealth Scientific and Industrial Research Organization (http://www.per.clw.csiro.au/topog/). TOPOG describes the topographic attributes of complex 3-D landscapes and can map the water table. However, it is intended for application principally to small watersheds less than 10 km^2 in area.

The U.S. Army Corps of Engineers Engineer Research and Development Center Coastal and Hydraulic Laboratory also provides WMS, the Watershed Modeling System (http://chl.wes.army.mil/software/wms/7.0/), for using topographic information to delineate watersheds and for providing stream flow and 2-D hydrology such as flood forecasting, surface ponding, infiltration analyses, and groundwater simulations. It also interfaces with GISs and incorporates DEMs to enhance analyses. WMS may be a useful model for our application because it is a comprehensive watershed modeling system, and because it is a system developed by the Department of Defense, its acquisition and integration may be simplified. However, it requires at least six days of setup time and thus may not provide the speed of execution needed for our seismic analysis requirements.

Although we have not explored each of these models in their entirety, the most useful model for seismic geomorphology analysis applications in denied areas appears to be TOPMODEL. TOPMODEL is a rainfall runoff

model based on landscape indices used to determine surface and subsurface flow (Beven 1997). TOPMODEL uses catchment topography and soil transmissivity to predict the elevation of the water table by computing a topographic index that uses the local slope and drainage area of any patch of land. Similar to the terrain relaxation filtering technique described above, TOPMODEL sets the water table at depths that are approximately parallel to the land surface. However, TOPMODEL uses weather and climate information and soil hydraulic conductivity to explicitly calculate the water-table depth. This model is generally best suited for catchments with shallow soils and moderate topography and without excessive dry periods. It has been applied to small watersheds (Wolock 1995), as well as to subcontinent-size watersheds (Chen and Kumar 2001). TOPMODEL could by used to estimate the water-table depth in denied areas because it is not as comprehensive, and thus not as complex or data-demanding, as other deterministic models described above and because it is easily interfaced with a GIS. It is thoroughly documented and tested, with a modular structure that allows it to be more efficiently modified and executed.

In general, TOPMODEL is a set of programs for modeling rainfall runoff in single or multiple watersheds in a semi-distributed way using DEMs. It is a variable-contributing-area model in which surface and subsurface saturated areas are estimated on the basis of simplified theory for down-slope saturated zone flows. The model assumes that the local hydraulic gradient is equal to the local surface slope and that all topographically similar points will respond similarly hydrologically. An estimate of soil transmissivity is necessary for model water-table calculations, a parameter that may be difficult to estimate in denied areas. However, overall, TOPMODEL is simple, versatile, and requires little data input, making it a practical candidate for application to the denied area seismic problem.

Recommendations

As noted above, none of these methods was fully explored during this project, but each was evaluated to the point that we can recommend which should be incorporated into a fully working GIS system. Each method provides capabilities that could be exploited, depending on the geologic conditions at a particular site of interest. The simplicity of the landscape relaxation method in areas of low relief and with water table cues such as surface water and well data make it applicable in limited areas. Similarly, the landscape classification method is simple and may be sufficiently accurate, given the availability of water-table data, to correlate to a landscape-

centered variable such as geomorphology or soil type. TOPMODEL, however, may be the most applicable model in denied areas. Although its deterministic structure does not guarantee accuracy, especially when variables such as soil hydraulic conductivity must be estimated, its topographic foundation and breadth of application suggest that it may be an optimal solution among currently available water-table estimation tools.

Fracture Properties

Fractures can serve as barriers to seismic propagation because they are often filled with materials (e.g., water and clay) with densities and thus seismic velocities different from those of the surrounding materials. Fractures are present not only in bedrock, but also in weathered material above bedrock, and they can reflect upward into the soil as well. It is for this reason that fracture properties—their distribution, length, orientation, and spacing—need to be determined within our model. Detailed ground-level fracture data are rarely available, particularly for denied areas, and typically the only way to obtain these data in denied areas is to predict fracture properties from lineation data (Fig. 37). Boyer and McQueen (1964), Segall and Pollard (1981), Mohammed (1986), and Ehlen (2001a), among others, have demonstrated the relationship between lineations and ground-level

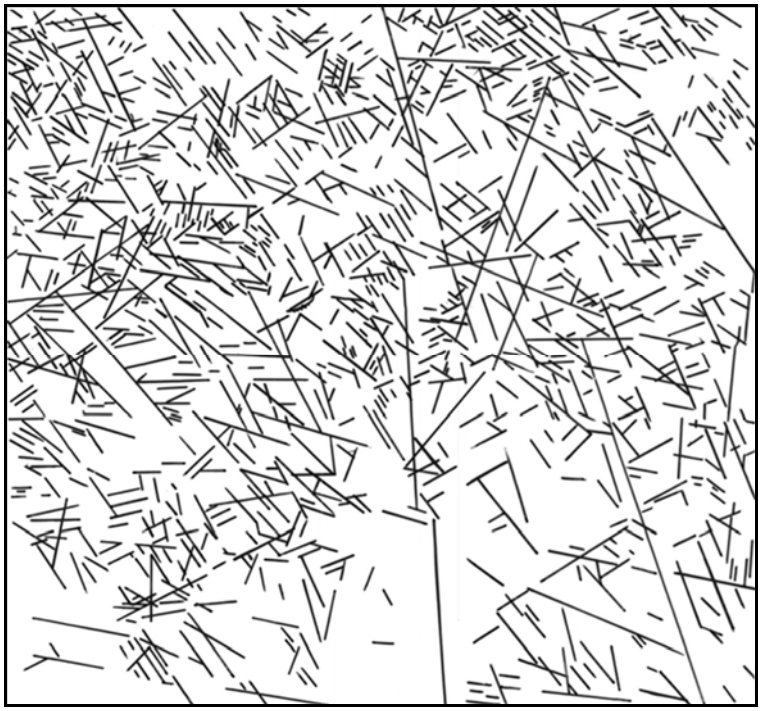

Figure 37. Typical digitized lineation overlay. The scale of this overlay is 1:21,200; north is at the top of the image.

fracture properties, and other studies have shown relationships between ground-level and subsurface fracture properties (e.g., Grout and Verbeek 1989, Narr 1996). Little research, however, has studied relationships between specific lineations, ground-level fractures, and subsurface fractures (e.g., Kane et al. 1996).

There are as yet no sufficiently accurate methodologies for automatically delineating lineations from aerial photography or satellite imagery (e.g., Ehlen et al. 1995), although significant advances have recently been made in automatically delineating fractures in the field using videography (e.g., on quarry walls) (e.g., Crosta 1997, Hadjigeorgiou et al. 2000, Post et al. 2001), such that automated procedures are now being used on a commercial basis. Lineation lengths and orientations (i.e., compass direction) can be automatically calculated from digitized lineation data. This is a simple matter of digitizing each lineation, either directly from geo-referenced digital imagery or from scanned, registered hard-copy lineation overlays. Once digitized, the length and orientation of each lineation can be calculated from the x_1, y_1, x_2, y_2 end-point positions using procedures developed as macros within ArcGIS by Douglas Caldwell at TEC. Fracture orientation can also be directly measured on geologic maps, but most small, local outcrop-scale fractures (joints) are not depicted on maps, which typically show only major structures such as folds and faults. Outcrop-level data are required for predicting subsurface fracture patterns.

A simple, effective procedure to determine lineation spacing once the lineations have been digitized was recently developed by Ghosh (2003) using ArcView. The digital procedure is similar to that usually used in the field to measure joint spacings and trace lengths. A “scanline” is drawn perpendicular to the lineation traces and then split into segments at the intersections with the lineations. The segments of the spilt scanline thus represent the spacings between individual lineations.

The data needed to fulfill the goals of this project, however, are ground-level fracture properties, some of which can be determined from lineation data using fractal theory. Ehlen (2001a) described methods for predicting fracture spacing and trace length using regression analysis of lineation data. These procedures, however, require specialized software and a level of expertise that the user of our fully developed GIS system is unlikely to have. Additional research using neural networks as a predictive tool not requiring similarly specialized or costly software or the same level of

expertise, has recently been completed; the results are very positive, indicating that it may, after all, be possible to accurately predict fracture properties from imagery (Ehlen, in prep.). These procedures will not likely be appropriate for our system, however, or be available for application during the lifetime of any follow-on effort.

Another approach to obtaining fracture spacing data is to develop estimates based on data in the published literature. Ehlen (2001b) discussed such a database with minimum, mean, median, and maximum joint spacings for common rock types. These data were re-compiled for the material types we included in Drainage 2 (Table 8). Thus, once a material type is determined using the logic tree process, our full GIS system can access such tables through the relational database, and appropriate fracture spacing values can be assigned for the material.

Table 8. Mean joint spacings for the end product material types in Drainage 2.

End Products	Joint Type	Mean Spacing (m)
Sedimentary or low-grade metamorphic rocks	vertical	0.45
	horizontal	0.31
High-grade metamorphic rocks	vertical	0.42
Crystalline rocks	vertical	0.61
	horizontal	0.25
Sedimentary rocks	vertical	0.45
	horizontal	0.31
Igneous rocks	vertical	0.59
	horizontal	0.27
Carbonate rocks	vertical	0.44
	horizontal	0.32
Volcanic rocks	vertical	0.08
	horizontal	0.16
Metamorphic or sedimentary rocks	vertical	0.45
	horizontal	0.31
Intrusive Rocks	vertical	0.59
	horizontal	0.25
Schist/slate	vertical	0.22
Serpentine*		
Metamorphic rocks	vertical	0.38

* There are no data available for serpentine.

Seismic Properties

Seismic properties, e.g., seismic velocity and bulk density, cannot be determined directly or inferred from imagery or map data. These properties are inherent to the material type and are typically determined by laboratory analysis of intact specimens. For our purpose of illustrating how an operational GIS would extract seismic properties from a relational database once the material type was determined, we compiled a partial database from data maintained by Dalhousie University and the Geological Survey of Canada (GSC 2001).

These data include compressional wave velocity and bulk densities for more than 2800 rock samples, e.g., phyllite, schist, and mudstone. We subdivided the rock data into broad groups and calculated the mean, standard deviation, maximum, and minimum for compressional wave velocity only for the groups we selected (Table 9). We found no database for unconsolidated material and used published data from Reynolds (1997) and Telford et al. (1975) as the source of this type of information.

Our goal in this effort was not to develop a definitive data set but to demonstrate proof-of-concept for the types of data manipulation capabilities and operations with relational databases that our GIS will have. We are aware that a fully developed look-up table will have to contain fewer combined material-type groups and narrower ranges of seismic properties and that the material-type end products in the table should coincide with the material-type end products in the three logic trees. However, we envision that the full GIS could extract appropriate values from numerous master databases for any inferred material and append that data to a polygon or 3-D matrix element.

Table 9. Seismic properties of some geologic materials.

Rock type	Compressional velocity (km/s) @ 10 MPA (GSC 2001)						Vp (m/s) (Reynolds 1997)		Density (g/cm³) (Reynolds 1997)		
	n	Mean	Med.	Min.	Max.	s.d.	Min.	Max.	Min.	Max.	Mean
Sandstones & shales	130	5.19	5.61	2.27	6.72	1.10					
Shale							2000	4100	1.77	3.20	2.40
Sandstones							1400	4500	1.61	2.76	2.35
Soft limestone							1700	4200	1.93	2.90	2.55
Hard limestone							2800	7000			
Carbonate (ds)	17	5.72	5.82	3.41	7.19	1.07	2500	6500	2.28	2.90	2.70
High-grade metamorphic and igneous rocks	1052	5.26	5.67	2.66	7.70	1.18					
High-grade metamorphic rocks	440	4.98	5.40	2.71	7.70	1.33					
Granitic rocks (felsic to intermediate)	260	5.41	5.66	3.19	6.64	0.82					
Basaltic rocks	325	5.70	5.99	3.05	7.66	1.04					
Granite							4600	6200	2.50	2.81	2.64
Basalt							5500	6500	2.70	3.30	2.99
Gabbro							6400	7000	2.70	3.50	3.03
Gneiss	316	4.87	5.32	2.71	7.30	1.28	3500	7600	2.59	3.00	2.80
Quartzite	16	5.24	5.53	3.50	6.29	0.91					
Volcanic rocks	154	5.68	5.78	3.53	7.30	0.57					
Metamorphic rocks	154	5.68	5.78	3.53	7.30	0.57					
Low-grade metamorphic rocks	153	5.26	5.51	2.64	7.16	1.10					
Slate/phyllite	24	5.68	4.87	2.64	6.69	1.21			2.70	2.90	2.79
Schist	60	5.59	5.69	3.46	7.06	0.79			2.39	2.90	2.64
Marble	9	5.72	5.86	4.87	6.30	0.47	3780	7000			
Metasedimentary rocks	60	5.16	5.69	3.00	7.16	1.23					
Serpentine							5500	6500			
Clay							1000	2500	1.63	2.60	2.21
Silt									1.80	2.20	1.93
Loess									1.40	1.93	1.64
Sand							200	2000	1.70	2.30	2.00
Sand (saturated)							1500	2000			
Gravel									1.70	2.40	2.00
Soil							100	600	1.20	2.40	1.92
Silt, sand, gravel							400	2300			
Permafrost							1500	4900			
Organic sediments*									0.10	1.00	
Glacial moraine							1500	2700			
Floodplain alluvium							1800	2200	1.96	2.00	1.98

* Includes range of densities for histosols, andisols, loamy A horizons, and clayey oxisol Ap horizons (Brady and Weil 1999).

5 DEMONSTRATIONS

Three demonstrations of our proof-of-concept GIS system were given. The first demonstration was given in March 2004 to the Defense Threat Reduction Agency Interagency Geotechnical Assessment Team (IGAT), an ad hoc group that has interests similar to ours and thus has encountered similar problems. The second demonstration was given to the CRREL Seismic Team in April 2004. Basic research needs expressed by this group provided the initial driving force for this project. The third and final demonstration in July 2004 was given to the Seismic Team members and various CRREL and TEC managers interested in the project. For purposes of the demonstrations, we used only the Drainage 2 logic tree to illustrate the system concept. Evaluations of Drainage 2 were also conducted as parts of the second and third demonstrations.

First Demonstration

The IGAT demonstration provided the first opportunity to present the logic tree concept in a storyboard framework, although this demonstration was a formal presentation with questions from the audience but no interactive participation. The purpose of this presentation was two-fold: First, to elicit feedback and second, to share ideas and approaches. The storyboard was used to step the IGAT members through the logic tree, with the user's current location within the logic tree and supporting images to enhance the decision-making process graphically embedded within each element of the storyboard (Fig. 38). We presented the need for our research and described the approach we were taking and the methodology we developed. This was followed by a non-interactive demonstration using the Yuma Proving Ground study area. We also made suggestions for future work.

The IGAT response to the briefing was positive. Our approach could provide information they need, especially with respect to depth to bedrock. However, our process in general provides information with insufficient detail for IGAT purposes, especially for water-table depth estimations. At the time of the demonstration, we had not yet implemented a method of estimating water-table depth.

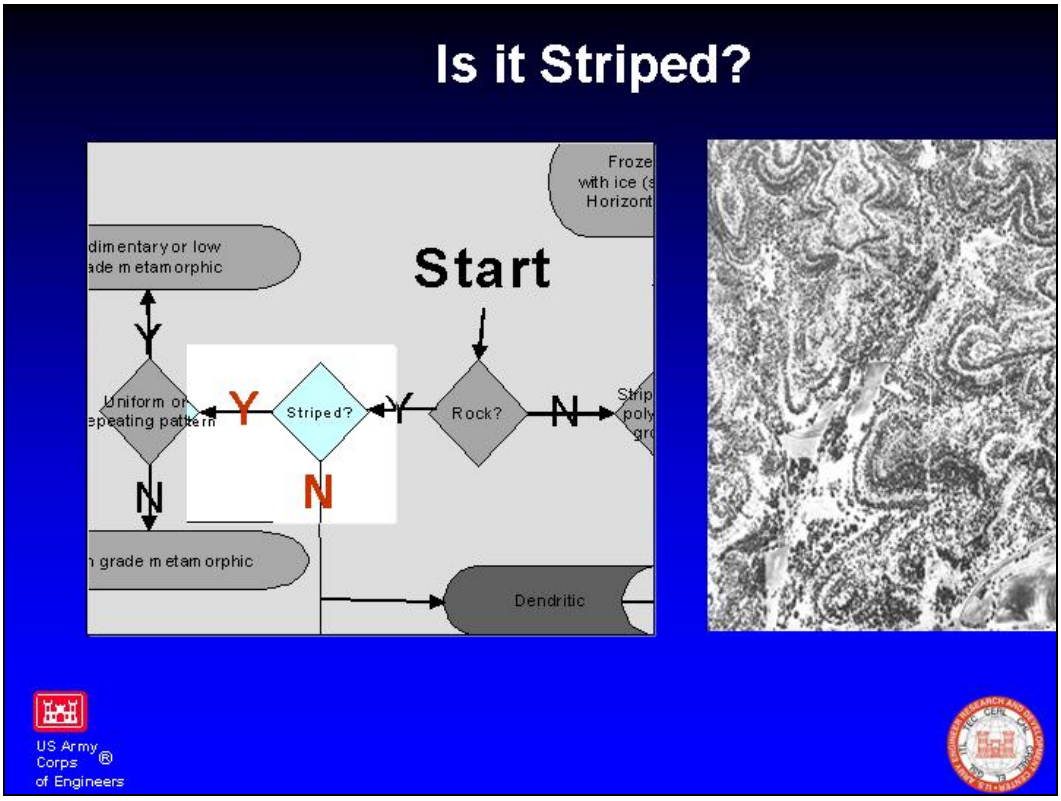

Figure 38. Illustration of the storyboard approach. The left side of the image shows the position of the user within the logic process. He has already determined that the landform polygon he is trying to classify contains rock. At this point, he is trying to determine whether or not that rock is striped. The right side of the image shows an example of striped rock provided to assist him in making this decision.

Second Demonstration

In this demonstration we discussed our concept about how to provide the required geologic data, presented our interface estimation methods and relational databases, outlined our plans for follow-on research, and discussed possible applications of our system to other topic areas. It was similar to the IGAT presentation in content, but there was more discussion and the presentation was interactive.

Some of the input we received addressed the effect of the scale of input data on the output inferences, the effect of image scale and spectral resolution, the value of stating the confidence levels in the system inferences, the value of including a road network data layer, and the importance of fracture data including statistics on fracture spacing.

- Image scale and confidence levels: We did address this issue in our evaluations, but we did not tally the results from this perspective, so we cannot quantitatively determine the effect of the scale of input data or provide confidence levels to our inferences. We did note that during the evaluations the analyst "felt" more confident about a decision on the way to an inference when large-scale input data were used.
- Road networks: We can easily provide the road network for any area. Even on small-scale imagery, either roads or road rights-of-way are visible and can be readily drawn on a map.
- Fracture statistics: We could easily include fracture statistics in addition to the mean as part of follow-on work; the data are currently available to do this.

Third Demonstration

This demonstration of our final concept used the Fort Irwin data set. We demonstrated four of the data layer manipulation capabilities: 2-D and 3-D viewing, zooming, data layer rotation for multiple perspectives, and data layer draping. The data layers available for this demonstration were multispectral satellite imagery, a satellite image orthophoto quad, a landform polygon map, a land cover map, a soils map, a 5-m-resolution DEM, and drainage patterns.

Dr. Keith Wilson, one of the participants, said our conceptual system is "definitely a positive step toward addressing the need for environmental characterization in data-poor areas." The participants hoped that we could continue the development of the system. They had the following comments and questions. First, the seismic velocity data available in the final relational database must contain values for a greater variety of materials and values for specific materials rather than for the lumped materials that we showed in our example table. In addition, seismic velocities for some materials had a sufficiently broad range that they encompassed the seismic velocities of nearly all of the materials on the logic tree, rendering the logic tree unnecessary. We are aware of these issues and the need for more detailed information, but such information would only be useful if our logic trees were expanded to include more detailed material type identifications: The data in the look-up tables must match the logic tree end products.

Second, the operation of the keynote landforms part of the system must be clearly defined so the analyst knows the value of and method for using this

feature. Our interpretation of one of the analyst's responses to the keynote landform section was that he felt the need to identify the polygon as a keynote landform and was uncomfortable when he was unable to easily do so (none of the landforms chosen for analysis by the analysts were keynote landforms). It was as if he thought he had failed if he did not identify a keynote landform and thus belabored the decision as to whether a keynote landform was present or not. Our intent is that this should be a quick process in which the analyst very rapidly recognizes if a keynote landform is present, and if not, he moves on to selecting the appropriate logic tree. The issue of how to use the keynote landforms "short cut" needs further consideration and clarification.

Third, we were asked whether the system allows for the use of analogs to infer geologic conditions. We explained how the use of analogs is controversial because different analogs must be used for different characteristics of the landscape, i.e., a geologic analog could be based on rock type or on geologic structure, and two areas analogous in rock type may not be analogous in geologic structure. For example, interbedded sedimentary rocks comprise significant proportions of the Appalachian Mountains as well as various mountain ranges in Nevada. Some would say then that these two areas could be considered analogs in terms of rock type. However, the climates are significantly different, so soil and overburden depths are different and strong rocks in one environment become weak rocks in the other because the rocks weather differently in the two different climates. Furthermore, the geologic structures in the two areas are also significantly different, leading to different types of landforms in the two areas.

We believe that different analog areas would be needed for each factor (e.g., climate, geology, vegetation) and that the analog concept in the broadest sense is not an appropriate means for obtaining the information our system is designed to produce. However, with this said, we are using a form of the analog concept to produce the look-up tables that contain required information that cannot be determined from imagery, e.g., fracture spacings, soil and overburden depths, and seismic velocities. We only use this approach, however, when there is no other way to obtain the desired information.

Fourth, we were asked if our logic trees could be tailored for and applied to a specific region. This is of course the case, and logic trees could easily be

extracted from our existing logic trees for specific areas. If this were to be done, the detail within the logic trees could be expanded significantly, and it is likely that accuracy would increase. Our purpose in this project, however, was to produce a methodology that could be applied in a global sense, a much more difficult task.

Finally, the effects of scale and the reliability of the material type inferences were discussed with respect to quantifying the results in terms of confidence limits and risk. These issues were also discussed during team meetings, logic tree evaluations, and the second demonstration, as noted above. We have not attempted to quantify the results in this manner; our evaluations were not intended to provide statistically valid data. We used the evaluations as a means to improve the logic trees, not to validate them statistically. We were primarily interested in providing first-order inferences of constituent material types, i.e., rock type to igneous, metamorphic, or sedimentary, and sediment type to clay, silt, sand, gravel, or a combination thereof. During this phase of the research, we were more concerned with evaluating the types of capabilities our system should have (i.e., 3-D layered display when fully developed) and showing that the concept could be developed into a functional system. We did not attempt to compile complete databases. Moreover, when we evaluated the interface data for the relational databases, we aimed to provide order-of-magnitude accuracy as defined during the initial phase of the project. Providing a statistical base to determine confidence and risk would be a major undertaking, but it could be—and should be—done in multiple evaluations of static logic trees as part of a follow-on effort.

6 Concept of System Operation

Step One

The system operator, a military terrain analyst, receives the location to be analyzed. He then determines what data are available for that area (Table 1) and compiles a set of GIS data layers from that data. Data availability will vary by location, but there will at least be some small- or continental-scale data, e.g., Landsat imagery, geology and/or soils maps, that are available globally. The system will use more synoptic, secondary data with the global data to put selected locations into a regional context to minimize the number of landforms and material types possible. For example, issues dealing with cold regions will not be addressed if the area of interest is located in a temperate environment. Tertiary, site-specific data will likely be rare for any particular site but, if available, may negate the need for applying our system's geologic analysis sequence.

Step Two

The analyst determines if the available maps and data are adequate to make the required inferences directly. If they are, the inferences are made. If they are not, the analyst uses the system's geologic analysis procedures. He loads all imagery of the area and data layers into ERDAS Imagine or ArcGIS and proceeds to step three.

Step Three

Landform unit maps with the polygons delineated but not classified and drainage-pattern maps will be provided to the analyst. The system will allow the analyst to automatically group like landforms into landform mapping units and to perform morphometric analyses for each polygon. See Table 10 for the types of analyses planned for the fully operational system.

Step Four

The analyst chooses which logic tree to use. If stereo imagery is available, he will most likely choose the landform logic tree; if not, he will choose one of the drainage logic trees, the choice depending on the complexity of the area and the scale or resolution of the data available. As noted previously,

Drainage 1 should be selected if the area of interest has complex geology and/or terrain and if high-resolution data are available. Drainage 2 performs well in all geologic and/or terrain environments, but because it provides generalized answers, it should be used only where the landform logic tree or Drainage 1 are not applicable.

Table 10. Prototype-GIS manual and functionality.

Manual to accompany prototype:
Include a glossary with pictures and drawings
Provide list of ancillary data and data layers so analyst knows what information is available
Define overall analytical/inferential process and approach
Give examples of trial runs through the process
Give guidance at the beginning of the analysis, with examples at decision points:
Show the flow of questions all at once
Identify a polygon based on the dominant (majority) feature
Scan around an image to get a "feel" for the region
Functionality:
Show keynote features with pictures and drawings before polygon analysis starts
Access relational databases and drop-down tables with various formats:
Weathering thickness
Overburden thickness
Provide ground water estimation
Meld fracture characteristics and rock/sediment properties
Develop the seismic property matrix and depth-to-bedrock estimation:
Slope projection (Matlab)
Soil type (to provide minimum estimate to bedrock)
Vegetation root depth estimation
Location relative to glacial maxima
Provide option to go back to the beginning of the analysis if end result is incorrect
Auto-classify all polygons that are similar once one of them is identified
Perform unsupervised classification spectral analyses/band ratioing to differentiate rocks vs. sediment and identify rock types

Step Five

The analyst identifies any polygons that are keynote landforms, which automatically provides the material type. If no keynote landforms are present, he begins the landform analysis using the selected logic tree. He chooses a polygon or group of polygons comprising one landform mapping unit and begins analysis. Multiple trees may be used to confirm inferences made. The answer to each question in each logic tree leads the analyst directly to the next question, and each question is illustrated with drawings or images of the possible answers to facilitate decision making. He can also call on any of the decision aids available to assist him in his choice.

Step Six

When the analyst has selected the material type for a polygon or like polygons, the system will populate a table with estimated interface data, i.e., depth to bedrock, water-table depth, fracture spacings, and seismic properties. The system will then use these data and the material inferences, similar to that shown in Figure 39, to automatically populate a 3-D, block-diagram-type of display (e.g., Kessler and Mathers 2004, 2006) for the polygon(s) that were analyzed. Steps five and six are then repeated for each landform mapping unit shown on the landform map.

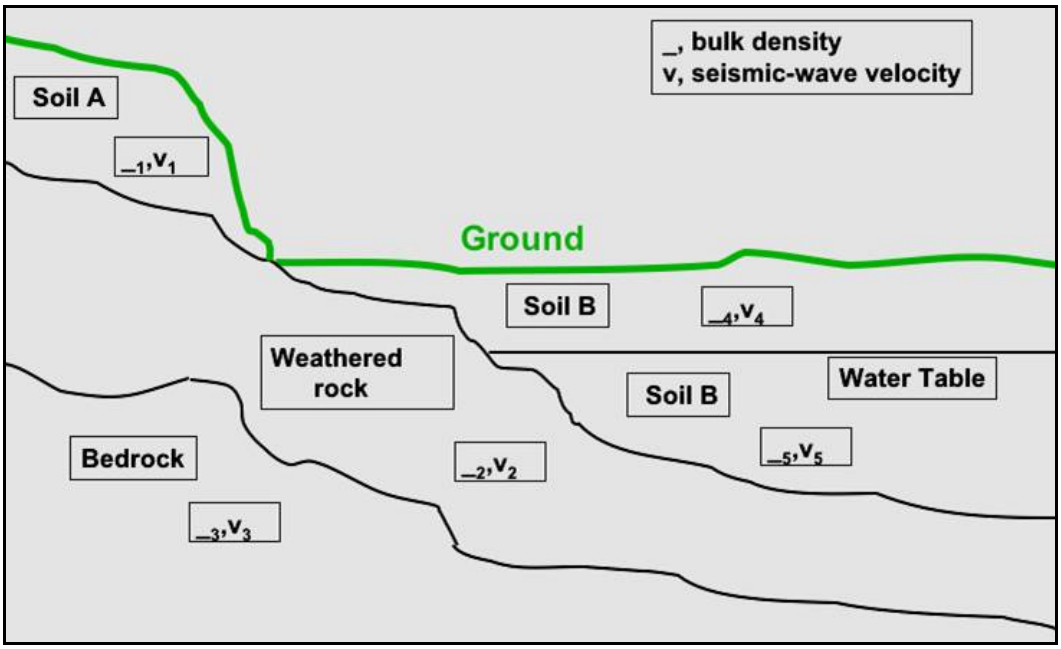

Figure 39. Hypothetical subsurface cross section with geological materials of differing densities and seismic velocities.

7 FUTURE DEVELOPMENT AND APPLICATIONS

This project has resulted in a proof-of-concept for an interactive, GIS-based terrain analysis system. We believe that additional research should focus on the development of a functional GIS graphical interface for the system. Figure 40 shows our concept of what such an interface window might look like. The development of such a window would require programming within the GIS to automatically link databases, access relational databases of various formats, and auto-classify polygons that have been determined to be the same. New data need to be incorporated as they become available or by further literature mining to provide better estimates of, for example, depth to bedrock for different rock types, region-specific data as needed, and specific rock and sediment seismic velocities.

A method to develop application data layers (e.g., for vehicle- and troop-movement corridors) from the results of analysis using our system would be particularly useful as a decision aid for seismic sensor deployment. Ultimately, the system could include algorithms in the background that screen out data fields where they are unlikely to occur, i.e., permafrost landforms and thus frozen soil should not be an option in keynote landforms or the logic tree used for arid areas such as Yuma Proving Ground or Fort Irwin.

A follow-on project would allow us to take our concept to a higher level. This would provide the opportunity to evaluate and develop methods and algorithms to estimate the thickness of unconsolidated sediment such as reported by Lawley and Booth (2004), to draw subsurface profiles using “profile maker” developed at Cornell University (Barazangi et al. 1998, Institute for the Study of Continents 2006, Seber et al. 2001), to populate 2-D and 3-D matrices with material types and properties, to draw subsurface 3-D diagrams, and to provide decision aids to the analyst, a need identified during our blind evaluations.

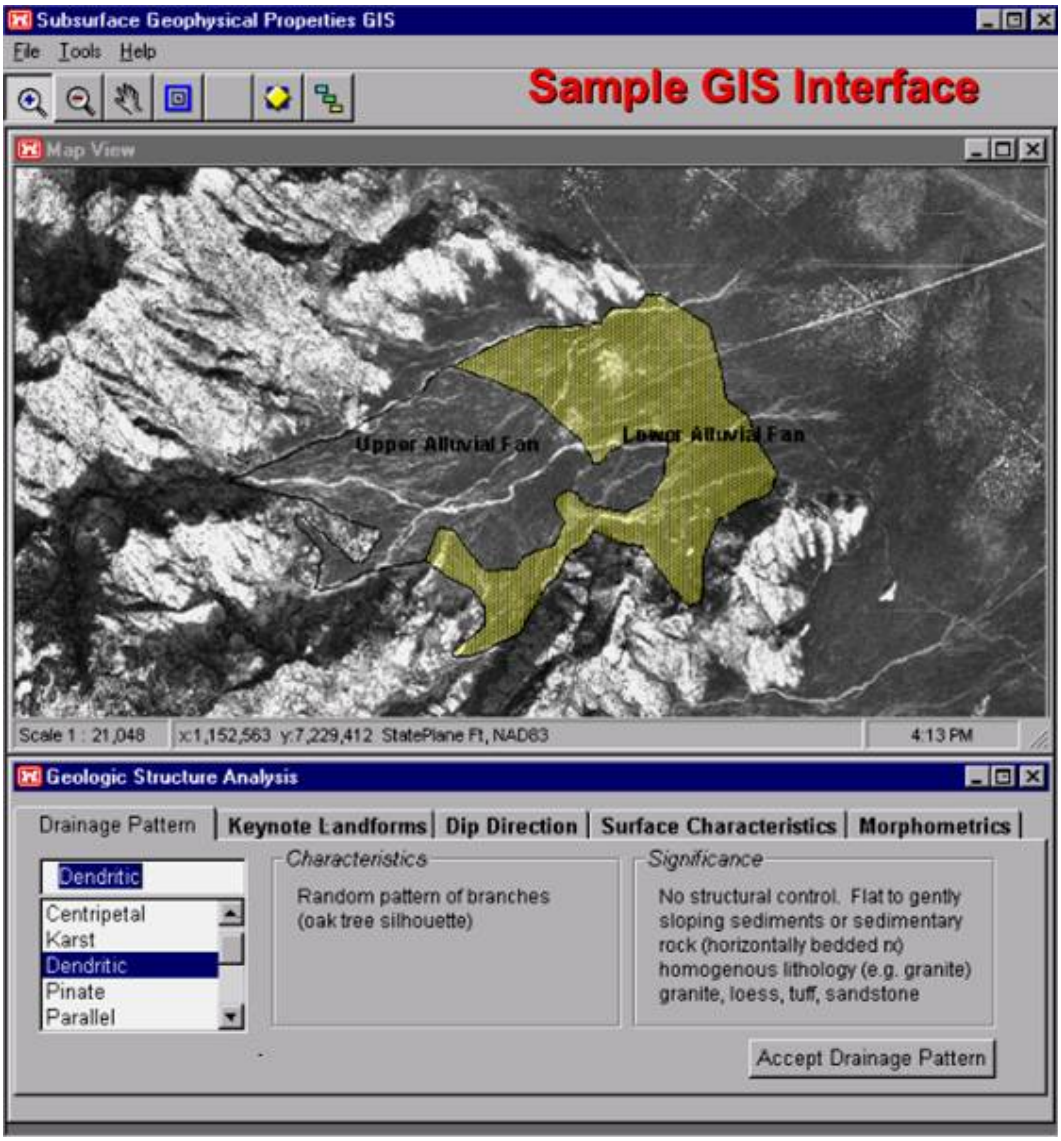

Figure 40. Conceptual GIS interface window with links to satellite imagery, the landform logic tree, seismic velocity and density databases, DEM, hydrology, roads, and landform vector layers.

8 CONCLUSIONS

The main contributions to science of this project are:

- Our concept, which integrates existing knowledge and technologies;
- Our logic trees, which define the basis for programming a GIS to follow a terrain analysis sequence;
- The slope projection method developed to estimate depth to bedrock; and
- The method developed to determine depth to the water table.

Furthermore, the proof-of-concept illustrates the feasibility of integrating the proven methods of traditional terrain analysis with a GIS.

The concept is robust. It works in diverse climates and geologic settings. A military terrain analyst with limited geological experience can correctly identify the material type 70–80% of the time using our Drainage 2, a simplified logic tree.

When fully developed, our system will provide a new capability to use the power of GIS and image processing software to manipulate available geospatial data and to complete a terrain analysis. The analysis will result in inferences on subsurface geologic conditions in locations where physical access is not possible, in estimates of geophysical properties, and in displays of the geological conditions and properties in 3-D matrices and diagrams.

9 REFERENCES

Anderson, J. F., E. E. Hardy, J. T. Roach, and R. E. Witmer. 1976. *A land use and land cover classification system for use with remote sensor data*. Professional Paper 964. Washington, DC: U.S. Geological Survey.

Barazangi, M., D. Seber, E. Sandvol, D. Steer, M. Vallve, and C. Orgren. 1998. *Digital database development and seismic characterization and calibration for the Middle East and North Africa*. Ithaca, NY: Cornell University Institute for the Study of the Continents, http://atlas.geo.cornell.edu/ctbt/geoid.html.

Beven, K. 1997. TOPMODEL: A critique. *Hydrological Processes* 11: 1069–1085.

Billings, M. 1954. *Structural geology*. Englewood Cliffs, NJ: Prentice-Hall.

Blodget, H. W., and G. F. Brown. 1982. *Geological mapping by use of computer-enhanced imagery in western Saudi Arabia*. Professional Paper 1153. Washington, DC: U.S. Geological Survey.

Boyer, R. E., and J. E. McQueen. 1964. Comparison of mapped rock fractures and air photo linear features. *Photogrammetric Engineering* 30: 630–635.

Brady, N. C., and R. R. Weil. 1999. *The nature and properties of soils*. 12th Edition. Englewood Cliffs, NJ: Prentice-Hall.

Brockway, D. G., and P. V. Nguyen. 1986. Municipal sludge application in forests of northern Michigan: A case study. In *Alternatives for treatment and utilization of municipal and industrial wastes*, ed. D. W. Cole, C. L. Henry, and W. L. Nutter, 477–496. Seattle: University of Washington Press.

Chen, J., and P. Kumar. 2001. Topographic influence on the seasonal and interannual variation of water and energy balance of basins in North America. *Journal of Climate* 14: 1989–2014

Crosta, G. 1997. Evaluating rock mass geometry from photographic images. *Rock Mechanics and Rock Engineering* 30: 35–58.

Dehn, M., H. Gartner, and R. Dikau. 2001. Principles of semantic modeling of landform structures. *Computers and Geosciences* 27(8): 1005–1010.

Ehlen, J. 1976. *Photo analysis of a desert area*. ETL-0068. Fort Belvoir, VA: U.S. Army Engineer Topographic Laboratory.

Ehlen, J. 2001a. Predicting fracture properties in weathered granite in denied areas. In *The environmental legacy of military operations*, ed. J. Ehlen and R. S. Harmon. Reviews in Engineering Geology XIV, 61–73. Boulder, CO: Geological Society of America.

Ehlen, J. 2001b. Joint spacing models: An alternative for joint property characterization. *Geological Society of America Abstracts with Programs* 33(6): A-66.

Ehlen, J. 2005. Above the weathering front: Contrasting approaches to study and classification of the weathered mantle. *Geomorphology* 67(1-2):7-21.

Ehlen, J. (in prep.) Predicting fracture trace length from imagery using neural networks.

Ehlen, J., R. A. Hevenor, J. Kemeny, and K. Girdner. 1995. Fracture recognition in digital imagery. In *Proceedings of the 35th U.S. Symposium on Rock Mechanics*, ed. J. J. K. Daemen and R. A. Schultz, 141–146. Brookfield, VT: A. A. Balkema.

Foley, M. G., K. A. Hoover, C. R. Cole, D. J. Bradley, J. L. Devary, L. G. McWethy, M. D. Williams, and S. K. Wurstner. 1994. *West siberian basin hydrogeology*. Final report prepared for the U.S. Department of Energy. Richland, WA: Pacific Northwest Laboratory.

Foster, N. H., and E. A. Beaumont. 1992. *Photogeology and photogeomorphology*. Geology Reprint Series 18. Tulsa, OK: American Association of Petroleum Geologists.

Frost, R. E. 1950. *Evaluation of soils and permafrost conditions in the territory of Alaska by means of aerial photographs*. Report for St. Paul District, U.S. Army Corps of Engineers. Lafayette, IN: Purdue University Engineering Experiment Station.

Frost, R. E., J. G. Johnstone, O. W. Mintzer, M. Parvis, P. Montano, R. D. Miles, and J. R. Shepard. 1953. *A manual on the airphoto interpretation of soils and rocks for engineering purposes*. Lafayette, IN: Purdue University School of Engineering.

Gatto, L. W., L. E. Hunter, C. C. Ryerson, J. Ehlen, and B. T. Tracy. 2002. Interpreting landforms from remotely sensed imagery to infer subsurface properties. *Geological Society of America Abstracts with Programs* 34(6): 478.

Geological Survey of Canada Atlantic/Dalhousie University (GSC) 2001. http://cgca.rncan.gc.ca/pubprod/rockprop/search_e.php, accessed 2003.

Gerrard, A. J. 1988. *Rocks and landforms*. London: Unwin Hyman.

Ghosh, K. 2003. Characterizing fracture distribution in layered rocks using geographic information system-based techniques. MS thesis, Florida International University.

Graff, L. H. 1992. *Automated classification of basic-level terrain features in digital elevation models*. TEC-0013. Fort Belvoir, VA: U.S. Army Topographic Engineering Center.

Grout, M. A., and E. R. Verbeek. 1989. Prediction of fracture networks at depth in low-permeability reservoir rocks, Piceance and Washakie Basins, western United States. Abstract. *American Association of Petroleum Geologists Bulletin* 73: 1158.

Hadjigeorgiou, J., F. Lemy, P. Côté, and X. Maldague. 2000. Development of a methodology for the automatic construction of discontinuity trace maps based on digital images. In *Pacific Rocks 'Rock Around the Rim,' Proceedings of the 4th North American Rock Mechanics Sumposium*, ed. J. Girard, M. Liebman, C. Breeds, and T. Doe, 681–686. Rotterdam: A. A. Balkema.

Institute for the Study of Continents. 2006. http://atlas.geo.cornell.edu/

Jensen, J. R. 1996. *Introductory digital image processing: A remote sensing perspective*. Englewood Cliffs, NJ: Prentice-Hall.

Kane, W. F., D. C. Peters, and R. A. Speirer. 1996. Remote sensing in investigation of engineered underground structures. *Journal of Geotechnical Engineering* 122: 674–681.

Kazmierski, J., E. Mills, D. Phemister, R. Nick, C. Riggs, R. Tefertiller, and D. Erickson. 2002. *Upper Manistee River Watershed Conservation Plan*. Master's Project. School of Natural Resources and Environment, University of Michigan.

Kessler, H., and S. Mathers. 2004. Maps to models. *Geoscientist* 14(10): 4–6.

Kessler, H., and S. Mathers. 2006. From geological maps to models—Finally capturing the geologists' vision. British Geological Survey, National Environment Research Council. http://www.bgs.ac.uk/news/press/mapstomodels.html.

Ketcham, S. A., M. L. Moran, J. Lacombe, R. J. Greenfield, and T. S. Anderson. 2002. Modeling ground loading by moving tracked vehicles in FDTD seismic simulations. In *Proceedings of the 2002 Meeting of the MSS Specialty Group on Battlefield Acoustic and Seismic Sensing, Magnetic and Electric Field Sensors, September 23–26, 2002, Laurel, MD*. Report 2002ACF02x. Laurel, MD: Applied Physics Laboratory, Johns Hopkins University.

Lawley, R., and S. Booth. 2004. Skimming the surface. *Geoscientist* 14(2): 4–7.

Leighty, R. D.B. D. Leighty, and M. D. Perkins, 2001. *Automated IFSAR terrain analysis system*. Final report, DARPA contract DAAH01-98-C-R148. Arlington, VA, DARPA, Distribution authorized to U.S. Gov't. agencies only; Test and Evaluation; 15 Mar 99. Other requests shall be referred to Defense Advanced Research Projects Agcy, ATTN: TI, 3701 N. Fairfax Dr., Arlington, VA 22203-1714.

Liang, Ta, R. B. Costello, G. J. Fallon, R. J. Hodge, H. C. Ladenheim, D. R. Lueder, and J. D. Mollard. 1951a. *A photo-analysis key for the determination of ground conditions. General analysis*. Land form reports 1. For the Amphibious Branch, Office of Naval Research, U.S. Naval Photographic Interpretation Center. Ithaca, NY: Cornell University School of Engineering.

Liang, Ta, R. B. Costello, G. J. Fallon, R. J. Hodge, H. C. Ladenheim, D. R. Lueder, and J. D. Mollard. 1951b. *a photo-analysis key for the determination of ground conditions. Sedimentary rocks.* Land form reports 2. For the Amphibious Branch, Office of Naval Research, U.S. Naval Photographic Interpretation Center. Ithaca, NY: Cornell University School of Engineering.

Liang, Ta, G. J. Fallon, R. B. Costello, R. J. Hodge, H. C. Ladenheim, D. R. Lueder, and J. D. Mollard. 1951c. *A photo-analysis key for the determination of ground conditions. Igneous and metamorphic rocks.* Land form reports 3. For the Amphibious Branch, Office of Naval Research, U.S. Naval Photographic Interpretation Center. Ithaca, NY: Cornell University School of Engineering.

Liang, Ta, D. R. Lueder, R. B. Costello, G. J. Fallon, R. J. Hodge, H. C. Ladenheim, and J. D. Mollard. 1951d. *A photo-analysis key for the determination of ground conditions. Waterlaid materials.* Land form reports 4. For the Amphibious Branch, Office of Naval Research, U.S. Naval Photographic Interpretation Center. Ithaca, NY: Cornell University School of Engineering.

Liang, Ta, J. D. Mollard, R. B. Costello, G. J. Fallon, R. J. Hodge, H. C. Ladenheim, and D. R. Lueder. 1951e. *A photo-analysis key for the determination of ground conditions. Glacial materials.* Land form reports 5. For the Amphibious Branch, Office of Naval Research, U.S. Naval Photographic Interpretation Center. Ithaca, NY: Cornell University School of Engineering.

Liang, Ta, R. B. Costello, G. J. Fallon, R. J. Hodge, H. C. Ladenheim, D. R. Lueder, and J. D. Mollard. 1951f. *A photo-analysis key for the determination of ground conditions. Windlaid materials.* Land form reports 6. For the Amphibious Branch, Office of Naval Research, U.S. Naval Photographic Interpretation Center. Ithaca, NY: Cornell University School of Engineering.

Lillesand, T. M., and R. W. Kiefer. 1987. *Remote sensing and image interpretation*. New York: John Wiley and Sons.

Loelkes, G. L., Jr., G. E. Howard, Jr., E. L. Schwertz, Jr., P. D. Lampert, and S. W. Miller. 1983. *Land use/land cover and environmental photointerpretation keys*. Bulletin 1600. Washington, DC: U.S. Geological Survey.

Matson, K. C., and J. E. Fells. 1996. Approaches to automated water table mapping. In *Proceedings, Third International Conference/Workshop on Integrating GIS and Environmental Modeling, Santa Fe, NM, January 21–26, 1996*. Santa Barbara, CA: National Center for Geographic Information and Analysis.

McMahon, W. 2003. S*oils database update*. Briefing to TEC GI TEM, 26 Sept 03.

Mikula, R., and H. Croskey. 2003. *Soil erosion and sedimentation control training manual*. Lansing: Michigan Department of Environmental Quality.

Mohammad, M. R. 1986. Jointing and air photo lineations in Jurassic limestone formations of Al-Adirab area, Tuwayq Mountain, adjacent to Ar-Riyadh, Saudi Arabia. In *International geomorphology*, ed. V. Gardiner. 2: 359–365.

Narr, W. 1996. Estimating average fracture spacing in subsurface rocks. *American Association of Petroleum Geologists Bulletin* 80, 1565–1586.

Post, R. M., J. Kemeny, and R. Murph. 2001. Image processing for automatic extraction of rock joint orientation data from digital images. In *Rock Mechanics in the National Interest, Proceedings of the 38th U.S. Rock Mechanics Symposium*, ed. D. Elsworth, J. P. Tinucci, and K. A. Heasley, 1: 877–884. Rotterdam: A. A. Balkema.

Reynolds, J. M. 1997. *An introduction to applied and environmental geophysics*. New York: John Wiley and Sons.

Rinker, J. N., and P. A. Corl. 1984. *Air photo analysis, photo interpretation logic, and feature extraction*. ETL-0329. Fort Belvoir, VA: U.S. Army Engineer Topographic Laboratory.

Seber, D., C. O. Sandvol, C. Brindisi, and M. Barazangi. 2001. Building the digital earth. In *Proceedings of the Geological Society of American Annual Meeting, 1-10 Nov 2001, Boston*. 33(6):176.

Segall, P., and D. D. Pollard. 1981. From joints and faults to photo lineaments. In *Proceedings, 4th International Conference on Basement Tectonics*, ed. R. H. Gabrielsen, I. B. Ramberg, D. Roberts, and O. A. Steinlein, 11–20. Oslo: Basement Tectonics Committee, Inc.

Telford, W. M., L. P. Geldart, R. E. Sheriff, and D. A. Keys. 1975. *Applied geophysics*. New York: Cambridge University Press.

Tracy, B., M. Campbell, J. Ehlen, L. Gatto, L. Hunter, and C. Ryerson. 2003. A GIS-based method to infer subsurface geology. In *Proceedings of the Military Sensing Symposia Specialty Group on Battlefield Acoustic and Seismic Sensing, Magnetic and Electronic Field Sensors, 6–8 October 2003, Baltimore, MD.* Paper ACC01BT1. Baltimore, MD: Applied Physics Laboratory, Johns Hopkins University.

United Nations Food and Agricultural Organization (FAO). 1998. *Digital soil map of the world and derived soil properties*. Land and Water Digital Media Series No. 1. Rome: United Nations Food and Agriculture Organization.

U.S. Army Topographic Engineering Center (TEC). 1996. *Desert tortoise habitat modeling and plant community mapping in the Mojave Desert*. Final report to the Government Applications Task Force Program Office.

U.S. Geological Survey (USGS). 1997. *Modeling ground-water flow with MODFLOW and related programs*. Fact Sheet FS-121-97. Washington, DC: U.S. Geological Survey.

Way, D. S. 1973. *Terrain analysis, A guide to site selection using aerial photographic interpretation*. New York: McGraw-Hill.

Webb, R. S., C. E. Rosenzweig, and E. R. Levine. 1991. *A global data set of soil particle size properties*. Technical Memo 4286. Washington, DC: National Aeronautics and Space Administration.

Wolock, D. M. 1995. Effects of subbasin size on topographic characteristics and simulated flow paths in the Sleepers River, Vermont watershed. *Water Resources Research* 31: 1989–1997.

REPORT DOCUMENTATION PAGE

Form Approved
OMB No. 0704-0188

1. REPORT DATE *(DD-MM-YYYY)*	**2. REPORT TYPE**	**3. DATES COVERED** *(From - To)*
September 2006	Technical Report	

4. TITLE AND SUBTITLE

A GIS System for Inferring Subsurface Geology and Material Properties: Proof of Concept

5a. CONTRACT NUMBER

5b. GRANT NUMBER

5c. PROGRAM ELEMENT NUMBER

6. AUTHOR(S)

Lawrence W. Gatto, Michael V. Campbell, Judy Ehlen,
Charles C. Ryerson, Lewis E. Hunter, and Brian T. Tracy

5d. PROJECT NUMBER

5e. TASK NUMBER

5f. WORK UNIT NUMBER

7. PERFORMING ORGANIZATION NAME(S) AND ADDRESS(ES)

U.S. Army Eng. Res. and Dev. Cen.
Cold Regions Res. and Eng. Lab.
72 Lyme Road
Hanover, NH 03755

U.S. Army Eng. Res. and Dev. Cen.
Topographic Engineering Lab.
7701 Telegraph Road
Alexandria, VA 22315

Sacramento District
U.S. Army Corps of Eng.
1325 J Street
Sacramento, CA 95814

8. PERFORMING ORGANIZATION REPORT NUMBER

ERDC TR-06-6

9. SPONSORING / MONITORING AGENCY NAME(S) AND ADDRESS(ES)

10. SPONSOR/MONITOR'S ACRONYM(S)

11. SPONSOR/MONITOR'S REPORT NUMBER(S)

12. DISTRIBUTION / AVAILABILITY STATEMENT

Approved for public release; distribution is unlimited.

Available from NTIS, Springfield, Virginia 22161.

13. SUPPLEMENTARY NOTES

14. ABSTRACT

This report describes the concept for a geographical information system (GIS) that can infer subsurface geology and material properties. The hypotheses were that a GIS can be programmed to 1) follow the fundamental logic sequence developed for traditional terrain- and image-analysis procedures to infer geologic materials; 2) augment that sequence with correlative geospatial data from a variety of sources; and 3) integrate the inferences and data to develop "best-guess" estimates. Structured logic trees were developed to guide a terrain analyst through an interactive, geologic analysis based on querying and mentoring logic primarily using imagery and map data as input. The logic trees allow a terrain analyst with limited geology background and experience to rapidly infer the most likely geologic material. A new surface projection method was also developed to estimate depth to bedrock, and an existing method to determine depth to the water table was significantly expanded. The concept was proven to be feasible during blind evaluations conducted at Camp Grayling, MI, a cool, temperate, vegetation-covered site, and at Yuma Proving Ground, AZ, and Fort Irwin, CA, both hot, arid, barren sites. The results show that an analyst can infer the correct geologic conditions 70–80% of the time using these inferential methods.

15. SUBJECT TERMS

Geographic information systems
Geologic analysis
Material properties
Terrain analysis

16. SECURITY CLASSIFICATION OF:			**17. LIMITATION OF ABSTRACT**	**18. NUMBER OF PAGES**	**19a. NAME OF RESPONSIBLE PERSON**
a. REPORT	**b. ABSTRACT**	**c. THIS PAGE**			**19b. TELEPHONE NUMBER** *(include area code)*
U	U	U	U	98	